To the Graduate Council:

I am submitting herewith a thesis written by Bei Fu entitled "Development of Multivariate Statistical Process Control for an Industrial Prototype Wastewater Bio-Treatment Plant." I have examined the final copy of this thesis for form and content and recommend that it be accepted in partial fulfillment of the requirements for the degree of Master of Science, with a major in Chemical Engineering.

Tsewei, Wang, Major Professor

We have read this thesis
and recommend its acceptance:

Paul Frymier

Duane D Bruns

Accepted for the Council:

Associated Vice Chancellor and
Dean of The Graduate School

Development of Multivariate Statistical Process Control for an Industrial Prototype Wastewater Bio-Treatment Plant

A Thesis
Presented for the
Master of Science
Degree
The University of Tennessee, Knoxville

Bei Fu
December 1999

DEDICATION

This thesis is dedicated to my parents

Mr. Da Fu and Mrs. Heqin Yan;

my brother Peng Yan;

my sister-in-law Ikuko Koizumi

and Mr. Almond Greenhall

whose love, dedication, inspiration and support I could never do without

ACKNOWLEDGMENTS

First of all, I would like to thank my parents, Mr. Da Fu and Mrs. Heqin Yan, whose sacrifice made it possible for me to have had two years' rewarding and challenging graduate study at the University of Tennessee, Knoxville. They will have my everlasting love.

I would like to thank all those who have assisted me in one way or another with my graduate studies in UTK. In particular, I would like to express my great gratitude to my major professor, Dr. Tsewei Wang, for her guidance, encouragement and assistance in both academic and life aspects, which made this project as well as my graduate study a truly enjoyable and intellectually stimulating experience.

I would also like to thank Dr. Paul D. Frymier, Dr. Duane. D. Bruns and Dr. Robert M. Counce for their concern, advice and correction during the preparation of this thesis.

Finally, I am grateful to James Grove and Brandon Schmidt for their previous research, which I could not do without.

Abstract

This research analyzes the feasibility of developing a Multivariate Statistical Process Control (MSPC) framework for monitoring and diagnosing a biological wastewater treatment plant. MSPC makes use of historical database of past successful operations as a reference to judge the normality of future operations. The projection method, Principal Component Analysis (PCA), is utilized not only to compress the originally correlated data but also to extract statistically meaningful information, by projecting the multivariate trajectory data onto a lower dimensional space, spanned by the Principal Components (PC' s) retained. From the established 'normal' operation domain, departure of new operating points from that of 'normal' domain can be detected by the use of several MSPC monitoring plots.

The proposed methodology generates monitoring charts by analyzing the process variables gathered in a reference database; new observations are analyzed by contrasting their projections onto the reference PC' s space against that of normal, using a variety of monitoring charts. Possible root causes can sometimes be identified when abnormal deviations have been detected. The capability of such MSPC scheme in monitoring and assessing the behavior of new wastewater treatment operations against the reference is illustrated through simulations of the bio-wastewater treatment plant under a variety of operating conditions.

The research first reviews the concepts and techniques of MSPC and the *Activated Sludge Model No. 1*. It then utilizes these techniques in creating the

monitoring and diagnosis framework for a wastewater bio-treatment plant using the activated sludge model No. 1 description as the process model. Simulation is carried out using the Matlab (version 4.2c) and Simulink™ as the programming platform. The MSPC framework is able to detect abnormal process deviations by comparing the projection of new observations onto the principal component subspace to the 'normal operation' region established from base case data. If current operating points fall inside this region, it implies that the current operation is 'normal'; If they fall or show a trend of migrating toward outside of the region, it implies emergence of abnormal operations. Usually, it is possible to trace back from the abnormal behavior to their assignable causes by analyzing contribution plots.

In this study, a reference database is generated based on the simulation of a large number of variations in the process operating conditions in the neighborhood of a nominal operating condition. These variations include: -21% to +21% changes in the influent nitrate concentration, $[NO_3^-]$, in the maximum growth rate of the heterotrophic biomass, $\mu_{m,\,H}$, in the half-saturation constant of COD, $K_{s,\,[COD]}$ and -15% to +15% changes in the influent ammonia concentration, $[NH_4^+]$. These deviations are defined as 'normal operation' deviations. Monitoring charts are obtained based on this simulated database. Acceptable regions are identified in these charts as the standards for monitoring all future processes. Three abnormal cases are simulated to validate the established base case PCA model. They represent 1) bigger than normal amount of changes in the operating conditions not

affecting the biological model; 2) bigger than normal amount of changes in the bio-process parameters altering the process model; 3) new biological event causing plant/model mismatch. Analysis results show that the indication of the migration, over time, toward a state of abnormality is clear and direct. Diagnosis is carried out by analyzing the contribution plot for each of the three abnormal cases. Results show that the PCA method can also identify the possible root causes for the observed abnormality. In addition, the interpretation of the principal components provides more insights to the behavior of the process variables. However, important implementation issues remain that must be addressed before it can proved to be effective when brought on line.

TABLE OF CONTENTS

CHAPTER	PAGE
1. Introduction	1
1.1 Motivation	1
1.2 Statement of Research Problem	5
2. Background	7
2.1 Multivariate Statistical Process Control (MSPC) and Recent Applications	7
2.1.1 Statistical Process Control (SPC)	7
2.1.2 A Comparison between Univariate Statistical Process Control (USPC) and Multivariate Statistical Process Control (MSPC)	8
2.1.3 Multivariate Statistical Process Control (MSPC)	12
2.1.3.1 General Information for MSPC and Principal Component Analysis (PCA)	12
2.1.3.2 Application of MSPC into Chemical Engineering Field	13
2.2 Configuration and Microbiology of the Wastewater Treatment Plant	15
2.2.1 Configuration of the Biological Wastewater Treatment Plant	15
2.2.2 Microbiology of the Treatment Processes	19
2.2.2.1 Fundamentals of Microbiology	19
2.2.2.2 Carbonaceous Material Biodegradation	20
2.2.2.3 Nitrification	20
2.2.2.4 Denitrification	21
2.2.2.5 Mass Balance-the Construction of the Wastewater Plant Dynamic Simulator	22
2.3 Application of MSPC to Wastewater Treatment Plant	26
2.4 Previous Work on the Wastewater Bio-treatment Plant	28
2.4.1 Grove' s Work	28
2.4.2 Schmidt' s Work	28
2.4.3 Fu' s Prior Work	33
3. Study Approaches	42
3.1 Generating Base Case Data Profile	45
3.2 Adding Measurement Noise	49
3.3 The Methodology of Principal Component Analysis (PCA)	51
3.3.1 Background Concepts of PCA	51
3.3.1.1 Covariance Matrix	51
3.3.1.2 Singular Value Decomposition (SVD)	52
3.3.1.3 Loadings and Scores of the PCA Model	54
3.3.2 A Simplified Illustration of PCA	56
3.4 Determining the Number of PC' s to Retain	58
3.4.1 Pretreatment	58

CHAPTER **PAGE**

3.4.2 Determining How Many PC' s to Retain 59
3.5 Establishing 'Normal Operation' Domain: Reference Scores and Squared Predictive Error (SPE) Charts 60
3.5.1 the Scores Chart 61
3.5.2 the SPE Chart 62
3.6 Monitoring Transient Responses 66
3.7 Simulating 'Abnormal Operations' 67
3.8 Modeling 'Abnormal Operations' with Base Case Profile 68
3.9 Diagnosing 'Abnormal Operations' Using Contribution Plots 69
3.10 A Literature Example for Fault-Detection by MSPC Monitoring Chart 70
3.11 Interpreting Principal Components 73
3.11.1 Loadings Plot 74
3.11.2 Variance-Retention Plot 75
3.11.3 Gabriel' s Plot for PC1, PC2 and PC3 76
3.11.4 Scores Plot 78

4. Results and Discussions 79
4.1 Generating Base Case Data Profile 79
4.2 Adding Measurement Noise 84
4.3 Determining the Number of Principal Components to Retain 84
4.4 Interpreting Principal Components 87
4.4.1 Loadings Plot 88
4.4.1.1 Principal Component 1 88
4.4.1.1.1 Open-Loop Time Response 90
4.4.1.1.2 Closed-Loop Time Response 93
4.4.1.2 Principal Component 2 96
4.4.1.3 Principal Component 3 99
4.4.1.4 Principal Component 4 and 5 105
4.4.1.5 Principal Component 6 105
4.4.2 Variance-Retention Plot 109
4.4.2.1 Principal Component 1 109
4.4.2.2 Principal Component 2 109
4.4.2.3 Principal Component 3 112
4.4.2.4 Principal Component 4 112
4.4.2.5 Principal Component 5 115
4.4.2.6 Principal Component 6 115
4.4.3 Gabriel's Plot for PC1, PC2 and PC3 115
4.4.4 Scores Plot for Samples Projected onto PC's 122
4.4.4.1 Principal Component 1 122
4.4.4.2 Principal Component 2 124
4.4.4.3 Principal Component 3 124
4.4.4.4 Other Principal Components 126

CHAPTER **PAGE**

4.5 Establishing 'Normal Operation' Domain 126
4.6 Simulating 'Abnormal Operations' 128
4.7 Validating PCA Model Using 'Normal'/'Abnormal' Cases and Identifying Causes for 'Abnormal' Cases 132
4.7.1 Normal Case: +15% Changes in the Influent [NO_3^-] and [NH_4^+] 134
4.7.2 Abnormal Case 1: +20% Changes in the Influent Flow Rate 139
4.7.3 Abnormal Case 2: +30% to +40% Changes in the Influent [NO_3^-] and +10% to +20% Changes in the Influent Flow Rate 143
4.7.3.1 Modeling Abnormal Case2 143
4.7.3.2 Identifying Cause for One Sample from Abnormal Case 2: +40% Change in the Influent [NO_3-] and +20% Change in the Influent Flow Rate 149
4.7.4 Abnormal Case 3: -50% to –40% Changes in the $\mu_{m,\,H}$ and +50% to +60% Changes in the $K_{s,\,[COD]}$ 152
4.7.4.1 Modeling Abnormal Case 3 152
4.7.4.2 Identifying Causes of One Sample from Abnormal Case 3: -50% Change in the $\mu_{m,\,H}$ and +60% Change in the $K_{s,\,[COD]}$ 157

4.7.5 Abnormal Case 4: New Biological Event - -30% to -20% Changes in $\mu_{m,\,A}$ 161
4.7.5.1 Modeling Abnormal Case 4 161
4.7.5.2 Identifying Causes of One Sample from Abnormal Case 4: -30% Change in the $\mu_{m,\,A}$ 164
4.7.6 Conclusion 167

5. Conclusions and Recommendations 168
5.1 Conclusions 168
5.2 Recommendations 169

Reference 171

Vita 177

LIST OF TABLES

TABLE		PAGE
2-1	Process Kinetics and Stoichiometry for Carbon Oxidation/Nitrification/ Denitrification (Henze, *et al.*, 1986)	24
3-1	Process Variables Incorporated in Reference Database Generation	48
3-2	Variations of the Operating Conditions in the Reference Database Generation	50

LIST OF FIGURES

FIGURE		PAGE
1-1	Implementation of Multivariate Statistical Process Control Scheme Envisioned for a Process	5
2-1	Measurement Trajectories from the SBR Example (Nomikos, 1995)	9
2-2	MPCA Monitoring Scores Chart from the SBR Example (Nomikos, 1995)	11
2-3	Flowsheet of Wastewater Bio-treatment Plant (Grove, 1995)	17
2-4	Internal Model Control Structure (Morari and Zafiriou, 1989)	30
2-5	Top Layer for Simulink™ Dynamic Simulator	31
2-6	PI Based Regulator Control for a –5% Setpoint Change in the Effluent [BOD] Controlled Variables: Effluent [BOD] and $[NH_4^+]$	34
2-7	IMC Based Regulator Control for a –5% Setpoint Change In the Effluent [BOD] Controlled Variables: Effluent [BOD] and $[NH_4^+]$	35
2-8	PI Based Regulator Control for a -15% Disturbance in the Influent Ammonia Controlled Variables: Effluent [BOD] and $[NH_4^+]$	36
2-9	IMC Based Regulator Control for a -15% Disturbance in the Influent Ammonia Controlled Variables: Effluent [BOD] and $[NH_4^+]$	37
2-10	PI Based Regulator Control for a –50% Change in the $\mu_{m,H}$ and +50% Change in $K_{s,[COD]}$ Controlled Variables: Effluent [BOD] and $[NH_4^+]$	38
2-11	IMC Based Regulator Control for a –50% Change in the $\mu_{m,H}$ and +50% Change in $K_{s,[COD]}$ Controlled Variables: Effluent [BOD] and $[NH_4^+]$	39
3-1	Flow Chart of the thesis work	46
3-2	Graphical Interpretation of PCA Method	57

3-3 Graphical Representation of Projection of Samples onto Reduced Space of PCA (Nomikos, 1995) 64

3-4 Monitoring Charts with Their 95% and 99% Control Limits for a New Normal SBR Batch. (Nomikos, 1995) 71

3-5 Monitoring Charts with Their 95% and 99% Control Limits for a New Abnormal SBR Batch (Nomikos, 1995) 72

4-1 2x2 IMC Closed-Loop Response with +21% Influent $[NO_3^-]$ and +15% $[NH_4^+]$ Changes 81

4-2 2x2 IMC Closed-Loop Response with +21% Influent $[NO_3^-]$, +15% $[NH_4^+]$, -21% $\mu_{m,H}$ and +21% $K_{s,COD}$ Changes 82

4-3 Scree Plot to Determine How Many PC's to Retain 85

4-4 Loadings Plot for PC1 89

4-5 Open-Loop Response with –10% Change in the Recirculation Ratio 91

4-6 Open-Loop Response with +10% Change in the Recirculation Ratio 92

4-7 2x2 IMC Closed-Loop Response with -21% Influent $[NO_3^-]$, +15% Influent $[NH_4^+]$, -21% $\mu_{m,H}$ and +21% $K_{s,[COD]}$ Changes (Sample 301)94

4-8 Loadings Plot for PC2 97

4-9 Open-Loop Response with –10% Change in the Sludge Age (x12) 100

4-10 Open-Loop Response with +10% Change in the Sludge Age (x12) 101

4-11 Loadings Plot for PC3 102

4-12 2x2 IMC Closed-Loop Response with -50% $\mu_{m,H}$ and +60% $K_{s,[COD]}$ Changes 104

4-13 Loadings Plot for PC4 106

4-14 Loadings Plot for PC5 107

4-15 Loadings Plot for PC6 108

4-16 Variance-Retention Plot for PC1 110

4-17 Variance-Retention Plot for PC2 111

4-18 Variance-Retention Plot for PC3 113

4-19 Variance-Retention Plot for PC4 114

4-20 Variance-Retention Plot for PC5 116

4-21 Variance-Retention Plot for PC6 117

4-22 Gabriel' s Plot for PC1, 2 and 3 118

4-23 Gabriel' s Plot for PC1, 2 and 3 (Different View from Figure 4-22) 118

4-24 Gabriel' s Plot for PC1 and 2 120

4-25 Gabriel' s Plot for PC1 and 3 120

4-26 Gabriel' s Plot for PC2 and 3 121

4-27 Scores Plot for PC1 for Samples 123

4-28 Scores Plot for PC2 125

4-29 Scores Plot for PC3 127

4-30 Scores Plot for Principal Components 1 and 2 129

4-31 Scores Plot for Principal Components 1, 2 and 3 129

4-32 SPE Plot for PC1- 2 130

4-33 SPE Plot (SPE versus Sample Number) 130

4-34 Scores Plot for Principal Component 1, 2 and 3. (. =Reference Data; + = Data from the Transient Response with +15% influent [NH_4^+] and +15% [NO_3^-] Changes) 135

4-35 SPE Plot for Principal Component 1 and 2 (. =Reference Data; + = Data from the Transient Response with +15% Influent [NH_4^+] and +15% [NO_3^-] Changes 135

4-36 SPE Plot over Time. (Transient Response with +15% Influent [NH_4^+] and +15% [NO_3^-] Changes. Upper SPE Bound is Obtained from the SPE of

Reference Case.) 136

4-37 2x2 IMC Closed-Loop Response with +15% Influent [NH_4^+] and +15% [NO_3^-] Changes 137

4-38 Scores Plot for Principal Component 1, 2 and 3. (. =Reference Data; + = Data from the Transient Response with +20% Influent Flow Rate Changes) 140

4-39 Scores Plot for Principal Component 2 and 3 (. =Reference Data; + = Data from the Transient Response with +20% Influent Flow Rate Changes) 140

4-40 SPE Plot for Principal Component 1 and 2 (. =Reference Data; + = Data from the Transient Response with +20% Influent Flow Rate Changes) 141

4-41 SPE Plot over Time (Transient Response with +20% Influent Flow Rate Changes. Upper SPE Limit is Obtained from the SPE of Reference Case) 141

4-42 2x2 IMC Close-Loop Response with +20% Influent Flow Rate Change 142

4-43 Monitoring Chart. Score Plot for Principal Component 1, 2 and 3 (.=Reference Data; + = Data of +15% Influent [NH_4^+], +21% $\mu_{m,\,H}$, -21% $K_{s,\,COD}$, +30%-+40% [NO_3^-] and +10%-+20% Flow Rate Changes) 144

4-44 Monitoring Chart. Score Plot for Principal Component 2 and 3 (. =Reference Data; + = Data of +15% Influent [NH_4^+], +21% $\mu_{m,\,H}$, -21% $K_{s,\,[COD]}$, +30%-+40% [NO_3^-] and +10%-+20% Flow Rate Changes) 144

4-45 Monitoring Chart. SPE Plot for Principal Component 1 and 2 (. =Reference Data; + = Data of +15% Influent [NH_4^+], +21% $\mu_{m,\,H}$, -21% $K_{s,\,[COD]}$, +30%-+40% [NO_3^-] and +10%-+20% Flow Rate Changes) 145

4-46 Monitoring Chart. SPE Plot (. =Reference Data; + = Data of +15% Influent [NH_4^+], +21% $\mu_{m,\,H}$, -21% $K_{s,\,COD}$, +30%-+40% [NO_3^-] and +10%-+20% Flow Rate Changes) 145

4-47 Monitoring Chart. Score Plot for Principal Component 1,2, 3 (.=Reference Data; + = Data of Transient Response of +15% Influent [NH_4^+], +21% $\mu_{m,\,H}$, -21% $K_{s,\,COD}$, +40% [NO_3^-] and +10% Flow Rate Changes) 146

4-48 Monitoring Chart. SPE Plot for Principal Component 1 and 2 (. =Reference Data; + = Data of the Transient Response of +15% Influent [NH_4^+], +21%

$\mu_{m,\ H}$, -21% $K_{s,\ COD}$, +40% $[NO_3^-]$ and +10% Flow Rate Changes) 146

4-49 Contribution Plot to t-score2 for Abnormality Case 2: +20% Change in the Influent Flow Rate and +40% Change in the influent $[NO_3^-]$ 150

4-50 Contribution Plot to SPE for Abnormality Case 2: +20% Change in the Influent Flow Rate and +40% Change in the influent $[NO_3^-]$ 150

4-51 Monitoring Chart. Scores Plot for Principal Component 1, 2 and 3 (. =Reference Data; + = Data of -50% to –40% $\mu_{m,\ H}$, +50% to +60% $K_{s,\ COD}$, Changes) 153

4-52 Monitoring Chart. Scores Plot for Principal Component 1 and 3 (. =Reference Data; + = Data of -50% to –40% $\mu_{m,\ H}$, +50% to +60% $K_{s,\ COD}$, Changes) 153

4-53 Monitoring Chart. SPE Plot for Principal Component 1 and 2 (. =Reference Data; + = Data of -50% to –40% $\mu_{m,\ H}$, +50% to +60% $K_{s,\ COD}$, Changes) 154

4-54 Monitoring Chart. SPE Plot (. =Reference Data; + = Data of -50% to -40% $\mu_{m,\ H}$, +50% to +60% $K_{s,\ COD}$ Changes) 154

4-55 Monitoring Chart. Scores Plot for Principal Component 1, 2 and 3 (. =Reference Data; + = Data of Transient Response of -50% $\mu_{m,\ H}$, +60% $K_{s,\ COD}$, Changes) 155

4-56 Monitoring Chart. SPE Plot for Principal Component 1 and 2 (. =Reference Data; + = Data of Transient Response of -50% $\mu_{m,\ H}$, +60% $K_{s,\ COD}$, Changes) 155

4-57 Contribution Plot to PC1 for Abnormality Case 3: -50% Change in the $\mu_{m,\ H}$ and +60% Change in the $K_{s,\ [COD]}$ 158

4-58 Contribution Plot to PC3 for Abnormality Case 3: -50% Change in the $\mu_{m,\ H}$ and +60% Change in the $K_{s,\ [COD]}$ 158

4-59 Contribution Plot to SPE for Abnormality Case 3 -50% Change in the $\mu_{m,\ H}$ and +60% Change in the $K_{s,\ [COD]}$ 159

4-60 Monitoring Chart. Scores Plot for Principal Component 1, 2 and 3 (. =Reference Data; + = Data of -30% to –20% $\mu_{m,\ A}$ Changes) 162

4-61 Monitoring Chart. Scores Plot for Principal Component 2 and 3

(. =Reference Data; + = Data of -30% to –20% $\mu_{m,A}$ Changes) 162

4-62 Monitoring Chart. SPE Plot for Principal Component 1 and 2 (. =Reference Data; + = Data of -30% to –20% $\mu_{m,A}$ Changes) 163

4-63 Monitoring Chart. SPE Plot (. =Reference Data; + =Data of -30% to –20% $\mu_{m,A}$ Changes) 163

4-64 Monitoring Chart. Scores Plot for Principal Component 1, 2 and 3 (. =Reference Data; + = Data of Transient Response of -30% $\mu_{m,A}$ Changes) 165

4-65 Monitoring Chart. SPE Plot for Principal Component 1 and 2 (. =Reference Data; + = Data of Transient Response of -30% $\mu_{m,A}$ Changes) 165

4-66 Contribution Plot to PC2 for Abnormality Case 4: -30% Change in the $\mu_{m,A}$ 166

4-67 Contribution Plot to SPE for Abnormality Case 4: -30% Change in the $\mu_{m,A}$ 166

NOMENCLATURE

Abbreviations

BOD	Biochemical Oxygen Demand
COD	Chemical Oxygen Demand
CSTR	Continuously Stirred Tank Reactor
GV	Gabriel' s Vector
IAWPRC	International Association on Water Pollution Research and Control
IAWQ	International Association on Water Quality
IMC	Internal Model Control
MBPC	Model Based Predictive Control
MIMO	Multi-Input Multi-Output
MPCA	Multi-way Principal Component Analysis
MPLS	Multi-way Partial Least Squares
MSPC	Multivariate Statistical Process Control
NOD	Nitrogenous Oxygen Demand
PC	Principal Component
PCA	Principal Component Analysis
PI	Proportional Integral (Controller)
PID	Proportional Integral Derivative (Controller)
PLS	Partial Least Squares (Projection on Latent Structure)
SBR	Styrene-Butadiene Rubber
SISO	Single-Input Single-Output

SPC	Statistical Process Control
SPE	Squared Predictive Error
SVD	Singular Value Decomposition
USPC	Univariate Statistical Process Control

Symbols, Upper Case

Symbol	**Meaning**	**Dimensions (as appropriate)**
CO_2	carbon dioxide	
$C_5H_7NO_2$	empirical formula for microbe mass	
E	residual matrix	mxn
F_e	effluent flow rate	volume/day
F_w	sludge wastage flow rate	volume/day
H^+	hydrogen ion	mass/volume
HCO_3^-	bi-carbonate ion	mass/volume
H_2CO_3	carbonic acid	
H_2O	water	
I	identity matrix	nxn
$K_{O,H}$	heterotrophic growth parameter	
K_{NO}	heterotrophic growth parameter	
K_s	Monod half saturation constant	mass/volume
$K_{s,\,COD}$	K_s for heterotrophic consumption of COD	mass COD/volume
N	nitrogen element	

NH_3	ammonia	
NH_4^+	ammonia ion	mass/volume
NO	nitric oxide	
NO_2^-	nitrite ion	mass/volume
NO_3^-	nitrate ion	mass/volume
NO_X	nitrate/nitrite ion	mass/volume
$N\text{-}NH_3/NH_4^+$	nitrogen as ammonia/ammonium ion	mass $N\text{-}NH_3/NH_4^+$
$N\text{-}NO_2^-/NO_3^-$	nitrogen as nitrite ion/nitrate ion	mass $N\text{-}NO_2^-/NO_3^-$
$N\text{-}NO_3^-$	nitrogen as nitrate ion	mass N as nitrate
N_2	nitrogen gas	
N_2O	nitrous oxide	
O_2	oxygen gas	
P	loadings matrix (orthonormal)	nxn
P^T	transpose of P matrix	nxn
P_k	P matrix of the first k columns retained	nxk
S	substrate concentration	mass/volume
S_{ALK}	alkalinity	molar units
S_I	soluble inert organic matter	mass COD/volume
S_{NH}	ammonia concentration	mass $N\text{-}NH_4^+$/volume
S_{ND}	soluble biodegradable organic nitrogen	mass N/volume
S_{NO}	nitrate concentration	mass $N\text{-}NO_3^-$/volume
S_O	oxygen concentration	mass COD/volume

S_s	readily biodegradable substrate concentration	mass COD/volume
SPE_i	SPE of the ith sample	1xm
T_k	scores matrix with k columns	mxk
U	SVD result matrix of X; orthonormal	mxm
U_k	U matrix of the first k columns retained	mxk
X	mean-centered and scaled matrix	mxn
X^T	transpose of X matrix	nxm
X_B	concentration of microbial mass	mass/volume
$X_{B,H}$	heterotrophic biomass concentration	mass COD/volume
$X_{B,A}$	autotrophic biomass concentration	mass COD/volume
X_e	effluent biomass concentration	mass COD/volume
X_I	particulate inert organic matter	mass COD/volume
Xi	the ith row of the X matrix	1xn
X_{ND}	particulate biodegradable organic nitrogen	mass N/volume
X_o	original simulated data matrix	mxn
X_{o-n}	original simulated data matrix with noise	mxn
X_p	particulate products arising from biomass decay	mass COD/volume
X_s	slowly biodegradable substrate	mass COD/volume
X_t	total mass of biomass in the system	mass COD
X_w	sludge wastage biomass concentration	mass COD/volume

Symbols, Lower Case

Symbol	Meaning	Dimensions (as appropriate)
b_H	decay ratio	day^{-1}
e	error between original projection data	
e_i	i^{th} row of E matrix	
k	number of principal components retained	
k_d	endogenous decay coefficient	day^{-1}
m	number of the rows in X matrix (number of observations)	
n	number of the columns in X matrix (number of variables)	
p_i	the ith loadings vector	nx1
p_r	the rth principal component	nx1
$p_r(i)$	the ith element of the rth principal component	1x1
t	time	day
t_i	i^{th} scores vector	
x1	$X_{B,H}$ from anoxic reactor	mass COD/volume
x2	$X_{B,A}$ from anoxic reactor	mass COD/volume
x3	S_s from anoxic reactor	mass COD/volume
x4	S_{NH} from anoxic reactor	mass $N\text{-}NH_4^+$/volume
x5	S_{NO} from anoxic reactor	mass $N\text{-}NO_3^-$/volume
x6	$X_{B,H}$ from clarifier	mass COD/volume
x7	$X_{B,A}$ from clarifier	mass COD/volume
x8	S_s from clarifier	mass COD/volume

x9	S_{NH} from clarifier	mass $N\text{-}NH_4^+$/volume
x10	S_{NO} from clarifier	mass $N\text{-}NO_3^-$/volume
x11	recirculation ratio	
x12	sludge age	
$x_{abnormal}$	a new abnormal observatrion	1xn
$x_{abnormal}(i)$	the Ith element in the $x_{abnormal}$ vector	1x1
x_i	i^{th} column of X matrix	mx1
x_{ij}	element on the ith row and j^{th} column of X matrix	
$x_{ij,\ projection}$	projection onto the k-dimensional subspace of the element on the ith row and j^{th} column of X matrix	

Symbols, Greek Characters

Symbol	**Meaning**	**Dimensions (as appropriate)**
μ_B	specific growth rate of biomass	day^{-1}
$\mu_{max.\ B}$	maximum growth rate of biomass	day^{-1}
$\mu_{m,\ H}$	maximum growth rate of heterotrophic biomass	day^{-1}
$\mu_{m,\ A}$	maximum growth rate of autotrophic biomass	day^{-1}
η_g	correction factor for anoxic growth of heterotrophs	
Σ	singular value matrix of X	mxn
σ	singular value	
$\hat{t}_r$	the rth t-score of the abnormal observation	
$\hat{Q}$	squared predictive error	

Chapter 1

Introduction

This is a feasibility study for a new tool of monitoring and diagnosing for an industrial prototype wastewater treatment plant. The focus of this study is to explore the effectiveness of Multivariate Statistical Process Control (MSPC) method as a handle for the plant personnel to assess whether the process operation is proper or not.

A MSPC monitoring and diagnosis framework is to be developed for a multi-stage biological wastewater treatment plant, in an attempt to offer an early warning of abnormal operation and to assign possible root-cause for the observed abnormality. The MSPC methodology applied in this study is Principal Component Analysis (PCA) – a strong component of the bag of tools used in MSPC. Provided that a historical operating profile data set is available, PCA then is able to reduce its data size, to extract statistically significant information and to establish a 'normal operation' region as a reference for assessing the state of future operation. The reference trajectory is used to represent the normal operation of the process and to evaluate the performance of new observations. New process observations are to be contrasted against this reference model and be classified as either normal or abnormal.

1.1 Motivation

The major purpose of an industrial wastewater treatment plant is to purify the quality of the wastewater by removing undesirable compounds (such as the

carbonaceous wastes and nitrogen compounds) in the waste stream coming from an upstream manufacturing plant. The waste streams entering the treatment plant will have some unavoidable fluctuations in both the feed rate and their various waste concentrations. Further, unknown differences between the process parameters of the real process and the model used to develop feedback controllers always exist. Therefore it is essential to have monitoring capability to detect, in time, significant deviation of actual performance of plant from that of expected. Thus, possible root cause can be identified and actions can then be taken to correct for these deviations, in an attempt to drive the system back to the region of 'normal operation', in order to meet effluent discharge standards.

The usual method to correct for output deviation from that of setpoint is to put in local feedback control loops. The outputs are fed back, to be compared with the desired value of the controlled variables. Any differences are then fed into the controller as error signals. Thus, control actions calculated from a specified control law can be implemented to compensate for the process deviation.

But for a complicated plant, local feedback control loops alone are not adequate. It is well established that feedback control loops eliminate the symptoms but not the root causes of a process upset. Its major deficiencies lie in the following aspects: 1) Using feedback loops, the system counteracts the output deviations by acting on non-zero errors. These errors go through the controller and change the inputs to the process. Hence, the cost of compensating for any deviation in the process output is a deviation in the process input from that of nominal. The system

deviation is now shifted from the output to that of the input. The cause for the deviation still exists. 2) In order to maintain the output at the desired value, corresponding input has to be changed. Suppose the output deviation becomes worse and worse, then the responsible input will also have to become more and more aggressive in an attempt to bring the system back to a normal state of operation. This might result in meeting against system constraints. For example, a ceiling coolant flow rate might be met and the plant can not be brought back to the normal reactor temperature state. 3) Feedback control only takes care of correcting for the deviation in the output. It does not take into account the effect on the input and intermediate variables. For a complex system, there are not only a large number of input and output variables, but also many correlated intermediate variables, whose effect on the system may not be known exactly. The entire operation profile, including the output, input and intermediate variables, needs to be compared to that of the 'normal' trend. Such that, even though the output appears to be normal, the monitoring system is still able to detect an overall shift over time from that of 'normality' and to recommend the operation personnel to take adjustment steps in time, before the effect becomes irreversible. Therefore, a tight monitoring and diagnosis of the overall plant operation is urgently needed to ensure the long-term success of the operation of the treatment system. Without timely and accurate measurements, local feedback control is unlikely to achieve the desired specific process goals. In the chemical industry, timely and accurate measurements are not always available. For instance, the biological process in this

study, most of the monitored variables are composition measurements. Composition sampling and analysis are usually made off-line in the laboratory, probably once or twice a day. In this case, local on-line feedback control loops designed to feedback directly these compositions are not feasible. In addition, control actions are usually based on off-line and intermittent measurements. Thus, tight control of the effluent concentrations, even when possible, is not feasible.

To achieve MSPC, the following implementation is envisioned. This implementation is considered for future application, only after practical implementation issues have been addressed and resolved. This is a possibility to achieve process monitoring in the future. Figure 1-1 is a block diagram of the layout for the envisioned MSPC scheme. It shows the relationship between the classical feedback control loop and the additional monitoring element riding on top of it. The new part is the "Multivariate Statistical Data Analysis" block. Plant-wide information is to be fed into this block. Through data reduction, multivariate analysis and model fitting, abnormal operation profiles can usually be detected and analyzed. Possible causes can then be attempted to be removed before the feedback control capacity is overwhelmed. The removal of the causes for deviation is to be carried out by an operator. The "Multivariate Statistical Data Analysis" acts as an alarm to warn the operators the existence of possible process 'abnormality' that may have emerged during the course of the operation of the treatment plant.

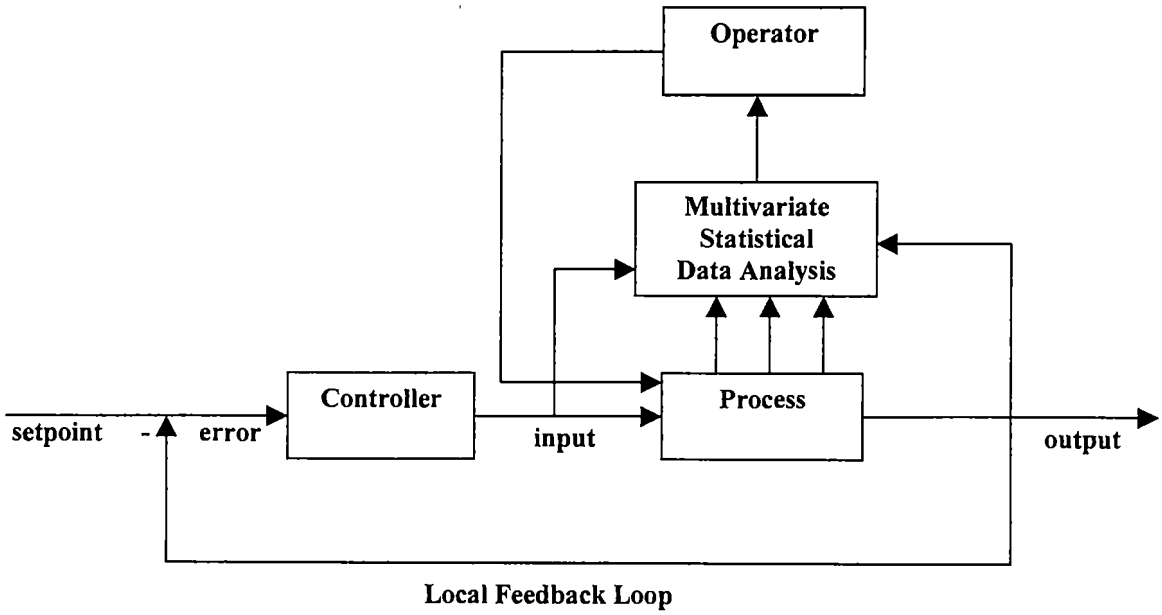

Figure 1-1. Implementation of Multivariate Statistical Process Control Scheme Envisioned for a Process.

1.2 Statement of Research Problem

The focus of this study is to develop a multivariate statistical monitoring and diagnostic framework for a wastewater biotreatment plant by using the principal component analysis methods. This framework can provide an early warning for abnormal operations and suggest process variables responsible for the deviation.

First, based on the historical operation data, a 'normal operation' PCA model will be developed and a desired multi-dimensional acceptable region for normal performance will be constructed using multivariate statistical method. If future process behavior lies inside the 'normal' region, process with good output will be indicated. Operation departing from this region represents possible faults.

Actions will be recommended to be taken to drive the process back to the 'normal' region. In this study, according to this logic, several perturbed cases with deviations larger than those used to develop the reference database, and those not included in the base case generation, will be simulated in order to assess the feasibility of the MSPC model developed. Variables that contribute to the deviation will be attempted to be identified.

Chapter 2

Background

2.1 Multivariate Statistical Process Control (MSPC) and Recent Applications

2.1.1 Statistical Process Control (SPC)

Modern plants have become more and more complex and vast amount of process data is usually available due to the advancements in automation and distributed control systems. These large quantities of data are an excellent information resource if significant and pertinent process information could be extracted from them easily and timely. Converting process data into useful operating information in a timely manner would greatly improve process quality and safety. Traditional data analysis methods may not be adequate when faced with stringent requirements for output product quality. This situation led to the application of statistical methods into the process control fields.

The objective of Statistical Process Control (SPC) is primarily to monitor the performance of a process over time to detect if it remains in a 'normal' state of operation according to that foretold by the historical data. Early warning and identification can be provided if any potential production problems, such as malfunctions, abnormal operations or significant disturbances, are present. Based on the warning, adjustment steps can be taken in time to reduce the off-specification production in order to maintain the product quality. The abnormal performance of a plant can cause many significant problems, such as bad product quality, low productivity, increased environmental problem and even plant

shutdowns. That is why quality control has become an extremely important part of today's plant operation programs.

2.1.2 A Comparison between Univariate Statistical Process Control (USPC) and Multivariate Statistical Process Control (MSPC)

Until recently, classical Univariate Statistical Process Control (USPC) method plays a major role in the quality control field. USPC monitors one quality variable at a time and ignores the collinear behavior between the variables. If a small set of variables are measured and all of them are independent, experimental results show that USPC approach is suitable for quality control. But with the advancement of modern technology and the power of computers, as industrial plants with complex structure being the norm, vast data set across a wide range of variables can still be logged and is available for analysis. It is less possible that they are all independent of each other. USPC is based only on the magnitude of the deviation of one variable and does not take into account the interactions among the variables. This method does not provide appropriate and adequate information about the overall state of the process if variable correlation exists. Therefore, it is not surprising that Multivariate Statistical Process Control (MSPC) approach has become more and more popular during the last few years. Figure 2-1 is an example to show the feasibility of MSPC.

This example is based on the semi-batch emulsion polymerization of Styrene-Butadiene in making latex rubber (SBR) (Nomikos, 1995). In this figure, both normal operation data and abnormal operation data are present. Since this is a

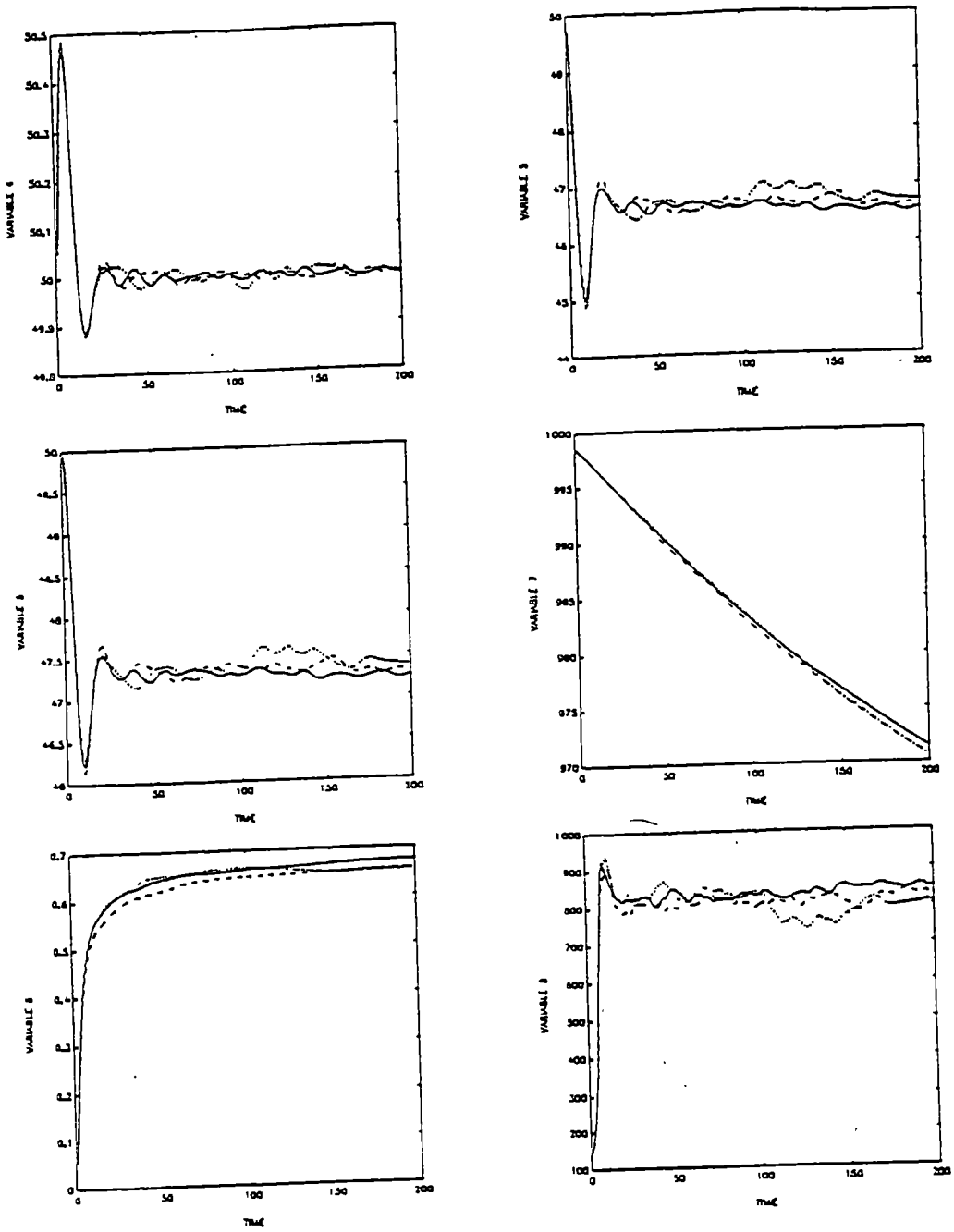

Figure 2-1. Measurement Trajectories from the SBR Example (-: normal batch; --: abnormal batch; ...: abnormal batch) (Nomikos, 1995)

USPC monitoring chart, each of the six figures shows the trajectories for several operations of one variable over time. Correlation among variables can not be depicted. In the figure, the solid line represents a successful batch; the dashed line and dotted line represent two unsuccessful batches. Apparently, there is not much observable difference among the good runs and the bad runs. Therefore, fault of the unsuccessful batches is not easily detectable by examining the plots of the individual variables.

Conversely, Multivariate Statistical Process Control (MSPC) handles data of this type very well. Visual inspection of the MSPC charts will be sufficient to detect the abnormal cases. Figure 2-2 is a monitoring chart showing the scores of data from fifty-two batch runs. By adding two unsuccessful batches, batch 51 and 52, to the reference batch database consisting of fifty successful batches, MSPC chart indicates the difference between these two sets clearly. In this figure, all fifty-two batches are projected onto the scores plane spanned by the first two principal components. The fifty good batches cluster more tightly in a region as shown in this plane. The two batches with fault fall well outside the cluster of the good batches. Therefore, while USPC is not adequate for fault detection graphically, MSPC works well in indicating process abnormalities. Through this example, it is shown that MSPC is appropriate for analysis of processes characterized by correlated measurements.

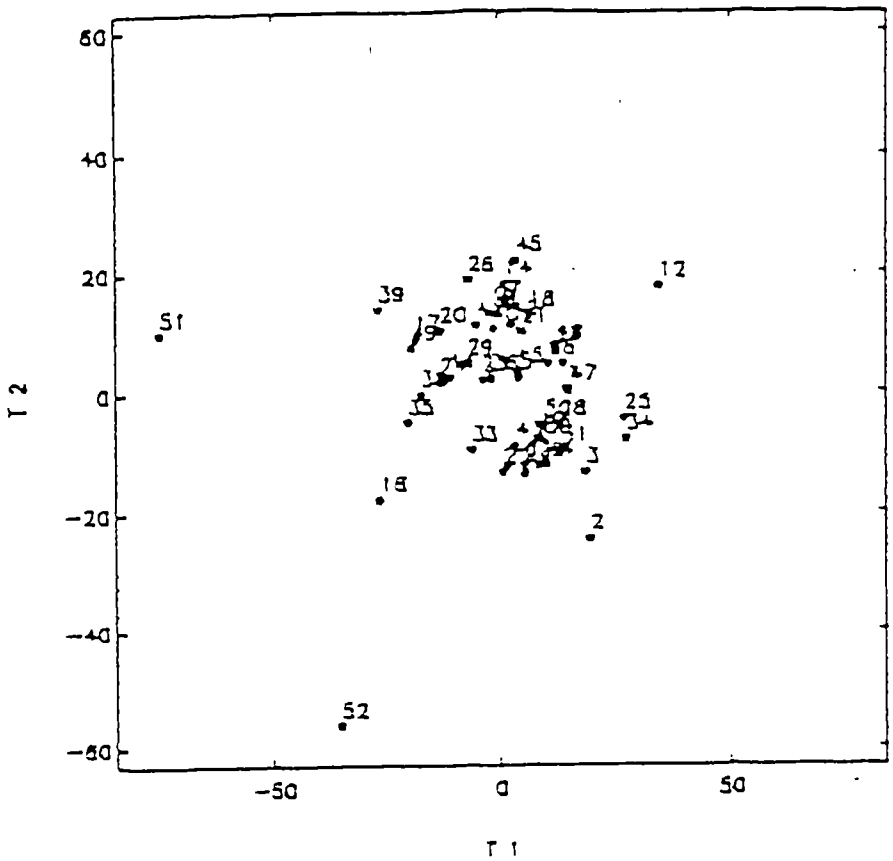

Figure 2-2. MPCA Monitoring Scores Chart from the SBR Example; Batches 51 and 52 are the bad batches. (Nomikos, 1995)

2.1.3 Multivariate Statistical Process Control (MSPC)

2.1.3.1 General Information for MSPC and Principal Component Analysis (PCA)

MSPC provides a systematic approach to the treatment of correlated process data. From the original data set, it extracts information that contributes the most to the variation of the data; it defines a set of new and fewer, so called, principal components or latent variables, and projects the original process variable measurements onto the much smaller dimensional space spanned by these principal component axes.

The basis of MSPC is the projection theory. One popular MSPC method is the Principal Components Analysis (PCA) (Wold, Wise, MacGregor, 1980's). Through MSPC, interrelated process data can be reduced to a much lower dimensional space, which reflects the truer dimensionality or the degree of freedom of the process, and are to be represented by a set of principal components. These principal components are formed by linear combinations of the original process variables. Principal Components are orthogonal to each other, therefore representing independent information. Usually, tens of process variables can be represented by just a few principal components without missing out on any significant system information. The highly correlated original data set can then be expressed by a reduced set of uncorrelated new variables, with a better insight into the process. MSPC may aid in separating the important information which

contributes the most to the variation of the process from noises and thus capturing the essence of the information.

PCA has a long history dating back to the beginning of the twentieth century (Pearson, 1901). It was first used in the field of social studies, psychology and anthropology. Recently, it has been used in the fields of data reduction, variable classification and providing early warning and identification of malfunctions, abnormal operations, significant process disturbances or impending equipment failure (Wold, 1987).

The essence of MSPC, including PCA, can be considered as practices in chemometrics application. Chemometrics is the 'science of relating measurements made on a chemical system to the state of the system, via application of mathematical or statistical methods' (Wise, 1996). As the use of modern instrumentation systems becomes more common, more and more data are recorded more frequently in the chemical processes. Therefore, the use of PCA emerged to be a powerful tool to analyze the chemical data. Chemometrics applies most effectively to inter-related data. PCA not only performs data compression but also extracts systematic information from the data set. PCA is a favorite tool of chemometricians for these purposes. PCA is chosen in this thesis work.

2.1.3.2 Applications of MSPC into Chemical Engineering Field

MSPC of chemical processes is an approach first shown possible by MacGregor, J. F. in the 1980's (MacGregor, *et al.*, 1987) and has since become an area for cutting-edge research and application during this decade. Recent popularity

is due to its applicability to more and more complex processes and showing success in detecting process abnormalities.

MacGregor as well as other investigators have already shown many results of application of MSPC method in the process industry. The MSPC method has been applied to a variety of different processes. Some recent applications include: 1) monitoring of fluidized bed reactors and extractive distillation columns (Kresta and MacGregor *et al,* 1991) (Chen and Mcavoy *et al*, 1998); 2) quality control of polypropylene production (Skagerberg and Lehtinen *et al*, 1992); 3) monitoring of low density polyethylene reactors (MacGregor and Skagerberg, 1994); 4) monitoring of batch and continuous processes (MacGregor and Koutodi, 1995); 5) study of batch polymerization reactors (Martin and Morris, 1996); 6) control of high-temperature short-time milk pasteurization process (Negiz and Cinar,1997); 7) solving of registration problems in fine pitch components for Printed Circuit Boards (Colon, GonzalezBarteto, 1997); 8) quality control of industrial titanium dioxide white pigment (Majcen and Rius *et al*, 1997); 9) analysis of polar compound of virgin olive oils (Evangelisti, Zunin *et al*, 1997); 10) analysis of the effect of inflow disturbances for fed-batch fermentative production of recombinant beta-galactosidase (Patnaik, 1997); 11) monitoring of emulsion batch processes (Neogi and Schlags, 1998); 12) investigation of the feasibility of monitoring sensor accuracy (Leger and Garland *et al*, 1998); 13) quality control of electrolysis process which produces extremely pure copper (Wikstrom, Albano *et al,* 1998); 14) real-time monitoring and detection of after-burning hazards of continuous catalyst

regenerators (You, 1998); 15) control of powder blending with near-infrared spectroscopy (Demaesschalck and Sanchez *et al*, 1998); 16) optimizing of oil spill dispersants as a function of oil type and weathering degree (Brandvik, Daling, 1998).

All of these applications show that the multivariate statistical analysis method is a very promising approach in the following two aspects: 1) identification of the occurrence of process deviation from that of 'normal operation' region; 2) identification of the combination of the process variables reflecting the deviation.

2.2 Configuration and Microbiology of the Wastewater Treatment Plant

2.2.1 Configuration of the Biological Wastewater Treatment Plant

Wastewater treatment in the United States is based mainly on the activated sludge process (Grady and Lim, 1980). An anoxic/oxic system is an example of this process and is a part of the wastewater bio-treatment plant in this study. This plant is the prototype for future treatment of industrial wastewater being considered by a major chemical company in the Gulf Coast, with the potential of several other similar plants being built in the near future.

The Bardenpho activated sludge process (Metcalf and Eddy, 1991) in this study consists of a biological system in series with a physical settlement system. They work together to reduce the waste material and to separate the solid and liquid fraction of the treated waste. The biological system features an anoxic reactor (without oxygen) followed by an aerobic reactor (with oxygen). Waste carbonaceous material degradation and nitrogen removal are carried out in this

system accompanied by biomass growth. Nitrogen removal in the Bardenpho process is through a two-step procedure – nitrification and denitrification. N-NH_3/NH_4^+ is first converted to N-NO_2^-/NO_3^- during nitrification in the aerobic reactor. N-NO_3^- is then converted into nitrogen gas and released to the atmosphere during denitrification in the anoxic reactor. The aerobic stage also removes almost all the organic matters of the wastewater stream. The third unit in the process is a physical settling system, the clarifier. The final step – separation of the suspended biomass solids and liquids is carried out in this unit by the force of gravity. No biochemical reactions take place in the settling tank. The clarified liquid is discharged into the receiving waterway. The separated suspended solids are divided into two parts. The majority of the solids are recycled back to the anoxic reactor. The remaining fraction exits the process through a bottom wastage stream where rate can be adjusted by the operator, and is an important manipulated variable for control consideration. A plant configuration is shown in Figure 2-3.

The Activated Sludge Model No. 1 (Henze, *et al.*, 1986) was used to develop the simulator model for the bio-wastewater treatment plant (Grove, 1995). This model utilizes Monod kinetics and accounts for carbonaceous degradation, nitrification and denitrification through the growth of heterotrophic and autotrophic microbes. It is assumed that all the reactors are well-mixed, continuously stirred tank reactors (CSTR). The *Activated Sludge Model No. 1* provides a series of ordinary differential equations, representing the kinetic mass balances for each of the thirteen process variables. Each equation represents the net generation rate of

one component in each of the two reactors. Depending on the stated dissolved oxygen level in the reactor, the model switches between aerobic and anoxic processes. The system is usually subject to daily flow and load fluctuations, but they can be assumed to operate at steady state when system stability is achieved in the long-term against these short-term cyclic variations.

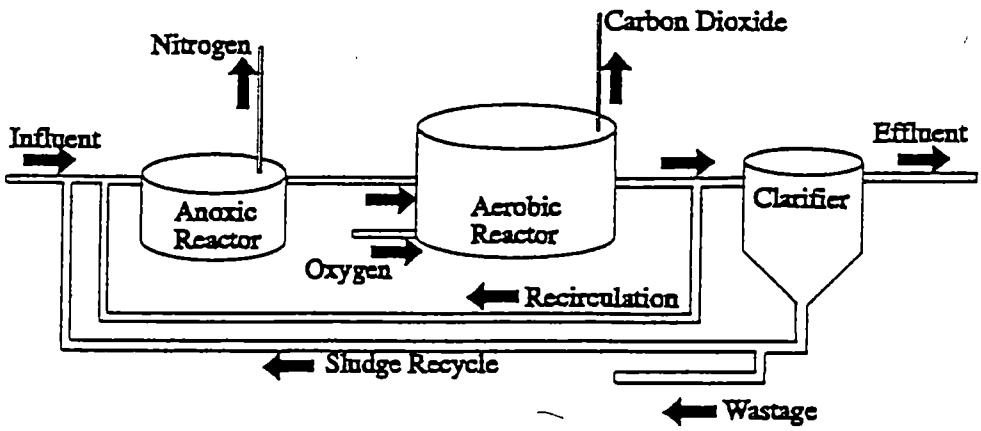

Figure 2-3. Flowsheet of Wastewater Bio-treatment Plant (Grove, 1995).

The objective of the bio-treatment is to reduce the amount of the carbonaceous wastes and nitrogen compounds to those less harmful to the environment when discharged, such as, water, carbon dioxide and nitrogen gas. Variables to be controlled to meet discharge permit standard usually are the effluent concentrations of carbonaceous waste-biological oxygen demand (BOD), ammonia, and/or nitrate. Two significant wastewater characteristics are its flowrate and

pollution load. Their ever-changing magnitude and model uncertainty and complexity make the controlling of the treatment process challenging. Therefore, the flow rate, the influent BOD, ammonia and nitrate concentrations are considered to be the system's input variables. The sludge age and recirculation ratio are selected as the manipulated variables for the design of feedback controllers. The recirculation ratio is defined as the ratio of the recirculation flow rate from the aerobic reactor to the anoxic reactor divided by the influent flow rate to the wastewater plant (Refer to Figure 2-3). The sludge age reflects the mean solids residence time in the reactor. It is assumed that the volume of the reactor is separately controlled to be constant at all times. Assuming the total mass of biomass in the system is X_t, effluent flowrate and biomass concentration in the effluent are F_e and X_e, sludge wastage flowrate and biomass concentration in the wastage are F_w and X_w, respectively, the definition of the sludge age is:

$$sludge \quad age = \frac{X_t}{F_w X_w + F_e X_e} \tag{1}$$

For $X_e \approx 0$, (1) becomes:

$$sludge \quad age = \frac{X_t}{F_w X_w} \tag{2}$$

It is the ratio of the total biomass in the system to the rate of solid removal of the system (Metcalf & Eddy, 1991; Orhon & Artan, 1994).

2.2.2 Microbiology of the Treatment Processes

2.2.2.1 Fundamentals of Microbiology

The biological processes occuring in the Bardenpho system are similar to the biological processes in other industrial applications. Microorganisms consume substrate/nutrition and convert them into either biomass or energy for cellular functions.

The growth rate of microorganisms with respect to the consumption of substrate is formulated as Monod kinetics (Monod, 1942, 1949, 1950):

$$\mu_B = \mu_{\max,B} \frac{S}{K_s + S} \tag{3}$$

where: μ_B = Specific growth rate of Biomass, day^{-1}

$\mu_{max,B}$ = Maximum specific growth rate of Biomass, day^{-1}

S = Substrate concentration, mass (e.g., COD or $N\text{-}NH_4^+$) $volume^{-1}$

K_s = Half velocity constant, same units as S, specific to that limiting substrate and microbe (Grove, 1995)

The net accumulation rate of microbes in a system where both cell growth and cell death are present has a first order exponential format (Shuler and Kargi, 1992):

$$\frac{dX}{dt} = \mu_{\max,B}\left(\frac{S}{K_s + S}\right)X - k_d X \tag{4}$$

where: X = Concentration of microbial mass, mass (COD) $volume^{-1}$

t = Time, day

k_d = Endogenous decay coefficient, day^{-1}

2.2.2.2 Carbonaceous Material Biodegradation

Large amount of carbonaceous material discharged into waterway is harmful to the ecological balance. A major goal of a wastewater treatment plant is to convert biodegradable organic compounds into chemical compounds which are less toxic to the receiving waterway. In the studied system, the aerobic tank is the primary unit for degradation of the carbonaceous compounds. It is designed to consume the carbonaceous material through the action of some heterotrophic microorganisms. They degrade organic carbon in wastewater as part of their food and energy source and these biosynthesis reactions use oxygen as the electron acceptor. The organic compounds are converted into carbon dioxide, cell mass, and a few other end products. There is also hetorotrophic degradation going on in the anoxic reactor, but at a slower rate. Microorganisms using CO_2 as their principal carbon source for biosynthesis are autotrophs and they are active in the nitrification process in the aerobic reactor. Microorganisms using organic compounds for biosynthesis are heterotrophs (Metcalf & Eddy, 1991; Orhon & Artan, 1994).

2.2.2.3 Nitrification

Similar to carbonaceous material, excessive amount of organically bound nitrogen compounds entering a waterway can also have deleterious effects on the ecological systems by imposing an oxygen load in the receiving water (Arcievala, 1981).

Autotrophic bacteria are capable of performing respiratory metabolism under aerobic conditions using inorganic compounds as their energy source. In this study, NH_3 and NO_2^- are oxidized to NO_3^- in the aerobic reactor, using HCO_3^- as the primary source of carbon, providing energy and raw material for cell growth. This process is called nitrification. The end product of nitrification is nitrate among others. It is then converted into nitrogen gas in the anoxic reactor in the process of denitrification and removed from the process.

Nitrification is carried out by two different physiological groups of nitrifying bacteria in the following sequence of reactions (Orhon & Artan, 1994):

$$2NH_4^+ + 3O_2 \rightarrow 2NO_2^- + 4H^+ + 2H_2O \tag{5}$$

$$2NO_2^- + O_2 \rightarrow 2NO_3^- \tag{6}$$

The overall equation describing the aerobic growth of autotrophs in association with nitrification of ammonia compounds can be expressed as (Metcalf & Eddy, 1991):

$$NH_4^+ + 1.83O_2 + 1.98HCO_3^- \rightarrow 0.021C_5H_7NO_2 + 1.041H_2O + 0.98NO_3^- + 1.88H_2CO_3 \tag{7}$$

where $C_5H_7NO_2$ represents microbial mass, and 4.3 mg of O_2 per mg of ammonia-nitrogen is required for its conversion to nitrate.

2.2.2.4 Denitrification

Denitrification and cell growth occur in the anoxic reactor in the absence of oxygen. Instead, the nitrates produced in the aerobic reactor serve as an electron acceptor. The heterotrophic microorganisms consume carbonaceous wastes present

for cell growth and generation of the nitrogen gas. The reduction of nitrate to nitrogen gas takes place in a sequence of reactions (Orhon & Artan, 1994):

$$NO_3^- \rightarrow NO_2^- \rightarrow NO \rightarrow N_2O \rightarrow N_2 \tag{8}$$

These reactions provide energy for the heterotrophic biomass growth occurring in the anoxic reactor. The overall nitrate removal as well as biomass synthesis can be expressed as (Metcalf & Eddy, 1991):

$$NO_3^- + 1.08 carbonunit + H^+ \rightarrow 0.065 C_5H_7NO_2 + 0.47 N_2 + 0.76 CO_2 + 2.44 H_2O \tag{9}$$

2.2.2.5 Mass Balance – the Construction of the Wastewater Plant Dynamic Simulator

According to the *Activated Sludge Model No. 1*, there are thirteen components of interest in the system. They are: soluble inert organic matter (S_I), readily biodegradable substrate (S_S), particulate inert organic matter (X_I), slowly biodegradable substrate (X_S), active heterotrophic biomass ($X_{B,H}$), active autotrophic biomass ($X_{B,A}$), particulate products arising from biomass decay (X_P), oxygen (S_O), N-NO_3^-/NO_2^- (S_{NO}), N-NH_4^+/NH_3 (S_{NH}), soluble biodegradable organic nitrogen (S_{ND}), particulate biodegradable organic nitrogen (X_{ND}) and alkalinity (S_{ALK}). For each of the thirteen components, a mass balance is carried out in the anoxic reactor, in the aerobic reactor as well as in the clarifier. There are eight major biological processes occurring in the system. They are: aerobic growth of heterotrophs, anoxic growth of heterotrophs, aerobic growth of autotrophs, 'decay' of heterotrophs, 'decay' of autotrophs, ammonification of soluble organic

nitrogen, 'hydrolysis' of entrapped organics and 'hydrolysis' of entrapped organic nitrogen.

Each mass balance is carried out by the formula of:

Input – Output + Generation - Consumption = Accumulation (10)

For such a system with multiple species as well as processes, the (Generation-Consumption) term in the above mass balance is consisted of several process kinetics and stoichiometry matrix, as presented in *The Activated Sludge Model No. 1*, listed in Table 2-1. All the symbols encountered in this table are noted on either the right or the left corner of the table.

In this table, rows represent the eight processes while columns represent the thirteen components described previously. Elements within this matrix comprise the stoichiometric coefficients, ν_{ij}. They characterize the mass relationship between each component and the individual process. The jth process rate, ρ_j, is listed in the last column of the matrix, depicting the reaction rate of each process. In the expression of ρ_j, the terms of $(\frac{S_O}{K_{O,H}+S_O})$ and $(\frac{K_{O,H}}{K_{O,H}+S_O})$ serve as 'switching functions'. They are responsible for switching the reactions to either aerobic reaction when oxygen is present or anoxic reaction when oxygen is absent. When O_2 is available, say, in the aerobic reactor, S_O is relatively large compared with $K_{O,H}$. Then the first term above approximately equals to one and the second term is almost zero. On the other hand, when O_2 is not available in the reactor, say, in the anoxic reactor, S_O approaches to zero. Then the first term equals to zero while the

Table 2-1. Process Kinetics and Stoichiometry for Carbon Oxidation/Nitrification/Denitrification (Henze, *et al.*, 1986)

Component → i	1 S_I	2 S_S	3 X_I	4 X_S	5 $X_{B,H}$	6 $X_{B,A}$	7 X_P	8 S_O	9 S_{NO}	10 S_{NH}	11 S_{ND}	12 X_{ND}	13 S_{ALK}	Process Rate, ρ_j $[ML^{-3}T^{-1}]$
j Process ↓	Soluble inert organic matter $[M(COD)L^{-3}]$	Readily biodegradable substrate $[M(COD)L^{-3}]$	Particulate inert organic matter $[M(COD)L^{-3}]$	Slowly biodegradable substrate $[M(COD)L^{-3}]$	Active heterotrophic biomass $[M(COD)L^{-3}]$	Active autotrophic biomass $[M(COD)L^{-3}]$	Particulate products arising from biomass decay $[M(COD)L^{-3}]$	Oxygen (negative COD) $[M(-COD)L^{-3}]$	Nitrate and nitrite nitrogen $[M(N)L^{-3}]$	$NH_4^+ + NH_3$ nitrogen $[M(N)L^{-3}]$	Soluble biodegradable organic nitrogen $[M(N)L^{-3}]$	Particulate biodegradable organic nitrogen $[M(N)L^{-3}]$	Alkalinity – Moles units	
1 Aerobic growth of heterotrophs		$-\frac{1}{Y_H}$			1			$-\frac{1-Y_H}{Y_H}$		$-i_{XB}$			$-\frac{i_{XB}}{14}$	$\mu_H\left(\frac{S_S}{K_S+S_S}\right)\left(\frac{S_O}{K_{O,H}+S_O}\right)X_{B,H}$
2 Anoxic growth of heterotrophs		$-\frac{1}{Y_H}$			1				$-\frac{1-Y_H}{2.86Y_H}$	$-i_{XB}$			$\frac{1-Y_H}{14\cdot 2.86Y_H}-i_{XB}/14$	$\mu_H\left(\frac{S_S}{K_S+S_S}\right)\left(\frac{K_{O,H}}{K_{O,H}+S_O}\right)\times\left(\frac{S_{NO}}{K_{NO}+S_{NO}}\right)\eta_g X_{B,H}$
3 Aerobic growth of autotrophs						1		$-\frac{4.57-Y_A}{Y_A}$	$\frac{1}{Y_A}$	$-i_{XB}-\frac{1}{7Y_A}$			$-\frac{i_{XB}}{14}-\frac{1}{7Y_A}$	$\mu_A\left(\frac{S_{NH}}{K_{NH}+S_{NH}}\right)\left(\frac{S_O}{K_{O,A}+S_O}\right)X_{B,A}$
4 'Decay' of heterotrophs				$1-f_P$	-1		f_P					$i_{XB}-f_P i_{XP}$		$b_H X_{B,H}$
5 'Decay' of autotrophs				$1-f_P$		-1	f_P					$i_{XB}-f_P i_{XP}$		$b_A X_{B,A}$
6 Ammonification of soluble organic nitrogen										1	-1		$\frac{1}{14}$	$k_a S_{ND} X_{B,H}$
7 'Hydrolysis' of entrapped organics		1		-1										$k_h \frac{X_S/X_{B,H}}{K_X+(X_S/X_{B,H})}\left[\left(\frac{S_O}{K_{O,H}+S_O}\right)+\eta_h\left(\frac{K_{O,H}}{K_{O,H}+S_O}\right)\left(\frac{S_{NO}}{K_{NO}+S_{NO}}\right)\right]X_{B,H}$
8 'Hydrolysis' of entrapped organic nitrogen											1	-1		$\rho_7(X_{ND}/X_S)$
Observed Conversion Rates $[ML^{-3}T^{-1}]$	$r_i=\sum_j \nu_{ij}\rho_j$													
Stoichiometric Parameters: Heterotrophic yield: Y_H; Autotrophic yield: Y_A; Fraction of biomass yielding particulate products: f_P; Mass N/Mass COD in biomass: i_{XB}; Mass N/Mass COD in products from biomass: i_{XP}														Kinetic Parameters: Heterotrophic growth and decay: μ_H, K_S, $K_{O,H}$, K_{NO}, b_H; Autotrophic growth and decay: μ_A, K_{NH}, $K_{O,A}$, b_A; Correction factor for anoxic growth of heterotrophs: η_g; Ammonification: k_a; Hydrolysis: k_h, K_X; Correction factor for anoxic hydrolysis: η_h

latter term could be approximated to be one. By means of this, the process rate expression is applicable to both aerobic and anoxic reactor.

To calculate the (Generation-Consumption) term for, say, the jth component, one needs to go down the jth column and add up all the $\nu_{ij}\rho_j$ (i =1 to 8) elements to obtain the overall reaction term for the jth component. An example is presented below to explain the procedure for calculating this term.

The fifth column represents the component of the active heterotrophic biomass. The cell generation rate of aerobic growth of the heterotrophs is $1\times\mu_H(\frac{S_s}{K_s+S_s})(\frac{S_O}{K_{O,H}+S_O})X_{B,H}$ (Refer to Section 2.2.2.1, Monod equation); the cell generation rate of the anoxic growth of the heterotrophs is $1\times\hat{\mu}_H(\frac{S_s}{K_s+S_s})(\frac{K_{OH}}{K_{OH}+S_O})(\frac{S_{NO}}{K_{NO}+S_{NO}})\eta_g X_{B,H}$, where η_g is the correction factor for anoxic growth of the heterotrophs; the rate of decay is $(-1)\times b_H X_{B,H}$, where b_H is the decay coefficient for the heterotrophs. The overall (Generation-Consumption) rate for the active heterotrophic biomass is:

$$1\times\mu_H(\frac{S_s}{K_s+S_s})(\frac{S_O}{K_{O,H}+S_O})X_{B,H}+1\times\hat{\mu}_H(\frac{S_s}{K_s+S_s})(\frac{K_{OH}}{K_{OH}+S_O})(\frac{S_{NO}}{K_{NO}+S_{NO}})\eta_g X_{B,H}-b_H X_{B,H}. \quad (11)$$

To obtain the overall mass balance for the active heterotrophic biomass in any unit operation, say, the aerobic reactor, input and output information are also needed. Referring the Figure 2-3, the flowchart of the treatment plant, the influent

flow of the aerobic reactor is the output of the anoxic reactor. This influent stream includes heterotrophic biomass. The output of the aerobic reactor is divided into two parts. One goes into the clarifier and the other goes back to the anoxic reactor as the recirculation flow. Both parts of the stream contain heterotrophic biomass, too. This wastewater treatment plant is considered to be a CSTR operation. The flowrate is considered to be always controlled at a steady value, in order to avoid overflow or washout conditions. Thus, every term in equation (10) is to be computed using known parameter values and the mass balance expression is then ready for the component of active heterotrophic biomass.

The dynamic simulator was built by carrying out the thirteen simultaneous mass balances in the anoxic reactor, the aerobic reactor and the clarifire by integrating the system of first-order differential equations derived by using the reaction rate terms as shown in Table 2-1.

2.3 Application of MSPC to Wastewater Treatment Plant

This activated sludge wastewater bio-treatment plant is characterized by a non-linear biological process with many bio-parameters. Several physical, chemical and microbiological factors affect the treatment results of the plant simultaneously. The biological processes are extremely sensitive to pH, temperature, and the dissolved oxygen level. The process can easily diverge from the desired operation profile. Thus, stringent monitoring is needed to more readily detect deviations, so as to avoid irreversible impact on the wastewater treatment system's output quality. Many variables are normally measured on and off-line in this process. They are

usually highly correlated. There are also a number of intermediate variables that are measurable. Since MSPC approach is suitable for dealing with correlated data, it is feasible to apply MSPC to the analysis of the system at hand. It is usually possible for this method to identify the process variable(s) accountable for the system's departure from the 'normal' operating trajectory.

Some researchers have already shown a strong interest in applying MSPC to the wastewater treatment field. Some recent reports are: 1) analysis of a waste treatment process (Schlags and Anani, 1998); 2) monitoring of an activated-sludge wastewater treatment plant (Teppola, Mujunen, 1998); 3) analysis of activated sludge plant (Teppola and Mujunen *et al*, 1997); 4) characterization of industrial effluent connected to municipal sewage treatment plants (Andren and Eklund *et al*, 1998). Their simulation results show the feasibility of applying MSPC for this type of system. Previous investigations for MSPC in wastewater treatment field are mostly carried out in Europe, Finland, Sweden, Denmark and Canada. Specific research was based on the data obtained from specific plant under specific operation condition and then was not able to represent the general case of the application of MSPC in wastewater treatment plant. In this study, MSPC is used in the simulation of a prototype of industrial wastewater bio-treatment plant in the United States. Effort will be made to make general discussions and conclusions. More effluent variables as well as some of the intermediate variables are monitored in this study to give more insight to the process at hand.

The activated sludge wastewater bio-treatment plant in this study is a complex system with nonlinear dynamic structure. A model predictive control strategy, the internal model control (IMC) (Morari, 1989), is applied. IMC has been shown to be superior to traditional PID in dealing with system nonidealities. With a 2x2 local IMC control loops in place, MSPC attempts to detect and identify occurrence of process operation deviating from that of acceptable limit. It is hoped that corrective actions can be taken by the operator before irreversible effect results.

2.4 Previous Work on the Wastewater Bio-treatment Plant

2.4.1 Grove's Work

Grove (1995) developed a dynamic simulator using the Matlab/Simulink™ platform for this multi-stage bio-wastewater plant. He studied the sensitivity of the open-loop dynamic responses of this system to perturbations and identified manipulated-controlled variable pairings, with respect to stability and performance requirement. He considered two by two decentralized output-input pairing and recommended desirable pairings based on the μ-interaction measure index (Grosdidier and Morari, 1985) for minimizing the effect of loop interactions.

2.4.2 Schmidt's Work

Based on Grove's work, Schmidt (1996) closed the two by two control loops by taking the recommended pairings but used linearized process models in designing for a feedback controller. He compared the performance of two base-level controller design approaches, that of the classical Proportional-Integral

Derivative (PID) tuned by traditional methods, and that of Internal Model Control (IMC), with respect to long-term stability, performance and ease of tuning when setpoint changed and when disturbances or plant/model mismatches were present.

First level unconstrained IMC was chosen in his study as the representing Model Based Control strategy, because it was easy to design and to understand after PID, but exhibited some nice control characteristics, not exhibited by the conventional PID controllers (Ogunnaike and Ray, 1994). These features included the built-in capability of compensating for process dead time, inverse response and tolerance of some degree of plant-model mismatch. Thus, while PID failed in stability when non-ideal process characteristics were encountered, IMC could always yield stable operation.

Figure 2-4 is a block diagram of IMC control. The major difference between classical feedback control and model-based control is that there is a model block in parallel with the process block in the latter. Thus, inputs entering the process will also go through the model. The outputs of the process and the model will be compared and if they are different, the difference will be fedback to the controller. Control actions will be taken to take care of this difference. For instance, when there is a disturbance or plant/model mismatch, the outputs from the process and from the model will not be the same. This deviation is the signal to be fedback. The system is then able to sense the occurrence of the disturbance event in time. Therefore, the capability of disturbance rejection and mismatch tolerance of the system is improved by applying model-based control strategy.

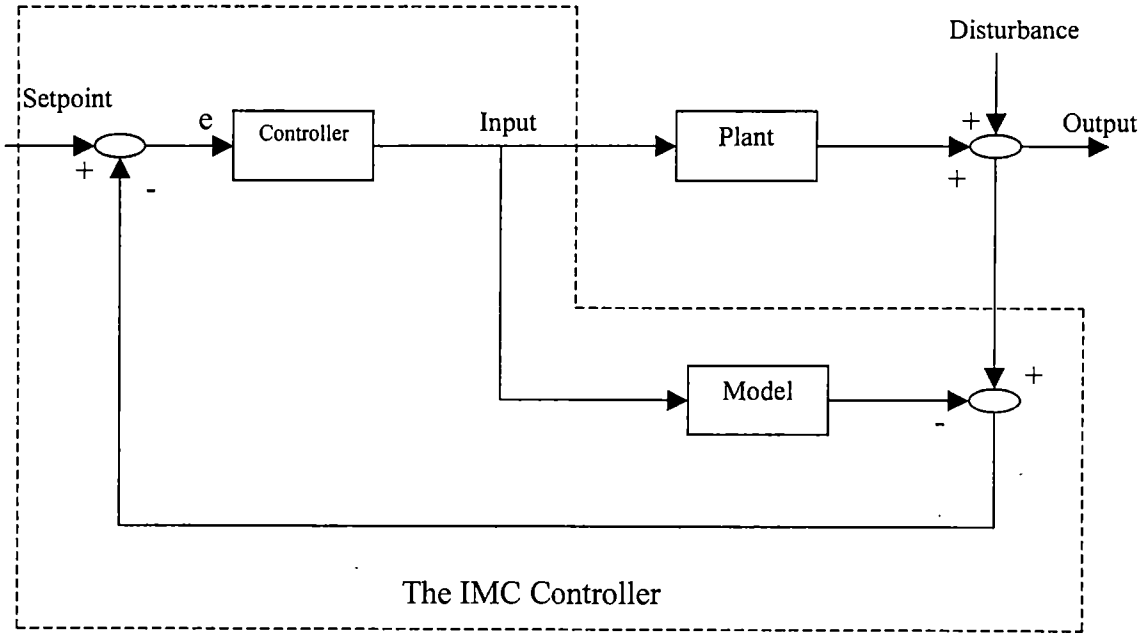

Figure 2-4. Internal Model Control Structure (Morari and Zafiriou, 1989)

Both PI and IMC control schemes in his study were decentralized multiple-loop controllers, which were simpler to design than a true multivariable controller by ignoring the inter-loop interactions. The drawback was that it would reduce the stability margin of the process. Decentralized controller is defined as follows: consider each manipulated variable paired with one process output variable on which it is deemed to have the most effect. The calculation for the manipulated variable is based only on the output variable to which it is paired. This is in contrast to that of the true multivariable controller, in which the calculation of each manipulated variable is based on all of the output or controlled variables. The decentralized control structure of this bio-wastewater treatment plant is shown in Figure 2-5. It is the top-level block diagram of the plant. In this figure, the

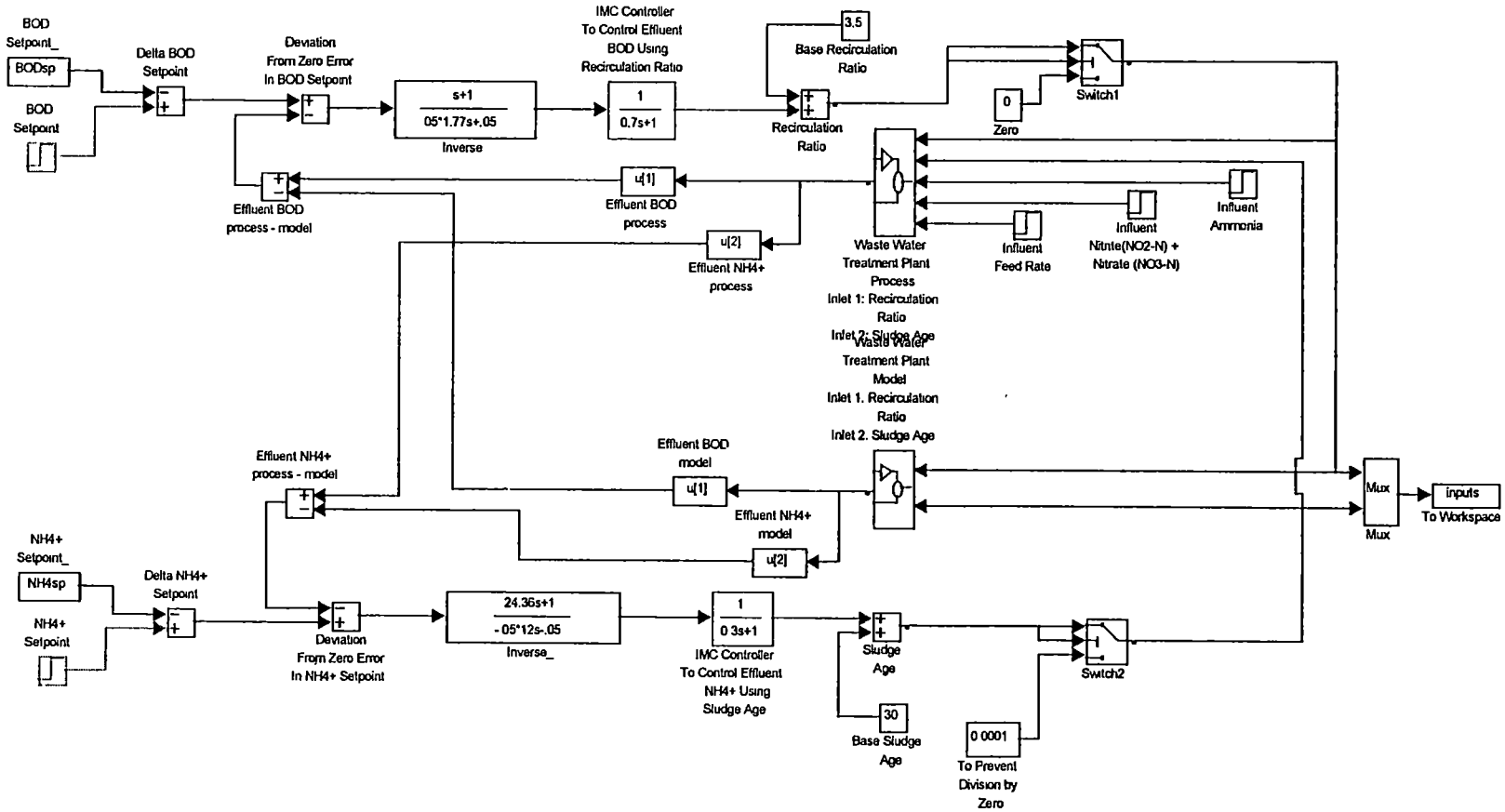

Figure 2-5. Top Layer for Simulink™ Dynamic Simulator

controlled variables are the effluent [BOD] and [NH_4^+]. The two manipulated variables, recirculation ratio and sludge age, are paired with the effluent [BOD] and [NH_4^+], respectively. The complex Multiple Input Multiple Output (MIMO) system is approximated by a decentralized two by two system, therefore much easier to handle. What is being sacrificed is the tight performance only a true MIMO controller will deliver.

Results of his study showed that: PI controller alone was not adequate in keeping long-term stability, for systems where non-ideal element was encountered (inverse response occurred in cases where ammonia was one of the two variables to be controlled, as the case in this thesis work). The performance of the 2x2 PI controllers became unstable even when the controller was detuned to increase the stability margin. Detuning only delays the onset of the instability after an introduction of either a setpoint or a disturbance step change. IMC had the obvious advantage in maintaining long-term stability under the same conditions. It was also easier to retune IMC to meet the performance criteria, because IMC had only one tuning parameter per loop, with built-in capability of compensating for process dead time and inverse response (Morari, 1989); while a PI loop had three parameters even before the addition of inverse-response compensator or Smith Predictors, in order to compensate for the process non-ideal characteristics. Schmidt attributed some model inaccuracies to the linear representation of the nonlinear process. However, because IMC did not take any input constraint

explicitly into consideration, it sometimes led to unrealistically big input actions, which could not be implemented in practice.

2.4.3 Fu's Prior Work

The last phase of the previous study was the incorporation of the original nonlinear model of the wastewater treatment plant into the process block in the feedback control loop. Results again showed that IMC was much more able to achieve long-term stability in the face of perturbation, compared with that of the PI controller. Detuning the PI controller could not avoid the onset of instability for cases with inverse response or long delay in the model. When plant-model mismatch was introduced into the process, PI controller would lead to impractical results. The performance of IMC could always meet the stability criteria by retuning, although IMC at times generated control actions that were too big or too rapidly changing to be practical. Again, since IMC had less tuning parameters than a PI controller does, the advantages in the ease of tuning were apparent.

Selected simulation results are shown here to display the advantage of IMC over PI controller with respect to long-term stability and performance, using nonlinear process model and a linear controller. Figures 2-6 to 2-11 are simulation results with the effluent [BOD] and [NH_4^+] being the controlled variables, with respect to setpoint tracking, disturbance rejection and plant-model mismatch

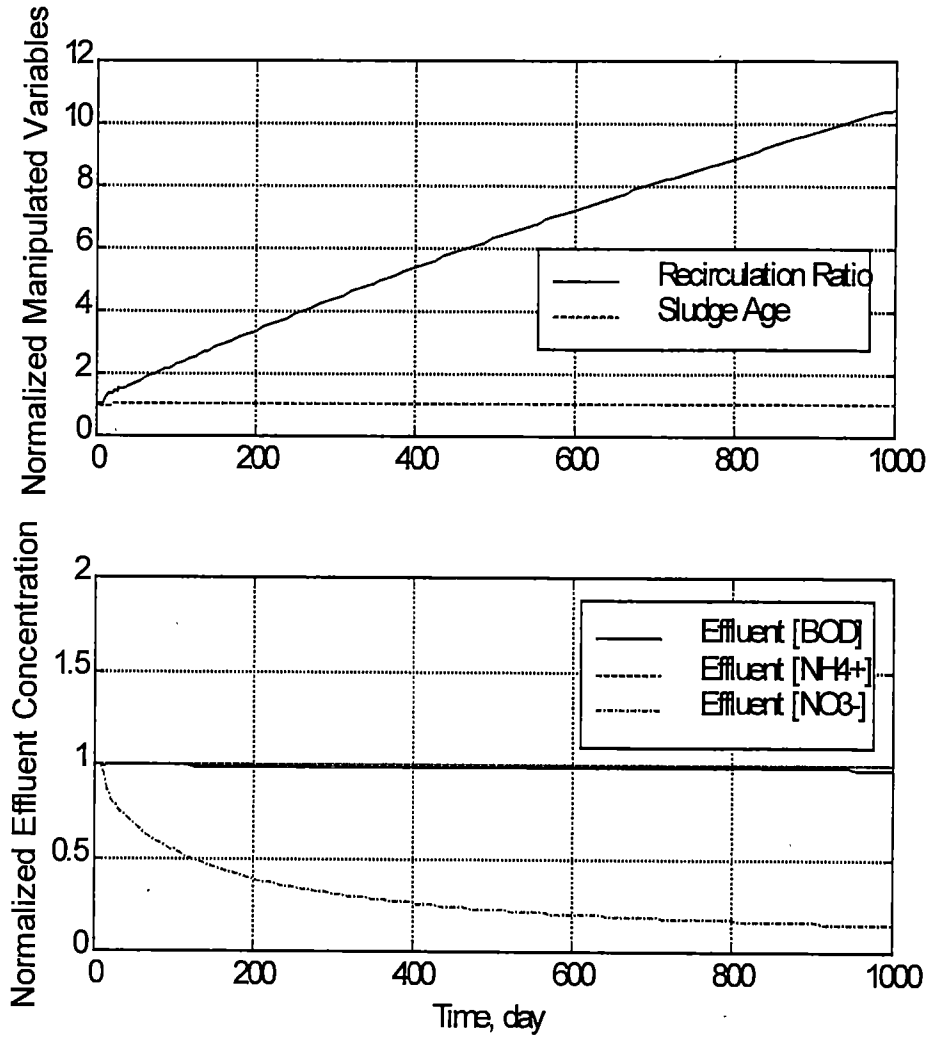

Figure 2-6. PI Based Regulator Control for a –5% Setpoint Change in the Effluent [BOD]
Controlled Variables: Effluent [BOD] and [NH_4^+]

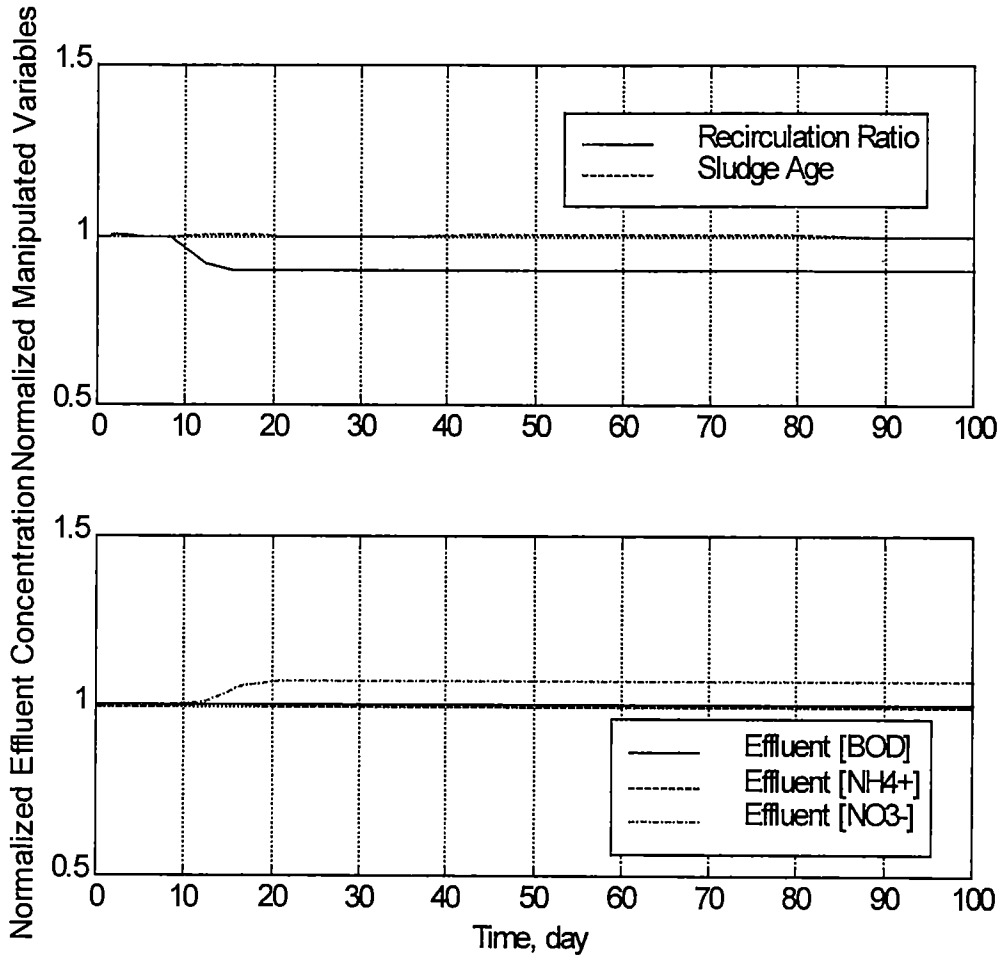

Figure 2-7. IMC Based Regulator Control for a –5% Setpoint Change In the Effluent [BOD]
Controlled Variables: Effluent [BOD] and [NH_4^+]

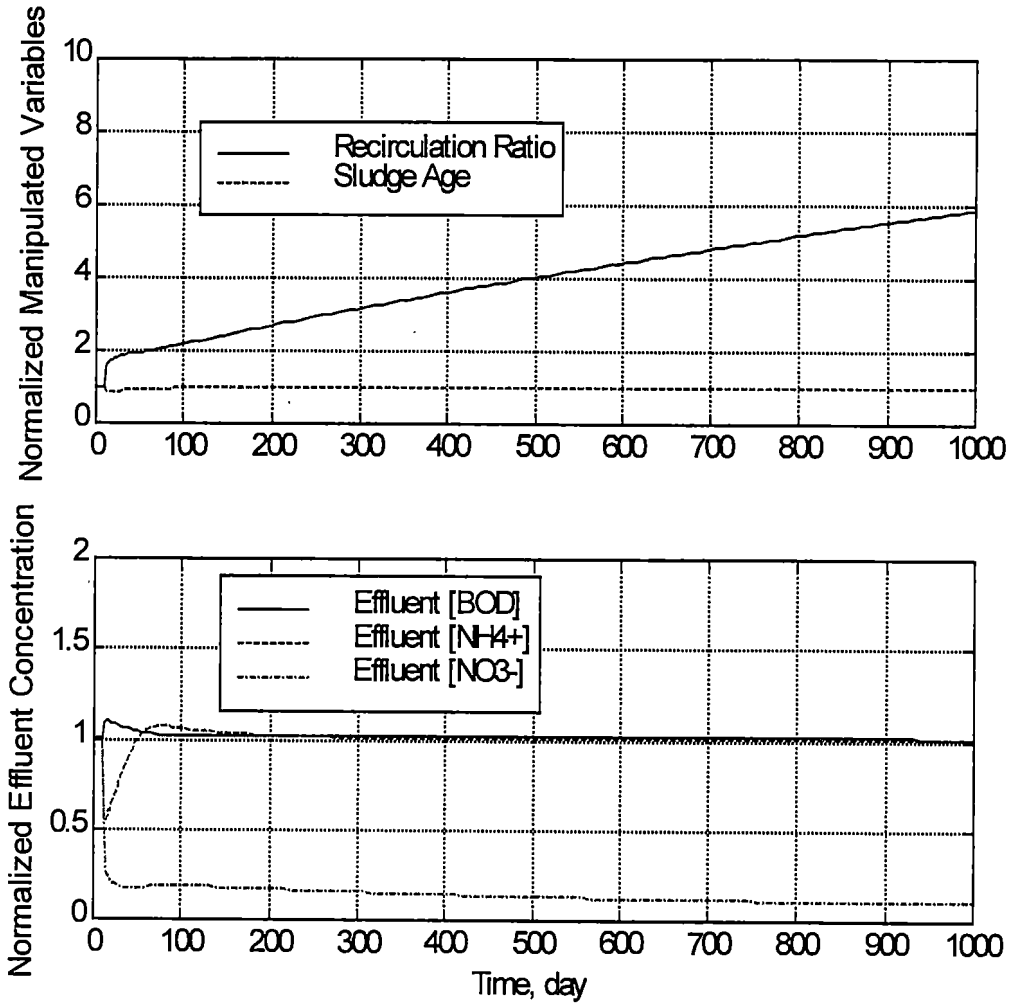

Figure 2-8. PI Based Regulator Control for a -15% Disturbance in the Influent Ammonia
Controlled Variables: Effluent [BOD] and [NH_4^+]

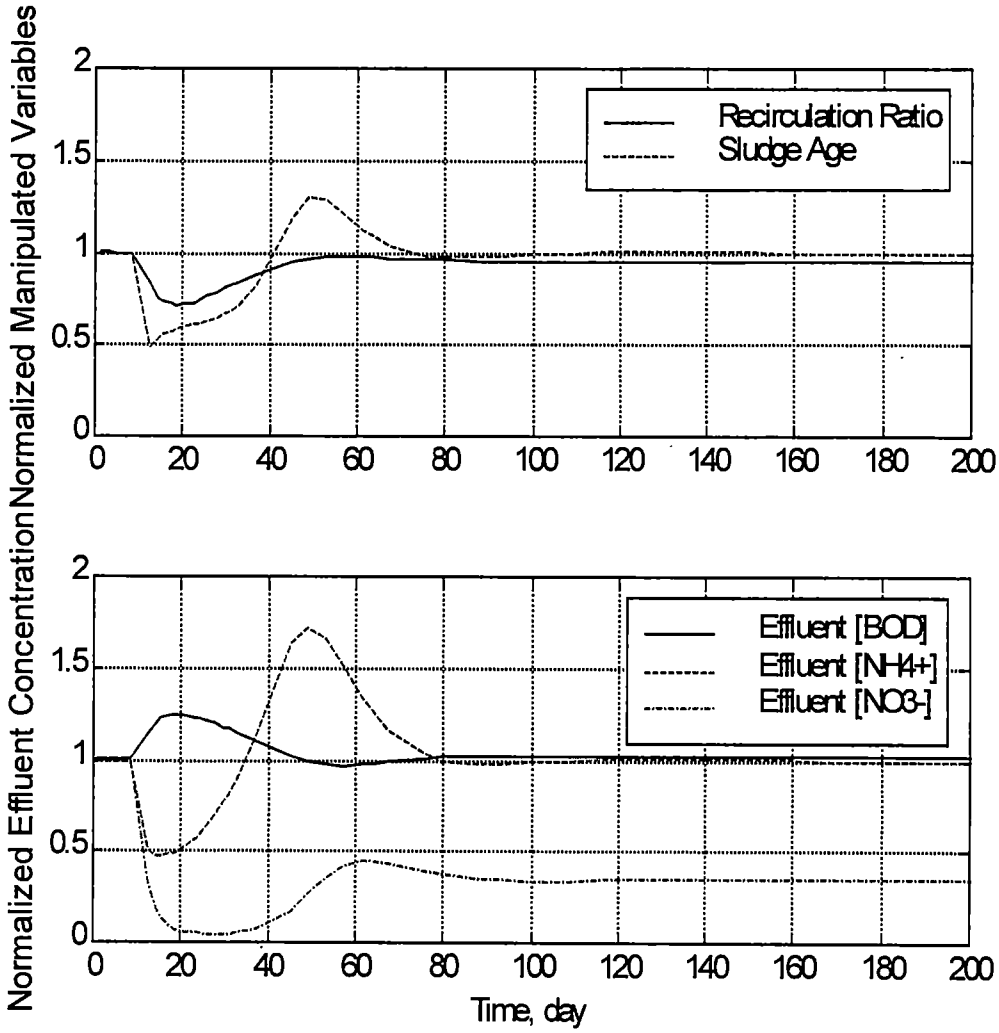

Figure 2-9. IMC Based Regulator Control for a -15% Disturbance in the Influent Ammonia
Controlled Variables: Effluent [BOD] and [NH_4^+]

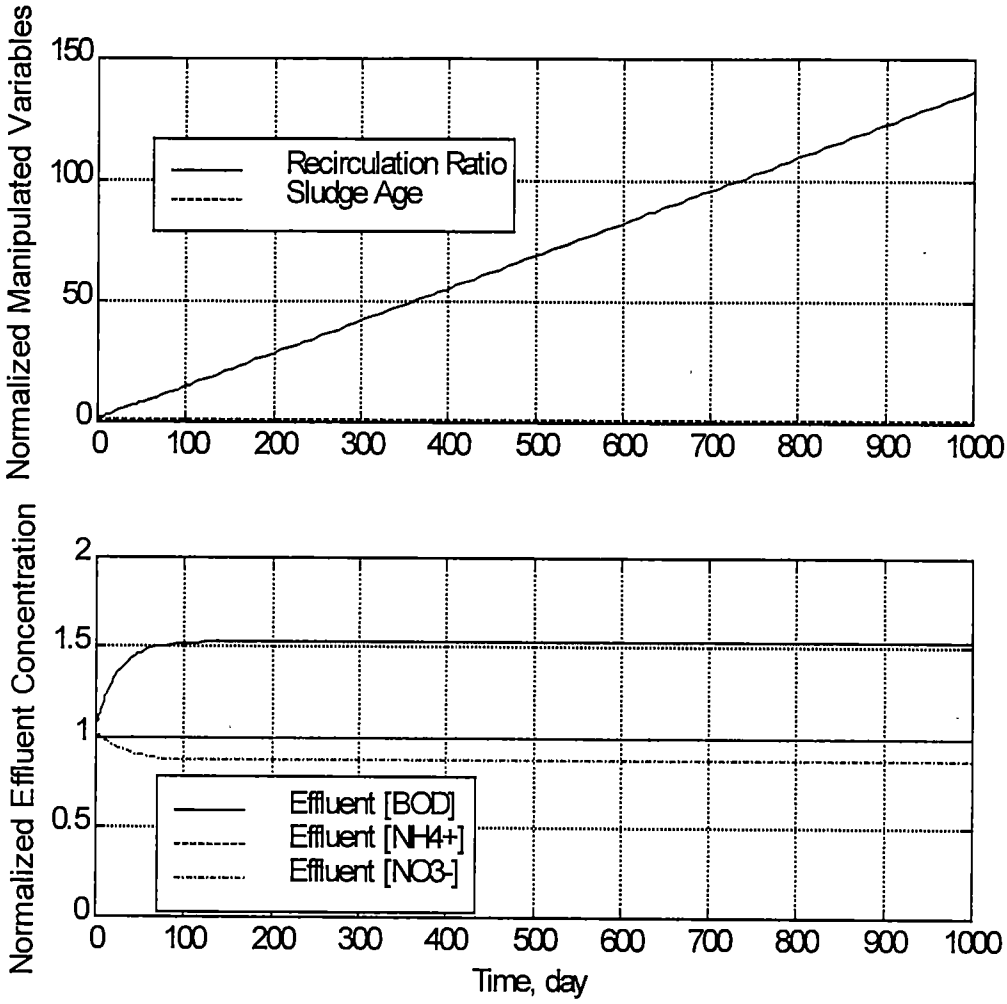

Figure 2-10. PI Based Regulator Control for a –50% Change in the $\mu_{m,H}$ and +50% Change in the $K_{s,[COD]}$
Controlled Variables: Effluent [BOD] and $[NH_4^+]$

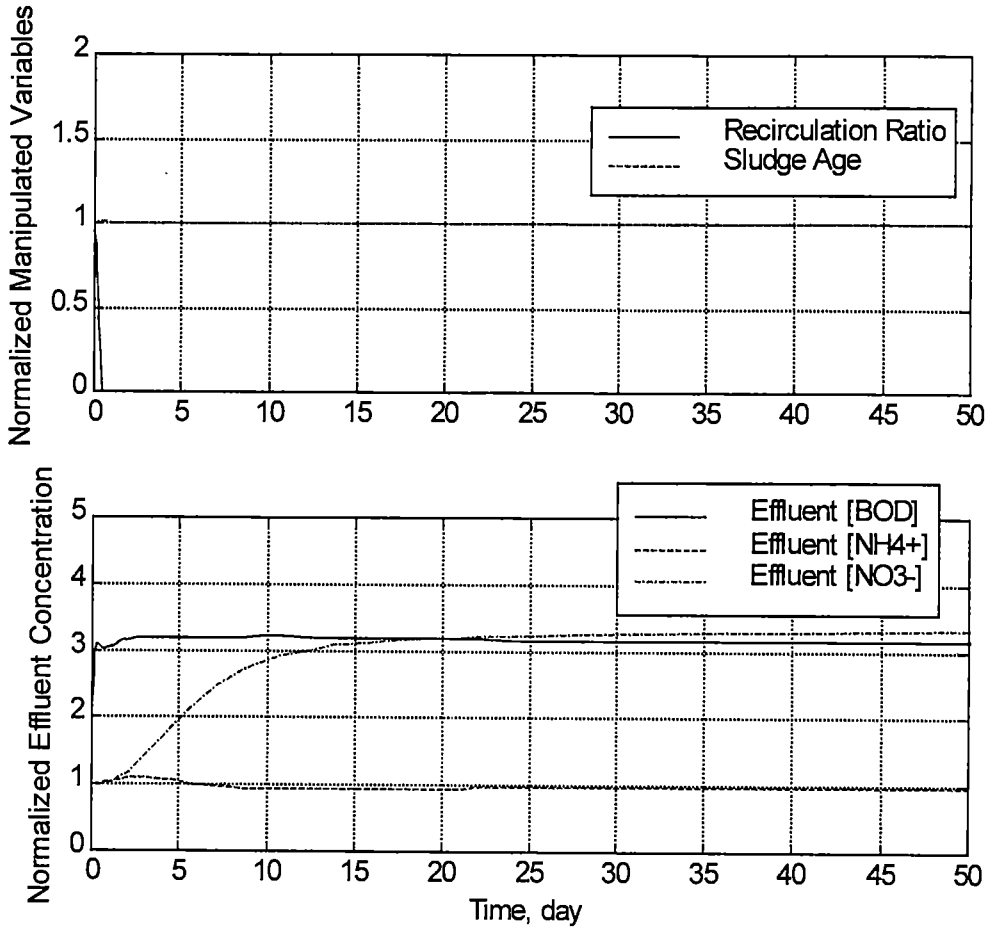

Figure 2-11. IMC Based Regulator Control for a –50% Change in the $\mu_{m,H}$ and +50% Change in the $K_{s,COD}$
Controlled Variables: Effluent [BOD] and [NH_4^+]

tolerance, respectively. Setpoint tracking is the ability of the process output to track the specified setpoint. Disturbance rejection is the ability of a controller to minimize the effect of perturbation on the process output. Plant-model mismatch is the difference in the dynamics that describes the actual plant and that that describes the model which was used for the controller design. Two primary goals of controller design are long-term stability and output performance.

Figures 2-6 and 2-7 are subject to a –5% setpoint change in the effluent [BOD]. As all the other operating conditions are same in the two figures, their difference is that, Figure 2-6 is the response curve when a PI controller is incorporated while Figure 2-7 shows the results when an IMC controller is incorporated. Apparently, for the former case, the system is still not stable at 1000 days. The recirculation ratio keeps increasing and the effluent [NO_3^-] keeps decreasing. In the contrary, for the IMC case, within 100 days, system settles down completely. Figures 2-8 and 2-9 show the result when a –15% disturbance in the influent [NH_4^+] is introduced. Again, the system with PI controller can' t achieve stability even after 1000 days. System with IMC, after a short-term transient response, settles down at around 100 days. Figures 2-10 and 2-11 are subject to a plant-model mismatch on biological constants, $\mu_{m,\ H}$ and $K_{s,\ COD}$. The results show again that PI fails in long-term stability while IMC yields stability within a reasonable time frame.

Based on the long-term stability requirement of the system, IMC has obvious advantages over PI. Therefore, IMC will be selected as the control algorithm for this study.

Chapter 3

Study Approaches

The objective of this study is to develop a multivariate statistical monitoring and diagnostic framework, for a multi-stage wastewater bio-treatment plant by using the principal component approach. Monitoring and diagnostic capability can provide an early warning for abnormal operational trend and to suggest process variables responsible for the observed deviations.

This study is carried out using the bio-wastewater treatment plant simulator developed by Grove (1995) in the Matlab™ platform. First, a controller scheme has to be chosen in order to provide feedback control capability, to correct for immediate and direct process deviation. Comparison of control design strategy between traditional PID controller and Internal Model Controller (IMC) was carried out by Schmidt (1996) and Fu (1998). They showed that IMC is superior to PID in the key aspect of maintaining stability, in the face of disturbance and plant-model mismatch. Therefore, IMC is chosen in this study as the default controller in the 2x2 feedback loops. The pairing of input to output variables were chosen based on the μ-interaction measure (Grosdidier and Morari, 1986) as well as on the system's steady state gains (Grosdidier, Morari and Holt, 1985). Two single-loop feedback controllers were designed.

In Schmidt's study, three cases, case I, II and III, with different controlled variables were chosen for study. In case I, effluent [BOD] and [NH_4^+] are the controlled variables. They are paired with recirculation ratio and sludge age,

respectively as the manipulated variables. In case II, effluent [BOD] and [NO_3^-] are under control whereas [NH_4^+] and [NO_3^-] are controlled in case III. In this study, case I with effluent [BOD] and [NH_4^+] as the controlled variables is chosen to carry out the MSPC procedure development. The motivation for this choice is explained further below.

In industrial wastewater treatment process, the major forms of nitrogen are: organic nitrogen, ammonia nitrogen, nitrite nitrogen and nitrate nitrogen. Among them, only the first two forms are significant for wastewater nitrogenous loading considerations, except for a few specific industrial discharges.

The primary impact of ammonia nitrogen in wastewater is the impairment of the dissolved oxygen balance in the receiving waters. The term NOD is created to refer to Nitrogenous Oxygen Demand. In the presence of nitrifying bacteria, for instance, in the aerobic reactor of the wastewater treatment system under this study, ammonia is readily converted into nitrate, and in the process consumes 4.3 gO_2/gN-NH_3. If the ammonia concentration is too high in the waterway, it will overload the oxygen balance, therefore upsetting the ecological system. Another significant impact of ammonia is that it is toxic to aquatic life, especially the free ammonia NH_3 form. Free ammonia NH_3 and ionized ammonia NH_4^+ are inter-convertible in wastewater. Ammonia nitrogen is also a major nutrient that will stimulate aquatic plant growth. Based on these considerations, the effluent standard guideline for nitrogen element was implemented together with an NH_4^+ concentration restriction

for many industrial bio-wastewater plants all over the world (Orhon & Artan, 1994).

Carbonaceous material removal is one of the major objectives of wastewater treatment. It is no doubt that effluent [BOD] is a significant quality variable for such plants. Besides [BOD], due to the importance of effluent concentration of ammonia to the receiving waterway, effluent [NH_4^+] is also chosen for monitoring the efficiency of the waste treatment plant. Case I is the case whose controlled variables are effluent [BOD] and [NH_4^+]. Therefore, case I is the case under study in this research.

The goal of a process monitoring system is to give warning when the operation starts to exhibit a trend of becoming 'out of control'. The reference domain, indicating 'normal operation', is established using historical data gathered when the process operation is deemed in a state of control under a variety of operating conditions, that will not be regarded as 'abnormal' if encountered again. This would be considered as the base case against which future observations will be compared. A series of PCA is to be carried out for data gathered to be included in the reference domain, and a desired multi-dimensional acceptable region defining the normal performance is to be constructed using multivariate statistical method. If future process behavior lies inside this region, then process with good output product quality will most probably result. Operation departing from this region represents possible abnormal operation. Actions would be recommended to be taken to drive the process back to the 'normal' region. According to this logic,

several perturbed cases with deviations larger than those used to develop the base case model, or not encountered by the base model operation will be simulated as well as analyzed and variables that contribute to the deviation will be attempted to be identified.

Several steps are involved in the research strategy to accomplish the study objectives. These steps are shown in the flow chart in Figure 3-1.

3.1 Generating Base Case Data Profile

Many effluent and intermediate process variables exist in this bio-wastewater treatment plant. Monitored variables are chosen from them so as to reflect their ready availability on either on-line or off-line basis. Each column of the data matrix, X_o, represents one monitored variable. In this study, the chosen process measurements (variables) (assumed to be available on a routine basis) consist of the following variables: the outlet concentrations of heterotrophic biomass, autotrophic biomass, BOD, NH_4^+ and NO_3^- from the anoxic reactor; the effluent concentrations of heterotrophic biomass, autotrophic biomass, BOD, NH_4^+ and NO_3^- from the clarifier; as well as the manipulated variables, the recirculation ratio and sludge age. They form the twelve columns of X_o, x1 to x12 in that order. The effluent concentrations of the various compounds from the clarifier are the key indicators of a wastewater treatment's efficiency. They are to meet some established specific discharge standard. Especially BOD and the nitrogen compound, they need to strictly meet the environmental legislation guidelines. These variables have to be monitored and logged constantly. A second class of

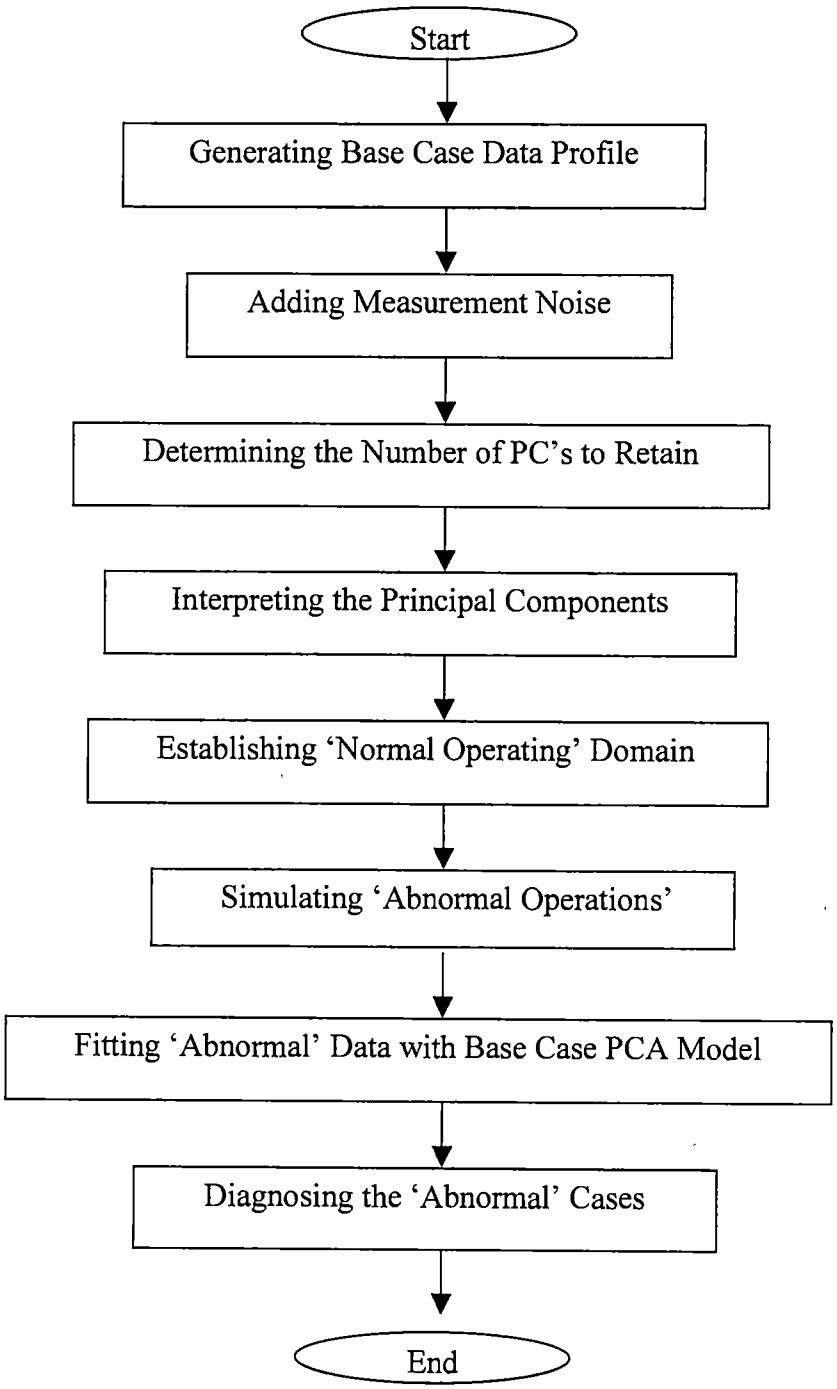

Figure 3-1. Flow Chart of the thesis work

variables that will also be monitored in this study consists of the intermediate variables. They are the effluent concentrations from the anoxic reactor. As mentioned in the previous chapters, one of the advantages of MSPC is that it takes into account all of the variables of interest from the process for the analysis, and not just the system outcomes. In this manner, the inter-relationship among the variables can be elucidated, and possible root causes for observed deviations can be identified, by observing which set of variables exhibit the deviant behavior. Therefore, if there is an abnormal shift occurring in some of the intermediate and non-monitored variables, it will manifest itself in the monitored process variables and actions can then be taken to remedy it if the cause variables are identifiable. The third group of the process variables included in the base case data matrix X_o includes the process inputs, or the manipulated variables, which respond to disturbance to the process and internal model change, so as to maintain the output variables at the desired setpoint. Thus, the reference database has a wide coverage of the plant information from variables representing the output, the input and the intermediate processes. Table 3-1 is a list of the twelve process variables chosen to be monitored.

Measurements represented in X_o are generated using a central composite design around a nominal operating point in the process variables x1 to x12.

The measured process variables in the X_o represent the steady-state process responses to changes in a few chosen operating conditions. In this study, these chosen operating conditions are: 1) disturbance: changes in the influent ammonia

Table 3-1. Process Variables Incorporated in Reference Database Generation

Variable Name	Component Name	Symbol
x1	Heterotrophic biomass (an)	$X_{B,H}$ (Anoxic Reactor Effluent)
x2	Autotrophic biomass (an)	$X_{B,A}$ (Anoxic Reactor Effluent)
x3	Readily biodegradable substrate (an)	S_S (Anoxic Reactor Effluent)
x4	NH_4^+ and NH_3 nitrogen (an)	S_{NH} (Anoxic Reactor Effluent)
x5	Nitrate and nitrite nitrogen (an)	S_{NO} (Anoxic Reactor Effluent)
x6	Heterotrophic biomass (c)	$X_{B,H}$ (Clarifier Effluent)
x7	Autotrophic biomass (c)	$X_{B,A}$ (Clarifier Effluent)
x8	Readily biodegradable substrate (c)	S_S (Clarifier Effluent)
x9	NH_4^+ and NH_3 nitrogen (c)	S_{NH} (Clarifier Effluent)
x10	Nitrate and nitrite nitrogen (c)	S_{NO} (Clarifier Effluent)
x11	Recirculation Ratio	Recirculation Ratio
x12	Sludge Age	Sludge Age

an: anoxic reactor

c: clarifier

concentration; changes in the influent nitrate concentration; 2) plant/model mismatches (Biological parameters being different from their values at the nominal operating point.): the maximum growth rate of the heterotrophs, $\mu_{m,H}$ and the half-saturation constant of the heterotrophic consumption of COD, $K_{s,[COD]}$ in the aerobic reactor. Table 3-2 provides detailed information about these operating condition changes.

The database representing the nominal case was generated by simulation based on the factorial design approach (Montgomery, 1994). In each complete trial or replicate of the simulation, effect of operating under all possible combinations of the seven levels from 79% to 121% (85% to 115% for influent ammonia concentration), of each of the factors are investigated. The seven levels ranging from 79% to 121% are evenly distributed. They are set at 79%, 86%, 93%, 100%, 107%, 114% and 121%, respectively (similar division approach for the 85% to 115% case). Therefore, there are 7^4, or 2401 sets of simulation observations to be included in the reference database. They form the 2401 rows of the X_o matrix. Each row represents one sample in the twelve variables of interest, obtained from operating under one of the 2401 sets of operation conditions.

3.2 Adding Measurement Noise

There are basically two types of noises, input noise and measurement noise. Input noise is added at the input end of the process and the noise goes through the dynamics of the process. Measurement noise occurs at the output end of the process. For measurement noise, it might be caused by some problems of the

Table 3-2. Variations of the Operating Conditions in the Reference Database Generation

Scenario Number	Conditions to vary	Symbol	Nominal Value	Amount of variation
1	Influent Nitrate Concentration	[NOx]	1000 mg $N\text{-}NO_3^-$/liter	79% -121% ×1000
2	Influent Ammonia Concentration	$[NH_4]$	300 mg $N\text{-}NH_4^+$/liter	85% -115% ×300 (*)
3	Maximum growth rate, heterotrophs	$\mu_{max,\,H}$	4 day^{-1}	79% -121% ×4
4	Half-saturation constant, heterotrophic consumption of [COD]	$K_{s,\,[COD]}$	10 mg [COD]/liter	79% -121% ×10

* Larger amount of change in the influent ammonia concentration caused numerical integration error in the simulation. Therefore, instead of 79% - 121% changes in the inlet ammonia, 85% - 115% was chosen.

laboratory instrumental analysis. In this study, only measurement noise is added to the raw values contained in the original data set X_o, and X_{o-n} denotes the noisy data set.

An amount of ±2.5% of the nominal level Gaussian random noise has been added to each column of the values in the simulated base case data matrix respectively to form the noisy database, X_{o-n}. With a relatively big data set of dimension 2401x12, noises of both positive and negative magnitudes are present on a more or less statistically equal basis. The ±2.5% level of noise is calculated based on the historically nominal steady-state values of each variable.

In practice, if the historical operating documents are available covering a wide range of operation conditions, the reference database can be obtained by including all the accessible data when the process was operated in a 'normal' state under statistical control. Therefore, it is very important that operating condition that should not be identified as 'abnormal' being present as part of the normal operation profile during the construction and data gathering phase of the base case.

3.3 The Methodology of Principal Component Analysis (PCA)

3.3.1 Background Concepts of PCA

3.3.1.1 Covariance Matrix

PCA is a method for modeling a set of data collected in a matrix X, in this study, the matrix, X_{o-n}. Data matrix X is made up with n column vectors x1, x2, x3, ..., xn, which characterize steady state process variables collected under different sets of operating conditions. The rows of X represent different observations. The

dimension of X depends on how many samples and how many process variables are to be monitored. The number of measured variables is chosen such that they fully represent the 'state' of the process operation. If the process is characterized by n variables and m samples are collected, X will be an mxn matrix, usually with m>>n. The data matrix is usually column mean centered to zero mean and scaled to unit variance, such that its covariance matrix is the same as its correlation matrix. Covariance matrix of mean-centered and scaled X with m samples and n variables can be formulated as:

$$\text{cov}\,ariance(X) = correlation(X) = X^T X \tag{1}$$

where: X = mean-centered and scaled matrix, mxn

X^T= transpose of the X matrix, nxm

3.3.1.2 Singular Value Decomposition (SVD)

PCA finds the combination of the process variables that represents the major variation in the data set. Mathematically, PCA is carried out by using the Singular Value Decomposition (SVD) (Strang, 1976) of the data matrix X, representing the process. An X matrix of dimension mxn, with m>n (more rows than columns) is decomposed by SVD into:

$$X = U\Sigma P^T \tag{2}$$

where, X = mean-centered and scaled data matrix, mxn

U = a matrix with orthonormal columns, mxn (the columns are referred to as the left singular vectors.)

Σ = diagonal matrix with positive and descending singular values, σ's, nxn

P = a matrix with orthonormal columns, nxn (the columns are referred to as the right singular vectors.)

Σ is a diagonal matrix containing the positive singular values, σ's, arranged in a descending order. The ratio of each of the σ's squared to the summation of all the σ's squared is an indication of how much variation each principal component represents compared with the overall process variation. More detail will be presented in Section 3.4.2.

The column vectors of U and P are the singular vectors. Singular vectors in U are called the left singular vectors and singular vectors in P are called the right singular vectors. Singular vectors are orthogonal to each other and with unit length. PCA provides a projection of the original data matrix X onto a reduced-dimensional subspace defined by the span of a chosen first few (k) right singular vectors of the data matrix. This set of chosen singular vectors from matrix P are called the PCA loadings. The PCA loadings are orthogonal to each other. Therefore, PCA mapping reduces the original matrix X into a lower-dimensional subspace of dimension, say, k, spanned by a set of known, orthogonal unit vectors, the first k right singular vectors. These singular vectors are weighted linear combinations of the original process variables, and the space they span captures the most dominant variations exhibited by the X matrix. These singular vectors are also referred to as the Principal Components (PC's) of a PCA model. The set of k specified principle components constitutes the process PCA model. All future process measurements will be 'fitted' by this model (i.e. be projected onto the

subspace spanned by these k principal axes). The residual will be assessed as to be within or out of the base case acceptable bounds.

3.3.1.3 Loadings and Scores of the PCA Model

The principal components can be identified by the resulting matrices of SVD of X, the U, Σ and P. The first principal component, or the first loadings, is given by the first column of the matrix P, p1. It lies in the direction describing the largest amount of variation of the process data of X. The first scores vector is obtained by: t1=X*p1, which has m elements. These m elements are the projections of the original m data points, or the m rows of X, onto the vector p1. The second PC is given by the second column vector of P, p2. It lies in the direction describing the second largest amount of variability in X and is orthogonal to p1. The elements of the second scores vector, t2=X*p2, represent the projections of the m sample objects onto p2, respectively. This procedure is repeated n times until all the scores vectors are calculated. The sum of the squares of the lengths of the projections of all the sample points onto the ith principal component, is equal to the square of the ith singular value. Thus the ith singular value indicates the relative amount of variability of the data points along the ith principal component.

Since the t_i and p_i pairs are arranged in the order according to the associated descending singular values of the data matrix, the first few t_i and p_i represent the directions of the biggest amount of the systematic variation exhibited by X. The first pair captures the largest amount of variability among all the pairs in the decomposition form. The second pair captures the second largest amount of

variation, and so on for the subsequent pairs. Therefore, among these n PC's, only the first k PC's will be retained. The rest are considered to represent noise and are lumped into an error matrix E. Decomposition of X ends up with the following formation:

$$X = T_k P_k^T + E = \sum_{i=1}^{k} t_i p_i^T + E \tag{3}$$

where T_k = scores matrix with the first k columns retained, mxk

P_k = loadings matrix with the first k columns retained, nxk

E = residual matrix, mxn

t_i = i^{th} column of scores matrix, mx1

p_i = i^{th} column of loadings matrix, nx1

E represents the residual matrix after k PC's are extracted to approximate the original data set. The product of the data measurements with the loadings are the scores. The scores of all samples onto the ith PC, is given by:

$$t_i = X * p_i \tag{4}$$

where: t_i = scores onto the ith principal component, mx1

p_i = the ith loadings vector of the PCA model, nx1

Loadings vectors as well as loadings plots give the information of the relative contributions of the original process variables to the specific PC's, thereby showing the correlation pattern among the process variables. This information will be very valuable in diagnosing the possible cause of malfunctions, as to what process variables are associated with the detected fault. The T_k matrix as well as the

scores plots represent the clustering pattern of the samples. Typically, just a few PC's are deemed enough to represent the original data information, due to the usually high degree of correlation among the process variables.

Thus, PCA provides an approximation of a data matrix, X, in terms of the product of two simpler matrices T_k and P_k, both with orthonormal columns. T_k captures the essential data pattern for the observations in X; P_k captures the essential pattern for inter-variable relationships. Plotting the column vectors of T_k and P_k against its index gives geometrical interpretation of the data matrix X; therefore the process (Refer to Section 3.11).

3.3.2 A Simplified Illustration of PCA

A simplified two-dimensional example is shown in Figure 3-2 to illustrate the interpretation of PCA. In this example, two original process variables are measured. Therefore, the data matrix X has two columns. It has been mean-centered, scaled and PCA has been carried out for it.

It is observed that these two variables are linearly correlated. Increasing one variable causes the increasing of the other, in general. The first right singular vector p1 (PC1) of the data matrix, indicates the direction in which the data has the greatest variability. The second right singular vector p2 (PC2), is orthogonal to p1 and represents the direction along which it is reasonable to assume that the data exhibit the next greatest variability. In this example, the p2 represents noise and inaccuracy in the measurements. Projections along the p2 direction should not be retained. By means of this, the original two-dimensional variable space is projected

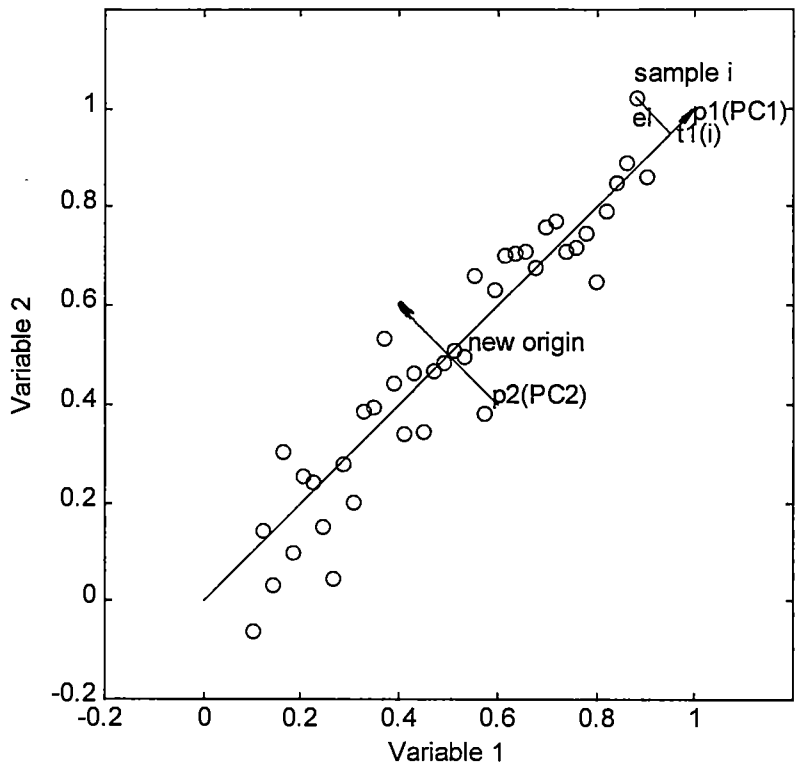

Figure 3-2. Graphical Interpretation of PCA Method

into a one-dimensional subspace spanned by p1, the first principal component axis. Now let' s consider the ith observation labeled as 'sample i' in Figure 3-2. The distance between its projection point onto p1 and the new origin is referred to as the scores of sample i along PC1, the ith element in the first scores vector, t1. The vector between sample point i and its projection onto vector p1 is the residual vector, e_i for the ith sample.

This example shows the application of PCA in reducing a two-dimensional data set to one-dimensional, without missing significant system variation information. What PCA ignores is considered to be the system noise. The principal component axes represent a new coordinate system onto which the data points are projected. And this reduced-space is spanned by the first k PC's, if k PC's are retained. The elements of the ith scores vector represent the length of the projections of all the sample points onto the ith principal component axis.

3.4 Determining the Number of PC's to Retain

3.4.1 Pretreatment

Before PCA is carried out, the noise-added reference matrix needs to be pretreated. The major steps for the pretreatment are mean-centering and scaling.

Centering to zero mean is carried out by subtracting the mean of each column of X from the corresponding elements of that column, such that the new mean of each column is zero. Scaling to unit variance is carried out by dividing each mean-centered column by the variance of the corresponding column, such that the new variance of each column is one. The usual purpose of scaling is to

standardize the measurement units between variables and to give equal weight to each variable's span in forming the new PC's.

The scaling is significant for the reason that PCA is a least-squares method, making variables with larger variance resulting in larger contributions to the loadings in the PCA model, an artifact of the magnitude of the numbers themselves. In order to avoid this, it is necessary to normalize the data matrix in some way so as to do away with the differences in scales. Variance scaling gives each variable the same influence on the model. Without scaling, problems similar to the following example will be met during PCA modeling. In a chemical process, one process variable can be pressure with the unit of Pascal. A magnitude in the order of 10^5 is normal for this. The other process variable can be the concentration of a very diluted solution, which can be a number as small as one in the order of 10^{-2}. In this case, without scaling, the latter variable is very likely to be neglected in the building of a process model since its absolute value is too little compared with that of the former variable. Therefore, its variance would seem insignificant in the process data. Systematic information may be lost due to the non-scaled data matrix representation. Therefore, the mean centered matrix needs to be normalized to, say, unity variance. After this normalization, the data matrix is now ready for singular value decomposition and subsequent PCA.

3.4.2 Determining How Many PC's to retain

The first and most significant step of PCA modeling is to decide how many Principal Components (PC's) to retain. In their studies, many investigators used

cross-validation method (Efron, 1983) to make this decision. In this study, a simpler and more intuitive method, via the scree plot, is applied.

Scree plot helps one to decide how many PC's to keep. It can be obtained by SVD to the mean-centered and scaled data set. As mentioned in Section 3.3.1.2, the data matrix X is decomposed into three simpler and more informative matrix, the U, Σ and P. The diagonal elements in Σ are the singular values, σ's. The percentage of process variation captured by each PC is computed by:

$$\% \text{ variation captured by the i}^{\text{th}} \text{ PC} = \frac{\sigma_i^2}{\sum_{j=1}^{n} \sigma_j^2} \times 100 \qquad (5)$$

where σ = singular value obtained by SVD of the data matrix X

The contribution of each PC to the overall variation is determined by the ratio of the square of each singular value to the sum of squares of all the singular values. The faster the rate of the magnitude of the singular values' decreases, the lesser number of PC's needs to be retained, and the more powerful the PCA approach is in the reduction of the dimensionality of the original data set. It implies that the original data is much more heavily correlated than otherwise.

3.5 Establishing 'Normal Operation' Domain: Reference Scores and Squared Predictive Error (SPE) Charts

The use of PCA monitoring charts is similar to that for Shewhart and EMWA control charts in the Univariate Statistical Process Control (USPC) (Shewhart, 1931). In USPC, sample data are collected and used to construct the

control chart, if a new sample value falls within the control limits and does not exhibit any systematic pattern, the process is deemed in control at the level indicated by the USPC control charts. A PCA model as well as MSPC control charts are derived from the similar philosophy, using the historical data that represent the normal operation profile. Under 'normal' operation, the process measurements usually cluster in a well-defined region of the 2-dimensional scores space spanned by t1-t2/t2-t3 or t_i-t_j, or the 3-dimensional scores space spanned by t_i-t_j-t_l, where i, j, l < k (k is the number of PC's retained), with correspondingly small values of Squared Prediction Error (SPE). This well-defined region is established as the 'normal operation' domain. Future process observations are then projected onto this 'normal operation' domain, and the associated SPE's are assessed. The two most popular graphical depictions of the reference model are the monitoring charts of two/three dimensional plots of the scores, and the SPE plot. These two types of Statistical Process Control charts are used in this study to monitor the process and to reflect potential deviations.

3.5.1 the Scores Chart

Perhaps the most attractive feature of PCA is that it converts a data matrix to a few informative plots, which lend themselves to some nice geometric interpretations. For instance, by plotting the columns t_i in the scores matrix T_k against each other, one obtains a picture of the objects and their configuration in k-dimensional scores space spanned by the k PC's retained. The first few component plots, t1-t2, t1-t3 or t1-t2-t3, *etc.*, display the dominant patterns in X.

Two/three dimensional scores plot is obtained by plotting the projections of each sample onto the first two/three PC's. The columns of the scores plot are calculated by equation (4) mentioned in the previous section. The coordinate of each point in this type of scores plot is given by the first few elements of each row of XP_k.

Scores of the ith sample = X_iP_k (6)

Where Xi = the ith row of the X matrix, 1xn

P_k = P matrix with the first k column retained, nxk

The result of equation (6) is a vector with k elements. It gives the coordinates of sample i in the k-dimensional PC space. For instance, if the scores plot of t1-t2-t3 is to be created, the first three elements of the result of equation (6) are used as the coordinates for the ith sample point in the three-dimensional subspace spanned by PC1, PC2 and PC3.

3.5.2 the SPE Chart

SPE plot is obtained by the following approach. Each pretreated sample point is projected onto the subspace spanned by the k PC's to arrive at the representative scores. The error vector between the pretreated sample point and its projection onto the k-dimensional subspace is referred to as the residual vector for that sample point. The residual matrix E is formulated as:

$$E = X(I - P_k P_k^T) \quad (7)$$

where: E = error matrix defined in equation (3), mxn

I = identity matrix, nxn

P_k = the matrix of the first k loadings vectors retained in the PCA model, nxk

P_k^T = the transpose of P_k, kxn

$P_kP_k^T$ = projection matrix onto the k-dimensional subspace, nxn

Where the ith row of E represents the residual vector for the ith sample.

A vivid graphical description of the errors is shown in Figure 3-3 (Nomikos, 1995). In this figure, the shaded plane represents the k-dimensional PCA subspace. Solid balls represent the original observations. Stars on the shaded plane represent the projection of observations onto the k-dimensional subspace. Distance between the ball and the corresponding star is the magnitude of the residual for each sample point.

The sum of squares of the elements in each sample row of the residual matrix forms the corresponding entry in the SPE vector. It represents the degree of misfit of that sample by the base PCA model. It can be expressed as:

$$SPE_i = \sum_{j=1}^{k}(x_{ij} - x_{ij,projection})^2 = e_i e_i^T = x_i(I - P_k P_k^T)x_i^T \tag{8}$$

where: SPE_i = SPE of the ith sample, 1x1

x_{ij} = element on the ith row and j^{th} column of the mean-centered, scaled matrix X, 1x1

$x_{ij,\,projection}$ = element on the ith row and j^{th} column of the projected X matrix, 1x1

e_i = i^{th} row of the E matrix,1xn

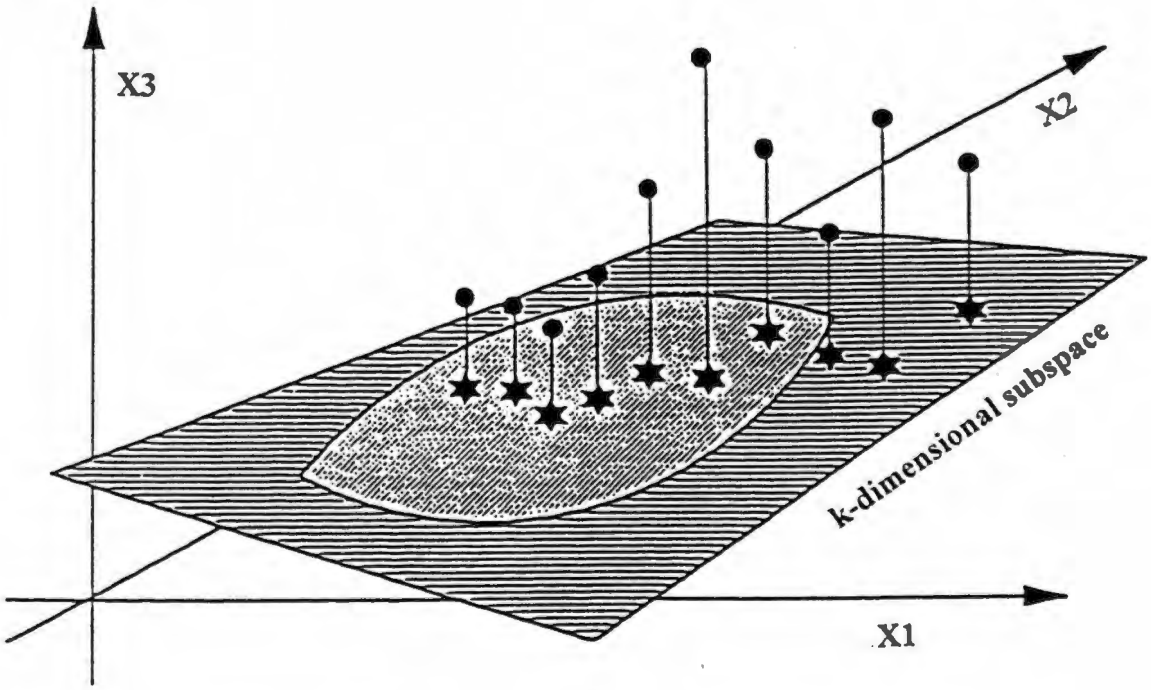

Figure 3-3. Graphical Representation of Projection of Samples onto Reduced Space of PCA (Nomikos, 1995)

x_i = i^{th} row of the X matrix, 1xn

SPE vs. PC1-PC2 plot is one of the most informative plots in monitoring the process performance. It contains both residual and scores information. Besides detecting and giving early warning of abnormal deviations in the process, this plot is also able to provide a handle to diagnose the type of process behavior that may have caused the present system's non-conforming behavior.

There are two categories of abnormalities that the SPE versus PC1-PC2 plot can show: 1) Process abnormality caused by a larger than normal shift in one or more of the process inputs, but the model itself remains unchanged. It means that, the relationship between the process variables and the product quality is not changed, but the associated values are all larger. In this case, a translation of the projected points in the scores plane will occur, because the new points are still normalized by the old variance for that column. But the SPE will remain inside the acceptable domain, because the PCA model should still fit the new points relatively well. For this type of process deviation, t1-t2-t3 should give a better detection of process behavior. 2) Process abnormality is caused by the participation of a new event which is not incorporated into the reference model development or the existence of plant/model mismatch unencountered previously in the base model development. In this case, the relationship among the process input and product variables has changed. Therefore, the associated SPE after fitting with the PCA model will increase, because the 'normal' PCA model does not fit or describe the new process data as well as before. This may or may not impact on the scores plot.

SPE plot is the best choice for this kind of abnormality detection. By means of identifying these two categories of abnormality, SPE versus PC1 and 2 plot classifies the two major directions in which deviation occurs. Root causes responsible for these abnormalities can sometimes be traced and identified.

3.6 Monitoring Transient Responses

Transient response plot is a display of the state of the process as a function of time under a certain operating condition. The location of the observation on the t-scores and the SPE charts exhibits the whole intermediate projection trajectory of such a sample onto the t-scores and the SPE reference domain, from the original steady state, being adjusted by the system to a new steady state. The final location of the observation in the transient response chart is determinant for assessing this specific operation, either in-control or out-of-control. Any transient response curve in this study starts at the origin, because the simulation of each case begins at the original nominal steady state, condition being used to carry out the mean-centering and scaling procedures.

First, the transient response simulation is carried out for a perturbed case included in the base case generation. That is, moderate changes in the influent [NO_3^-] and [NH_4^+]. Since this scenario is deemed as a normal operation when the reference database is generated, the steady state value of this case should be within the 'normal operation' domain. The perturbation is entered at t=10 days. System may exhibit large, even abnormal transient deviations soon after that time point. But in this study, only the final steady state value is of interest. Therefore one

should examine the behavior of process variables within the time window spanning at least the duration of the process time constant before an assessment of in or out-of-control is made.

Transient response test is also carried out to all the abnormal cases simulated in this study. For instance, a perturbed case with a new event that is not considered in the base case creation, is, a larger influent flow rate. If this new event makes the plant model to be mismatched from the real process, then out-of-bound operation will be expected in the SPE plot. If the new event does not result in plant/model mismatch, then it will not result in an increased SPE. And it may or may not exhibit abnormal deviation in the scores chart. Since the influent flow rate only appears in the forcing function term in the mass balance of all the twelve monitored variables, an increase in the flow rate will not result in a plant-model mismatch. Therefore, an abnormal deviation in SPE plot is not expected.

3.7 Simulating 'Abnormal Operations'

To evaluate the capability of such a series of multivariate statistical process control charts to detect abnormal operating deviations, several cases of faults would be simulated.

As explained previously, abnormalities can enter the system through two different ways. The first type of abnormalities is generated by having a larger than normal change in one or more of the process input variables. In this case, the essential relationship among the process variables has not been altered. Therefore, this type of the abnormality is expected to cause a possible shift only in the t_1-t_2 -t_3

scores trajectory plot. The second type of abnormalities is the introduction of a new perturbation to the system that was not encountered in the generation of the reference data set. It may change the t-scores plot, if it results in changing the magnitude of the monitored variables. It may or may not influence the SPE plot, depending on whether this perturbation occurs in the forcing function terms or the state variable coefficient terms in the mass balance kinetic equations. The third and fourth type of abnormalities result from the presence of additional plant/model mismatches and events of different nature not included in those used in the construction of the reference data, respectively. These classes of abnormality will invariably increase the associated SPE values and cause the migration of the SPE trajectory from within the acceptable region toward that of without. For these cases, the reference PCA model no longer 'fits' the new data as well as before, because some model parameters would most probably have changed. Therefore, the associated SPE would increase.

In this study, four 'abnormal' cases representing the above four types of abnormality are simulated and diagnosed.

3.8 Modeling 'Abnormal Operations' with Base Case Profile

Base case data have been generated. Cases of several abnormal operations have been simulated. Projection of the new data onto the reference PCA axes will then be carried out. They are to be projected onto both the two/three dimensional scores chart and the SPE chart. If the new operating points are located away from the bulk of the acceptable region in either chart, it would indicate that an abnormal

condition may exist and the computer can then issue a warning to the operating personnel to take actions. Further analysis of these drifts in the monitoring charts may help in finding out the root cause of the abnormal deviation, by identifying the combination of the process variables responsible for the misfit.

3.9 Diagnosing 'Abnormal Operations' Using Contribution Plots

When abnormality is detected, causes of the deviation need to be investigated. Process variables responsible for large t-scores and SPE can be found by plotting the contribution of each measurement variable to the deviation. This kind of plot is called contribution plot. Although contribution plot alone may not provide complete diagnostic information the operating personnel need in order to adjust the operation of the process, it will clearly identify the group of measurement variables responsible the most for the detected deviation (Nomikos, 1995).

The percentage of contribution of the ith process variables to the rth t-scores is given by:

$$\%\ contribution\ of\ the\ i^{th}\ variable = \frac{100}{\hat{t}_r} x_{abnormal}(i) p_r(i) \qquad (9)$$

where $x_{abnormal}$ = a new abnormal observation, 1xn row vector

$x_{abnormal}(i)$ = the ith element in the $x_{abnormal}$ vector, 1x1

p_r = the rth principal component, nx1

$p_r(i)$ = the ith element of the rth principal component, 1x1

$\hat{t}_r$ = $x_{abnormal} * p_r$, 1x1

The percentage of the contribution of the ith process variables to this SPE is given by:

$$\%\ contribution\ of\ the\ i^{th}\ variable\ =\ \frac{100}{\hat{Q}} e^2(i) \qquad (10)$$

where $e = x_{abnormal}(I-P_kP_k^T)$ according to equation (5), I is a nxn identity matrix, 1xn

e(i) = the ith element in the error vector

$\hat{Q}$ = ee^T, 1x1

By plotting each of the two '% contribution' of all the variables versus variable number, one obtains an approach to trace back the possible root causes of the current unacceptable deviation. Examples of making use of the contribution plots to diagnose abnormality will be shown in the next chapter.

3.10 A Literature Example for Fault-Detection by MSPC Monitoring Chart

A simulation study presented by Nomikos and MacGregor (1995) of monitoring the process mentioned in Chapter two, a semi-batch emulsion polymerization of Styrene-Butadiene in making a latex rubber (SBR), results in the following monitoring charts as seen in Figures 3-4 and 3-5.

In these figures, the t-scores and SPE charts are presented with their 95% and 99% control limits. These limits were established from analyzing the historical data set when the variations were considered 'normal'.

The t-scores charts are plotted using the first two PC's in both cases. Nominal t-scores operation region is represented by the area inside their 95% and 99% control limits, respectively. SPE charts are plotted over time. Acceptable

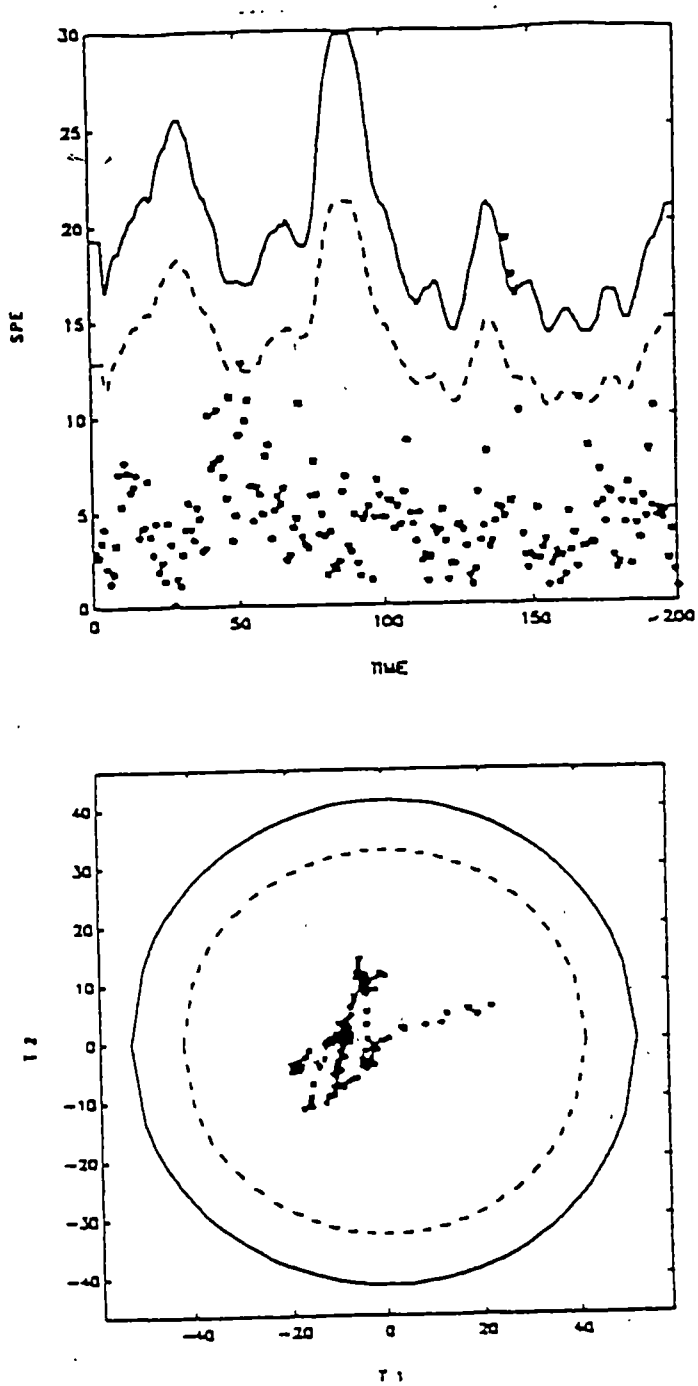

Figure 3-4. Monitoring Charts with Their 95% and 99% Control Limits for a New Normal SBR Batch. (-: 99% Control Limits; --: 95% Control Limits; ...: New SBR Batch) (Nomikos, 1995)

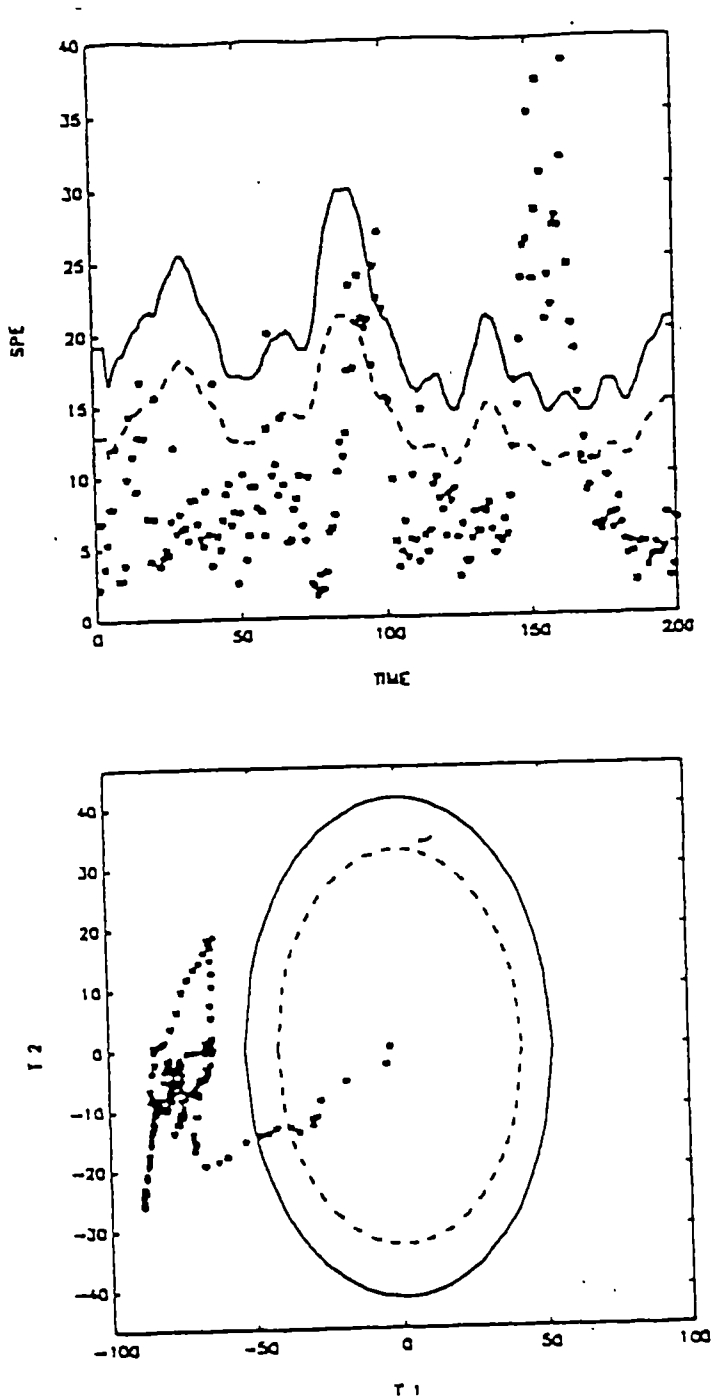

Figure 3-5. Monitoring Charts with Their 95% and 99% Control Limits for a New Abnormal SBR Batch (-: 99% Control Limits; --: 95% Control Limits; ...: New SBR Batch) (Nomikos, 1995)

operation region for SPE is represented by the area within their 95% and 99% control limits. The interpretation of the monitoring charts is straightforward.

Figure 3-4 shows the projection of a new SBR batch onto the reference region. The projected points are all well within the control limits for both the SPE and the t-scores. This indicates that the new batch is considered a 'normal' batch. While in Figure 3-5, the situation is different. Several sample values exceed the 99% SPE control limit, starting from about t=140 units of time. A detection of the abnormality is also obtained from examining the corresponding t-scores plot. Since the abnormal batch has a problem present from the very beginning, the observations in the t-scores starts at origin and gradually drifts out of the control limit and stays outside the 'normal operation' region as time goes on. This is a clear indication for the existence of a process fault. In this example, MSPC provides an intuitive way of analyzing and viewing originally complicated process data and effectively indicating process abnormality.

3.11 Interpreting Principal Components

The essential purpose of PCA is to reduce a large number of correlated process variables to a much smaller number of PC's while retaining as much as possible variation exhibited by the original process data.

In addition to substantially reducing the dimensionality of the problem, MSPC produces decoupled process vectors more readily interpretable. In the PCA approach, these process vectors are those principal components retained. PCA is more satisfying if intuitively reasonable interpretations can be provided for the

make-up of the first few PC's or even to all of the PC's that have been retained. More insights to the process can generally be obtained by observing and understanding the pattern of data distribution as well as clustering in a lower k-dimensional subspace, where k denotes the number of PC's retained.

There are several types of graphical approach to interpret the process data, such as the loadings plot, the variance-retention plot, the Gabriel's plot and the scores plot.

3.11.1 Loadings Plot

Plots of the coefficients of the loadings vectors are called the 'loadings plots'. Loadings plot tells us the contribution of the original variables to each of the principle components retained. In addition, loadings plot shows the correlation between the original process variables in the database. For the first few principal components representing most of the system variability, the interpretation of correlations among the process variables is generally easier and more apparent. These process variables who contribute more highly to each principle component are regarded to be more correlated to each other.

Referring to Figure 4-9 in the next chapter, it is an example of the loadings plot. It is the loadings plot for the second PC in the PCA model of this study. Obviously, the two original process variables that contribute the most to this principal component are X2 and X7, the autotrophic concentration from anoxic reactor and from clarifier. PC2 is primarily made up by these two variables.

Meanwhile, this figure shows that X2 and X7 are highly positively correlated with each other.

3.11.2 Variance-Retention Plot

Variance-retention plot essentially delivers information similar to the loadings plot. They differ in that the variance-retention plot provides a handle for the graph-reader on the exact amount of variation contributed by each of the process variables for each PC rather than only knowing which variable contributes more onto each PC. In other words, variance-retention plot is quantitative while loadings plot is more qualitative. In variance-retention plot, the height of each bar stands for the weight of that variable in its contribution to that particular PC. Compared with the loadings plot, the deficiency of variance-retention plot is that it is able to show which variables are correlated without delivering the information whether they are positively correlated or negatively correlated.

Figure 4-18 can be referred to as an example of the variance-retention plot. This is the variance-retention plot for the same PC used to interpret the loadings plot in the previous section. Covariance matrix is calculated by $X^TX=(U\Sigma P^T)^T(U\Sigma P^T)=P\Sigma^2P^T$ (11). Variance-retention plot for a specific PC (the ith PC) is generated by plotting the ith column of the product of the ith column of the loadings matrix P, the square of the ith singular value and the transpose of the ith column of loadings matrix P versus the index number. As shown, PC2 explains more than 90% of the overall variation of X2 and X7. The variables X2 and X7 are dominant in constructing PC2 compared with the rest ten process variables.

3.11.3 Gabriel's Plot for PC1, PC2 and PC3

There is another graphical representation of the PC loadings, the Gabriel's plot (Gabriel, 1971,1972, 1978). Different from the loadings plot and the variance-retention plot, Gabriel's plot gives correlation information of the process variables over the first three PC's instead of one PC at a time. The Gabriel's plot is created in a 3-dimensional subspace spanned by PC1, 2 and 3. The twelve Gabriel's vectors (GV) in 3-d space are calculated by the following formula:

$$GV = \Sigma_3 P_3' = U_3' X \tag{12}$$

where GV represents Gabriel's vectors, 3x12

Σ_3 is obtained from SVD in equation (2), 3x3

P_3 is the first three loadings vectors, 12x3

U_3 is obtained from SVD with the first three columns retained, 2401x3

X is the mean-centered, scaled data matrix, 2401x12

Each vector in the 3-dimensional Gabriel's plot represents the portion of the corresponding original process variables represented by the first three PC's. The directions and lengths of the vectors lend themselves to meaningful interpretation.

Since the data has been normalized in the original n-dimensional space, the variable length as retained by the k PC's retained can be compared with each other to arrive at the following conclusions: 1) Vectors with relatively longer vector lengths are well represented by the retained PC's; relationship of these vectors can be discerned from this plot. 2) Vectors with appreciably shorter vector length imply they are poorly represented by the retained PC's; It also implies that these variables

are highly correlated with those who exhibit longer vector lengths in the Gabriel's plot. Gabriel's plots in a subspace spanned by other principal components should be used to study variable relationships involving those vectors. 3) The proximity of the Gabriel's vectors to each other indicates the correlation among them. 4) Both positive and negative correlation patterns can be detected by examining the clustering pattern of the vectors in the Gabriel's plot.

Beside the length of the vectors, the angle between any two vectors also possesses important process information. The angle between two vectors implies their pairwise correlation. The smaller the angle, the stronger the linear correlation between the two variables. When the angle is close to 0°, these two variables give more or less the same information. One of the two variables is therefore redundant. One variable can be deleted without losing much independent information. When the angle is close to 180°, the corresponding two variables are strongly negatively correlated. When the angle is 90°, the two vectors are orthogonal to each other, which implies the two variables are totally independent. If variables are all orthogonal to each other, then the original set of process variables can be considered as independent of each other. There is no redundant information. For this kind of system, PCA will not reduce the system dimensionality. Conversely, if variables are closely related to each other, either positively correlated or negatively correlated, PCA will be a powerful approach to reduce the size of the original data to a much lower dimensional set without missing out on much system information.

3.11.4 Scores Plot

Other than the scores plot discussed in Section 3.5, scores of all the samples can be plotted for each PC one at a time. This is the type II scores plot. The x-axis for this plot is sample index numbers, from, say, 1 to 2401. The y-axis is the scores of each sample for that particular PC. Each scores plot corresponds to one PC. Since the scores are orthogonal to each other, each scores plot is independent of all the other scores plots. This type of plot delivers information on which samples are more similar to each other with respect to each principal component.

The approach to obtain this type of PC is to use the result of equation (4). The vector t_i is the scores of all samples onto the ith principal component. Plotting the components of each t_i over sample number gives the scores plot for the ith PC.

Chapter 4

Results and Discussions

Using the Principal Component Analysis (PCA) approach, Multivariate Statistical Process Control (MSPC) scheme with monitoring and fault diagnostic capability is developed for a prototype of an industrial biological wastewater treatment plant,.

The study is carried out using the bio-wastewater treatment plant simulator developed by Grove (1995). Simulation is carried out in the Simulink™ platform of Matlab. The MSPC is implemented on top of the plant with a 2x2 decentralized local feed back controller in place. Comparison of control design strategy between traditional PID controller and Internal Model Controller (IMC) has been carried out by Schmidt (1996) and Fu (1998). These studies show that IMC is superior to PID in many respects, especially with respect to stability issues. Therefore, IMC is chosen in this study as the controllers used in the feedback loops.

The detailed chronological steps of this thesis work was in the flow chart in Figure 3-1. The major tasks include generating base case profile, carrying out PCA, establishing 'normal operating' domain, simulating abnormal cases and fitting abnormal cases with PCA model.

4.1 Generating Base Case Data Profile

Process variables chosen in this study consist of the process input, output and intermediate variables. The twelve variables to be monitored are: 1) outlet concentrations from the anoxic reactor: heterotrophic biomass, autotrophic

biomass, BOD, NH_4^+ and NO_3^-; 2) treatment effluent concentrations from the clarifier: heterotrophic biomass, autotrophic biomass, BOD, NH_4^+ and NO_3^-; 3) the manipulated variables: recirculation ratio and sludge age (refer to Table 3-1 for a listing of these variables). Each of the twelve columns of the original data matrix X_o represents one monitored variable.

These twelve process variables' behavior is monitored under changes made to a few chosen operating conditions. In this study, the controlled variables are the effluent [BOD] and [NH_4^+]. They are paired with the manipulated variables, recirculation ratio and sludge age, respectively (Grove, 1995, Schmidt, 1996). The chosen operating conditions undergoing changes are the influent [NH_4^+], the influent [NO_3^-], the maximum growth rate of heterotrophs, $\mu_{m,\ H}$ and the half-saturation constant $K_{s,\ [COD]}$ for the heterotrophic consumption of COD. Using a central composite design around the nominal operating point (Refer to Table 3-2), the amount of change is -21% to +21% from their nominal values except for the influent [NH_4^+], which is from -15% to +15% change from the nominal influent [NH_4^+] value. Based on factorial design principle, with seven levels of each of these four variables, 2401 operating conditions are simulated. Each of the 2401 rows of the original data matrix X_o represents the steady state results of one operating condition, and constitutes, one sample.

In this study, the simulation time has been chosen to be 500 days. At this time, the system is guaranteed to have reached steady state, as shown in Figures 4-1 and 4-2. In these cases, the operating conditions consist of the most challenging

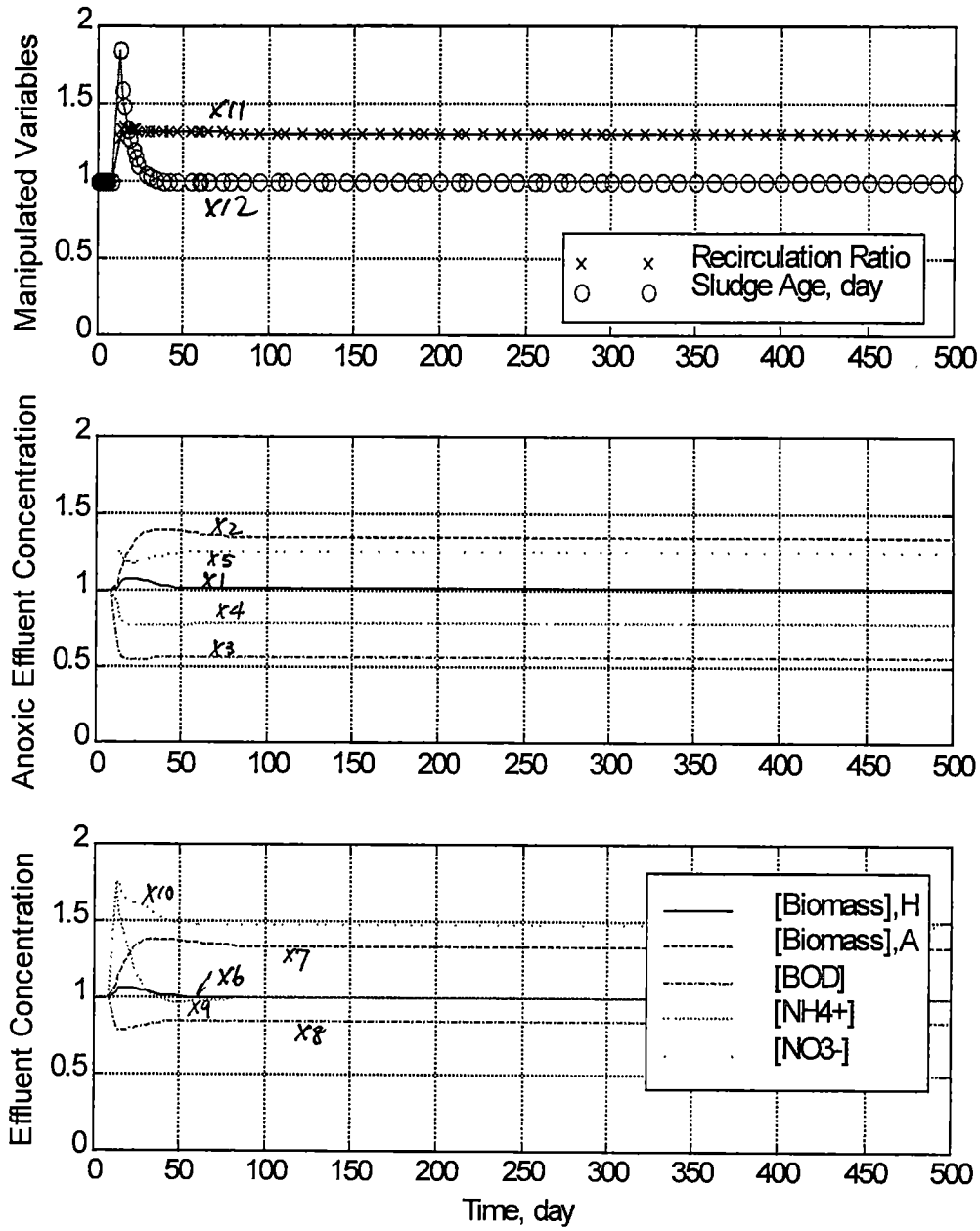

Figure 4-1. 2x2 IMC Closed-Loop Response with +21% Influent $[NO_3^-]$ and +15% $[NH_4^+]$ Changes
(Y axis is normalized value)
Controlled Variables: Effluent [BOD] and $[NH_4^+]$

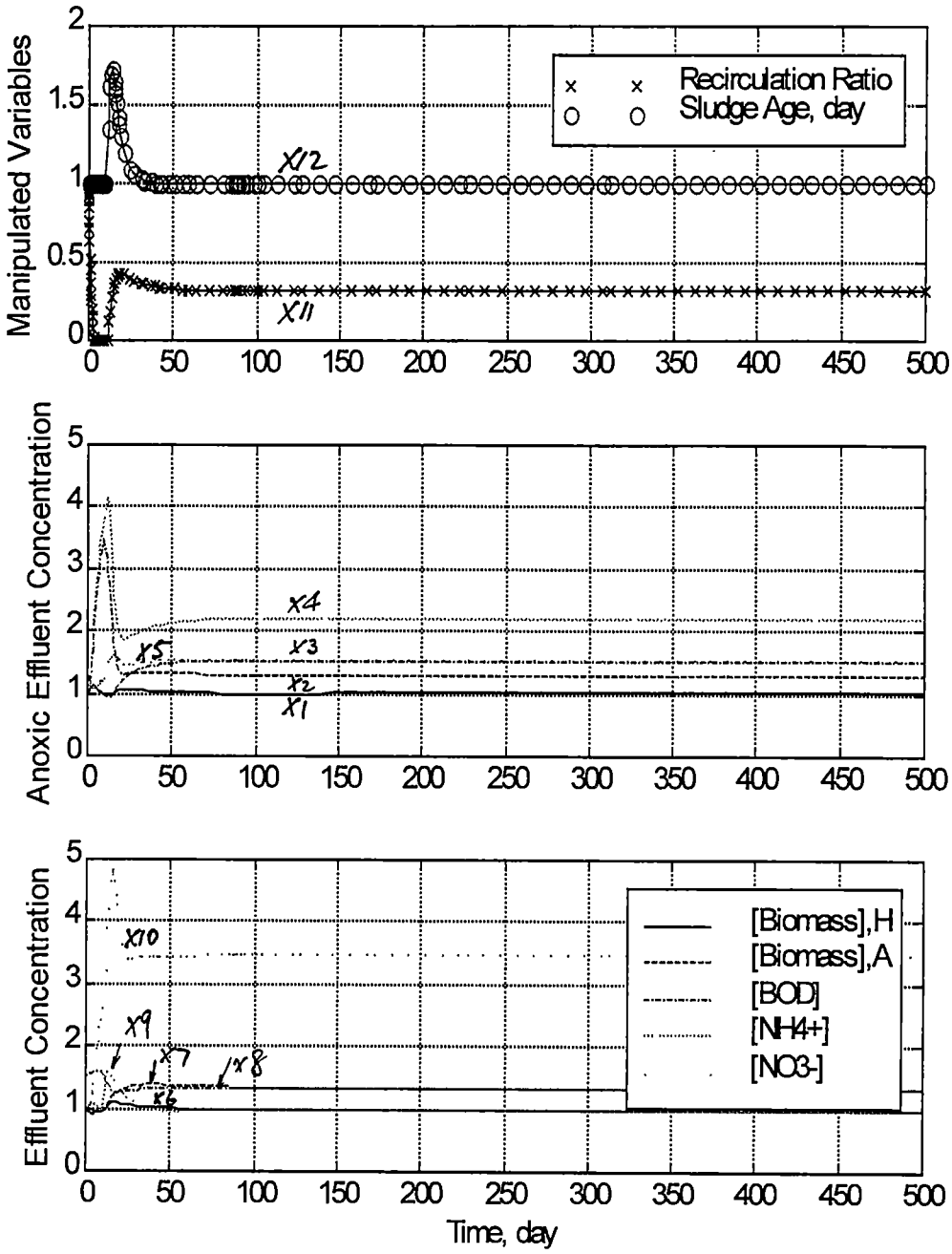

Figure 4-2. 2x2 IMC Closed-Loop Response with +21% Influent $[NO_3^-]$, +15% $[NH_4^+]$, -21% $\mu_{m,H}$ and +21% $K_{s,COD}$ Changes (Y axis is normalized value) Controlled Variables: Effluent [BOD] and $[NH_4^+]$

combinations. Challenging condition refers to the combination of operating condition that is likely to cause systematic instability if the controller used is not an effective one. If 500 days is sufficient for the system with the most challenging conditions to achieve steady state, it will be more than sufficient for systems under other operating conditions to reach stability. Some disturbance simulations are presented below to support this assumption.

Figure 4-1 is the time response curve of the 2x2 decentralized IMC closed-loop controller for a +21% increase in the influent $[NO_3^-]$ and a +15% increase in the influent $[NH_4^+]$ initiated at t=10 days. The levels of +21% and +15% are the maximum changes of the influent $[NO_3^-]$ and $[NH_4^+]$ in the base case, respectively. The top plot of Figure 4-1 is a plot of the normalized manipulated variables over time. The manipulated variables are recirculation ratio and sludge age in this study. The middle plot shows the five normalized outlet concentrations of the stream from the anoxic reactor. The bottom plot shows the relationship between the normalized effluent concentrations and the simulation time. From the observation of all the twelve process variables, it is concluded that: the system is disturbed at the tenth day when the influent $[NH_4^+]$ and $[NO_3^-]$ are changed to larger values; It takes the process variables around 50 days to reach their new steady-state values. Therefore, 500 days are more than enough to reach new steady state for this case.

The operating condition of Figure 4-2 is a +21% increase in the influent $[NO_3^-]$, a +15% increase in the influent $[NH_4^+]$ starting at t=10 days and a –21% variation in $\mu_{m,\ H}$ and a +21% variation in $K_{s,\ [COD]}$ starting at t=0 day. More

variations from the nominal case yield bigger overshoot after ten days when disturbance is introduced by positive changes in the influent [NO_3^-] and [NH_4^+]. But it does not vary the relative time period in which the process reaches new steady state. This time period is less than 50 days.

Figures 4-1 and 4-2 show that the system reaches steady-state around 50 days in the worst scenario. Therefore, all the other conditions are assumed to lead to new steady state even sooner. Based on these tests, 500 days is more than enough for the process to achieve a new steady state. Therefore, the measurements in the matrix X_o reflect the steady state values for each sample and each variable.

4.2 Adding Measurement Noise

A ±2.5% Gaussian-distributed random noise has been added to each of the simulated data matrix X_o to form the noisy matrix X_{o-n}. Noise added directly to the system measurement is considered to be the measurement noise.

4.3 Determining the Number of Principal Components to Retain

Before PCA is carried out, data matrix X_{o-n} needs to be mean-centered and scaled. Centering is carried out by subtracting the mean of each variable from the corresponding measurement of each sample; Scaling is carried out by normalizing the mean-centered data with the variance of each variable. Data matrix is now ready for PCA.

The scree plot is obtained using equation (5) in Section 3.4.2. Figure 4-3 is the scree plot from which the number of principal components to be retained is determined.

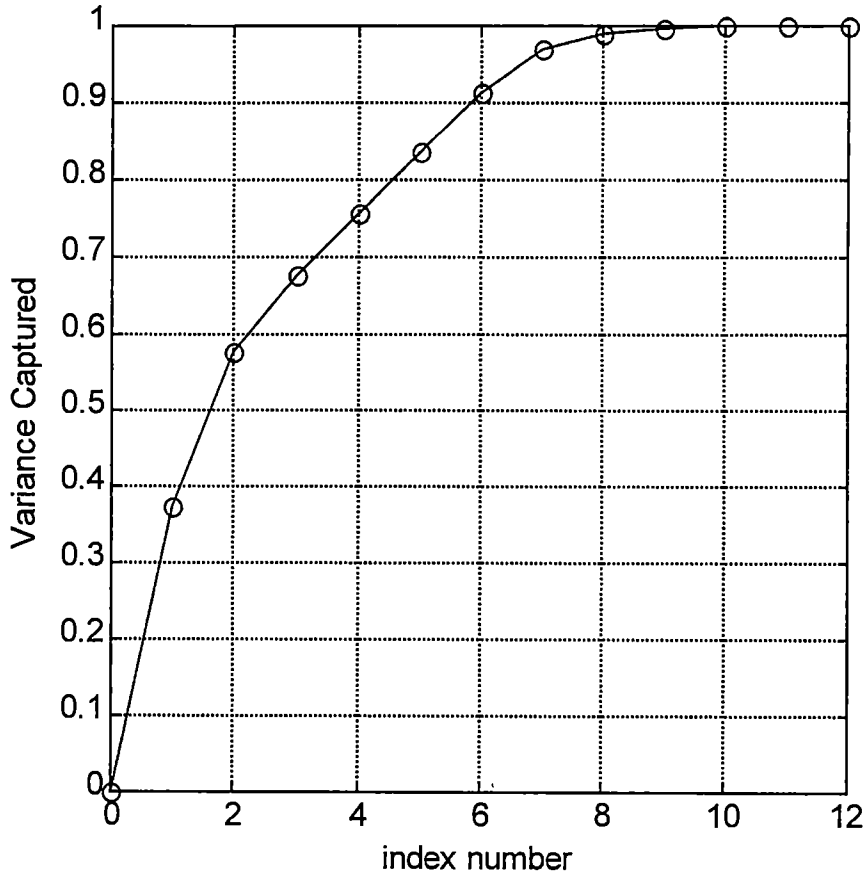

Figure 4-3. Scree Plot to Determine How Many PC's to Retain

Figure 4-3 shows that the first PC captures 37% of the original variance. The second PC captures an additional 20%. These two PC's alone have already retained more than half of the system variability. Each of the subsequent PC's represents less than 10% of the overall variability. It is decided that the first six PC's are to be retained in building the PCA model. They together reflect 91% of the original data variance. The last six principal components are considered to provide no additional statistical significance. They are regarded as arising from noise. The dimensionality and the effective rank of the database are then reduced to six.

The base case PCA model has been built using the projection of the original data to the 6-dimensional subspace representing the majority of the total variance of the original data. The principal component axes come from the first six right singular vectors of the SVD of the pretreated data matrix, as shown in Equation (2) of Section 3.3.1.2.

Because four independent process inputs/parameters are changed during the simulation to obtain the base case process variable values that represent the 'normal' operation profile, the degree of freedom of the base case should be three (because the data is mean-centered, which takes away one degree of freedom). But the number of PC's kept in this study is six. Normally, one does not know the true degree of freedom exhibited by the base case data. Therefore, the number of PC's to be retained may sometimes exceed that of the true degree of freedom of the

process. The additional dimension is assumed to have come from noise. This is one source of possible model misfit for assessing future data.

To test the hypothesis, a second database was generated by the same method of simulation but without additional noise. After similar pretreatment, PCA is also carried out on this database. The scree plot of this database shows that the first three PC's capture 61.10%, 21.90% and 12.60% of the total system variance, respectively. The forth PC represents only 2.36% variance (probably from round-off error effect of the computer computation). This result conforms the fact that the inherent process degree of freedom is 4. The two additional PC's in the noisy data modeling are therefore attributable to the addition of measurement noise.

4.4 Interpreting Principal Components

The essential purpose of PCA is to reduce a large number of correlated process variables to a much smaller number of PC's while retaining as much as possible variation of the original process through the associated process variables. In this study, six PC's are retained to keep 91% of the total variation exhibited by the original data set. The dimensionality of the problem is thus reduced from twelve to six. This methodology has not only simplified the analysis for the process, but also extracted the most significant information of the system. SVD creates scores vectors as well as loadings vectors (Principal Components). More insights to the process can be obtained by observing and understanding the distribution and clustering pattern of these vectors in the lower dimensional space.

Graphical representations for the six retained principal components are given in the following section.

The loadings plots, the variance-retention plots, the Gabriel's plots and the scores plot for the base case will now be presented and discussed.

4.4.1 Loadings Plot

A loadings plot tells us the relative weights of the original process variables in the make-up of each of the retained principal components. It also gives information for the correlation between the process variables.

4.4.1.1 Principal Component 1

Figure 4-4 is the loadings plot for PC1, which contributes 37% to the overall variation. It shows that PC1 is heavily loaded with x3 ($S_{S\ (Anoxic\ Reactor\ Effluent)}$), x4 ($S_{NH\ (Anoxic\ Reactor\ Effluent)}$), x8 ($S_{S\ (System\ Effluent)}$), x10 ($S_{NO\ (System\ Effluent)}$) and x11 (Recirculation Ratio). Among them, x3, x4, x8 and x10 are positively correlated. They are negatively correlated with x11. Other process variables' contribution to PC1 is negligible compared with them. Therefore, PC1 represents a linear combination of x3, x4, x8, x10 and x11. This correlation pattern implies that the manipulated variable of recirculation ratio mainly has an impact on x3, x4, x8 and x10 under the set of operating conditions chosen for the construction of the base case data. Opposing variations are expected between x11 and x3, x4, x8 and x10. In other words, an increase in x3, x4, x8 and x10 results in a decrease in the recirculation ratio, x11.

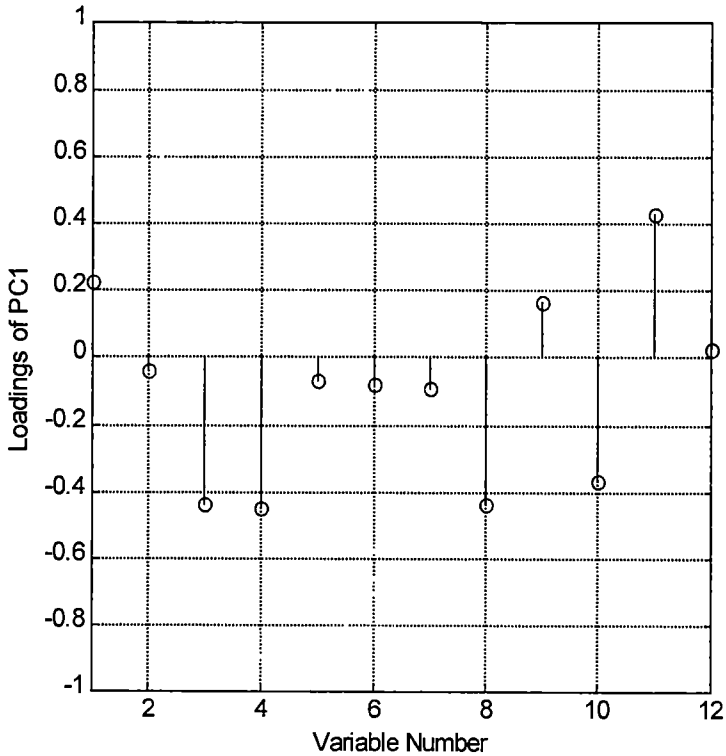

Figure 4-4. Loadings Plot for PC1

4.4.1.1.1 Open-Loop Time Response

Variable correlation observed from Figure 4-4 is tested by the simulation of the wastewater treatment plant with respect to the changes exhibited by these variables. Figures 4-5 and 4-6 are the open-loop time response curves for changes made in the recirculation ratio. For a process without disturbance, the relationship between the manipulated variables and the process outputs do not change when the loop is closed to form a closed-loop control. Open-loop response gives important information to the system's sensitivity to the manipulated variables. Therefore, open-loop response has been carried out first in this study to validate the variable correlation relationship.

Figure 4-5 shows the open-loop time response when the input variable of the recirculation ratio has a –10% change initiated at t=10 days from its nominal value. The two groups of curves represent the anoxic reactor's effluent concentrations of biomass, [BOD], [NH_4^+], [NO_3^-] and the system's effluent concentrations of biomass, [BOD], [NH_4^+] and [NO_3^-], respectively. In Figure (a) (anoxic reactor effluent), the normalized anoxic effluent [BOD] (x3) and [NH_4^+] (x4) concentrations are observed to deviate from their nominal values greatly, starting at t=10 days. Responding to the 10% negative change in the manipulated variable - recirculation ratio, x11, these two variables yield less than 10% positive changes of their original values. In Figure (b), for system effluent, shows that normalized [NO_3^-] (x10) has a +7% change with respect to the –10% change in the recirculation ratio. In addition, normalized [BOD] concentration from the effluent

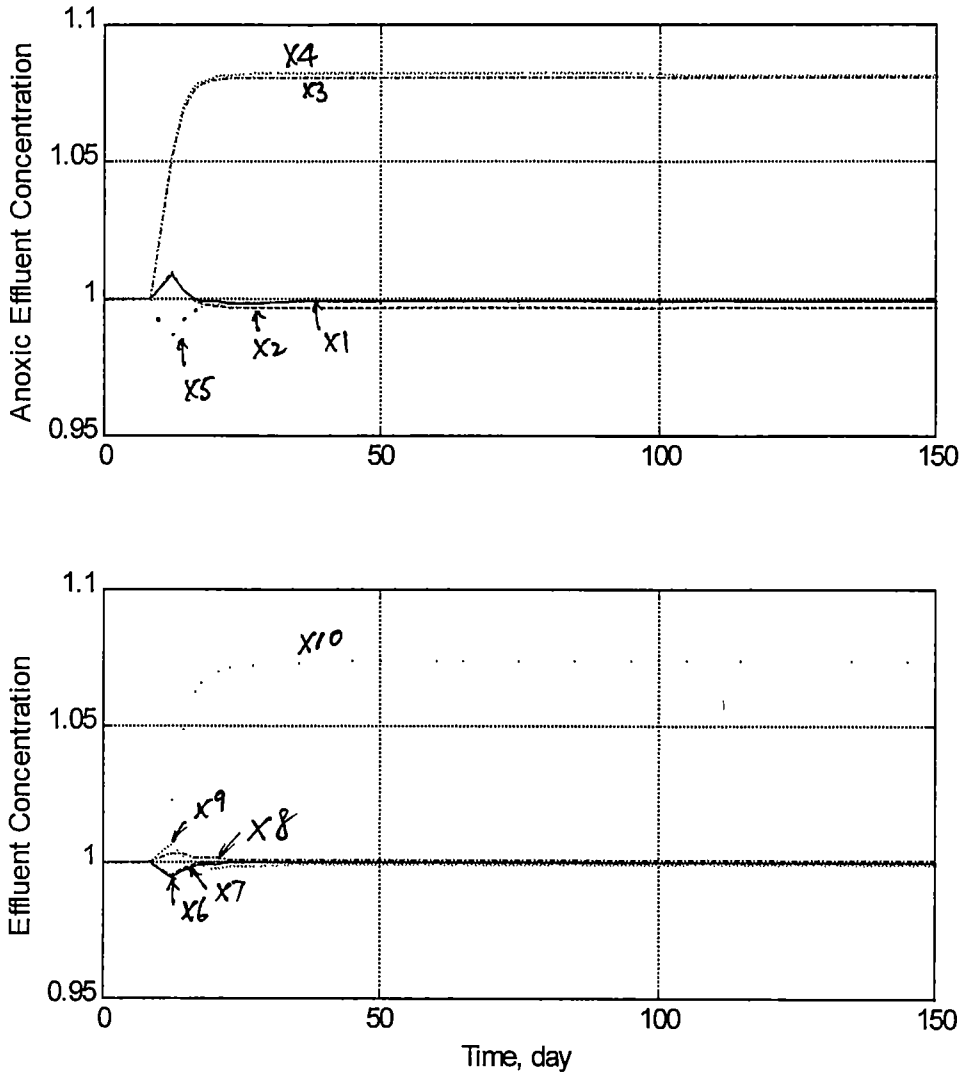

Figure 4-5. Open-Loop Response with –10% Change in the Recirculation Ratio

a) b) Process Variables: [Biomass], $_H$ (x1, x6), -; [Biomass], $_A$ (x2, x7), --; [BOD] (x3, x8), -.; [NH_4^+] (x4, x9), ...; [NO_3^-] (x5, x10), . .

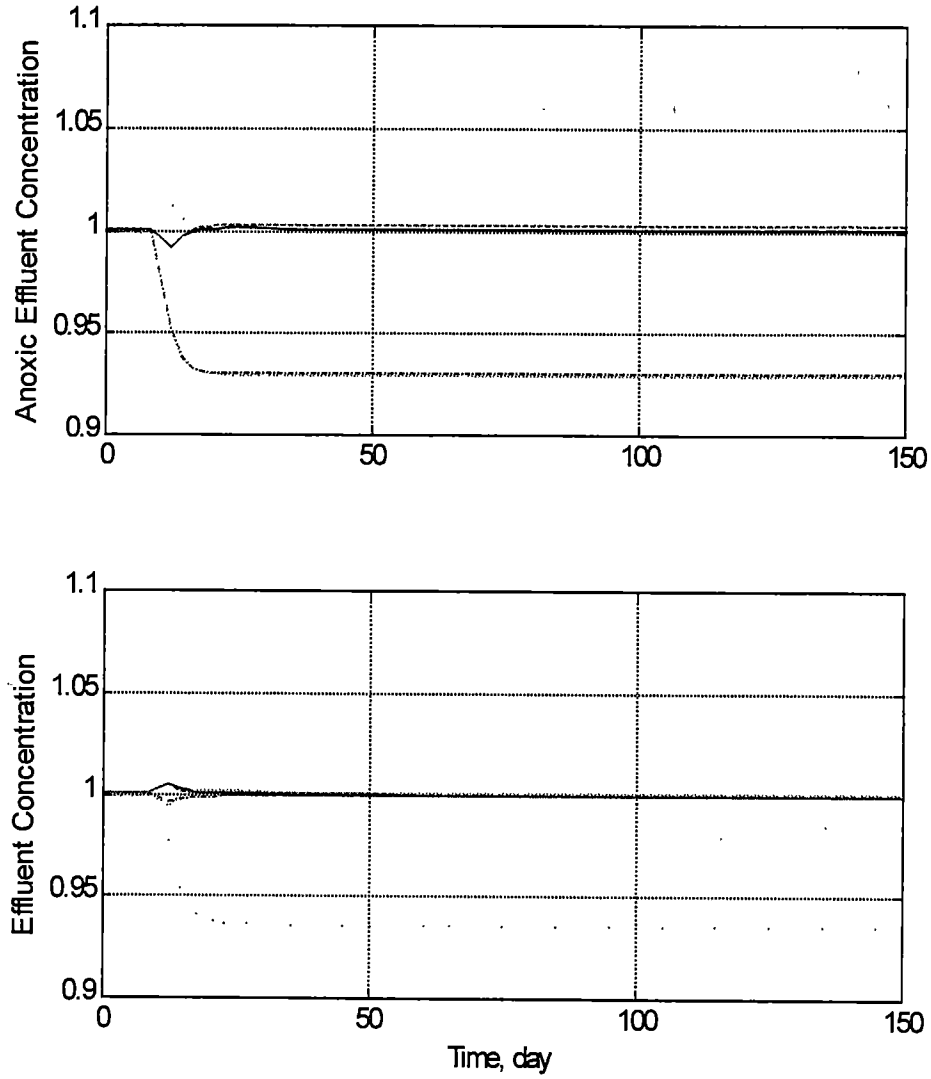

Figure 4-6. Open-Loop Response with +10% Change in the Recirculation Ratio
a) b) Process Variables: [Biomass], $_H$ (x1, x6), -; [Biomass], $_A$ (x2, x7), --; [BOD] (x3, x8), -.; [NH_4^+] (x4, x9), ...; [NO_3^-] (x5, x10), . .

(x8) has also some positive response in Figure (b). But it is not as obvious as that of x3, x4 and x10. But recall that each variable in the base case data matrix is scaled by the variance of each process variable in the data set. Since the levels of response observed in the open-loop simulation are unscaled, one can not compare directly the relative magnitude between the scaled and unscaled contributions made by each process variable. It was found that the scaling factor for x8 is 100 times smaller than all the other variables. Therefore, it is concluded that a –10% change in x11 leads to a positive change in x3, x4, x8 and x10. These observations support the correlation pattern observed from the loadings plot for PC1.

Similarly, Figure 4-6 shows the time response trends of the ten process concentration variables in response to a positive 10% change in the recirculation ratio at t=10 days. Monitored variables x3, x4, x8 and x10 result in negative shifts from that of nominal. This figure also supports that x3, x4, x8, x10 and x11 are correlated and it is a negative correlation between these two groups.

4.4.1.1.2 Closed-Loop Time Response

Figure 4-7 is the closed-loop time response of sample 301 in the reference database. The effluent [BOD] and $[NH_4^+]$ are under control. This is the sample with the heaviest score coefficient onto PC1 among all the 2401 samples. Its operating conditions are: –21% change in the influent $[NO_3^-]$, +15% $[NH_4^+]$, -21% $\mu_{m,\ H}$ and +21% $K_{s,\ [COD]}$. Apparently, recirculation ratio (x11) drops to zero (no recirculation) as a function of time, while the anoxic reactor effluent concentrations

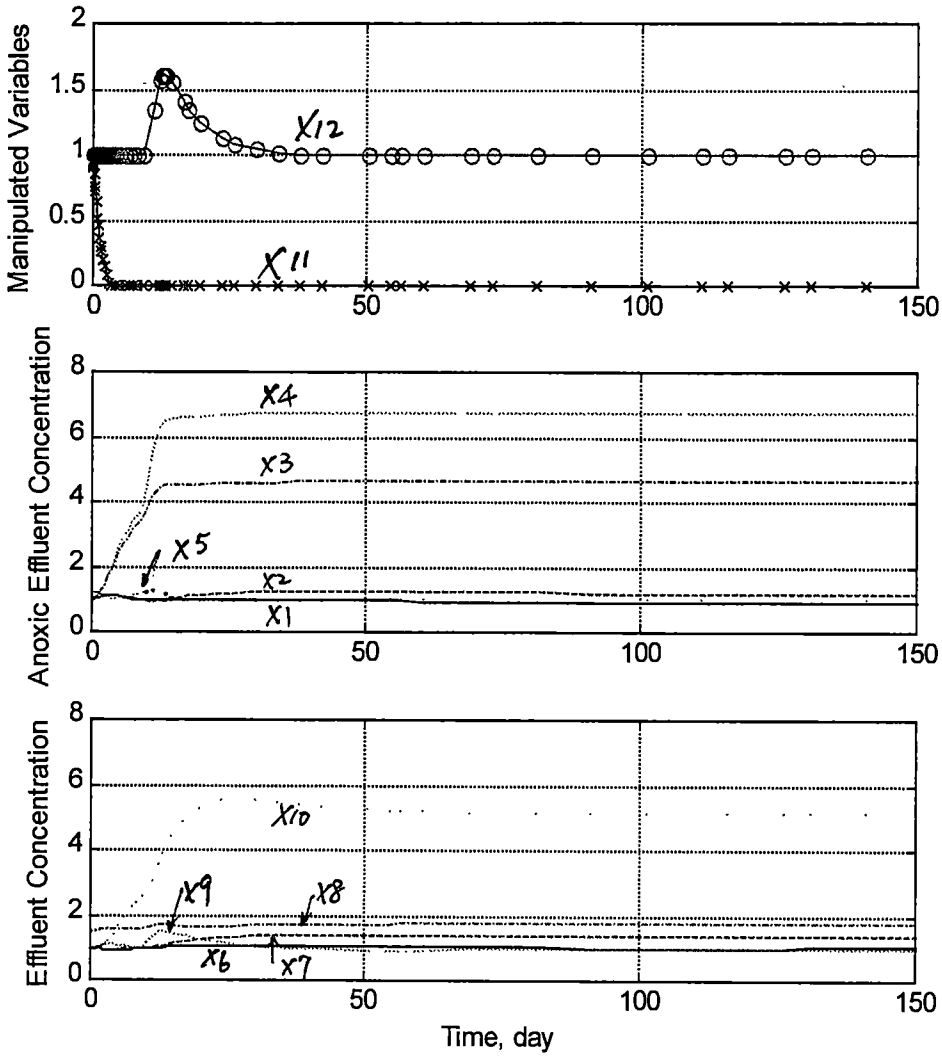

Figure 4-7. 2x2 IMC Closed-Loop Response with -21% Influent [NO_3^-], +15% Influent [NH_4^+], -21% $\mu_{m,\,H}$ and +21% $K_{s,\,[COD]}$ Changes (Sample 301)
a) Manipulated Variables: Recirculation Ratio (x11), x; Sludge Age (x12), o
b) c)Other Process Variables: [Biomass], $_H$ (x1, x6), -; [Biomass], $_A$ (x2, x7), --; [BOD] (x3, x8), -.; [NH_4^+] (x4, x9), ...; [NO_3^-] (x5, x10), . .
Controlled Variables: Effluent [BOD] (x8) and Effluent [NH_4^+] (x9)

of [BOD] (x3) and [NH_4^+] (x4) increase enormously. They rise to five to seven times of their nominal steady state values. For system effluent concentrations, [NO_3^-] (x10) climbs to more than five folds of its original value. The effluent [BOD] (x8) increases by 50%. These observations also properly support the correlation pattern obtained from the loadings plot, Figure 4-4.

The wastewater treatment process in this study consists of an anoxic reactor, an aerobic reactor and finally a clarifier. Denitrification is carried out in the anoxic reactor. Ammonia concentration is not changed in this section. The high loading of the influent [NH_4^+] in sample 301 leads to the large ammonia concentration in the anoxic reactor effluent, which is x4 in the database. Ammonia is consumed in the nitrification reaction occurring in the aerobic reactor to produce nitrate; the more ammonia entering the reactor, the more ammonia is converted into nitrate. Therefore, x10, the nitrate concentration in the effluent also increases, and it is not one of the controlled variables. These are the major effects of the bigger influent ammonia concentration on the overall process. Both low value of the $\mu_{m,\,H}$ and high value of the $K_{s,\,[COD]}$ decrease the rate of biomass growth, therefore the rate of BOD degradation. Sample 301 was simulated with –21% change in the $\mu_{m,\,H}$ and +21% change in the $K_{s,\,[COD]}$. [BOD] under these operating conditions varies from their nominal values. [BOD] coming out from the anoxic reactor is variable x3 and the effluent [BOD] is variable x8. The variables, x3, x4, x8 and x10, are all primary loadings variables for PC1 according to Figure 4-4. Therefore, the time response plot supports the observation obtained from the loadings and scores plots.

Some of the previous time response figures can also be referred to in showing the correlation pattern of the loadings plot 4-4. Figure 4-1 is such an example. The top figure exhibits about 30% increase in the recirculation ratio. The middle figure shows –45% and –20% decrease in x3 and x4, respectively. The bottom figure shows a negative variation in x8 and a positive variation in x10. Ignoring the uncontrolled variable, x10, this case could be a very good physical interpretation to the mathematical PCA model. Besides Figure 4-1 and Figures 4-2, later figure shown on page 135 and 141 tell the same story for the relationship between the process variables of x3, x4, x8, x10 and x11. On page 135, the final recirculation ratio (x11) increases while x3, x4 and x8 decrease. X10 again does not follow the correlation pattern implied by Figure 4-4. It is not a controlled variable. In the figure on page 141, although the final steady-state value of the recirculation ratio stays at unity, it has a transient period from t=10 to 30 days. Behaviors of those variables in the transient period also follow the correlation pattern. It is concluded that these variables do exhibit strong collinear relationship among them. Therefore, multivariate statistical process control approach reflects the interactive pattern among variables in analyzing the correlated system data.

4.4.1.2 Principal Component 2

Figures 4-8 shows the variable loadings for PC2, which contributes 20% to the overall variability. The second PC is loaded mainly with autotrophic biomass concentration in both of the effluent streams, x2 ($X_{B,\ A\ (Anoxic\ Reactor\ Effluent)}$) and x7 ($X_{B,\ A\ (System\ Effluent)}$). It is also somewhat loaded by x10 ($S_{NO\ (System\ Effluent)}$). They are

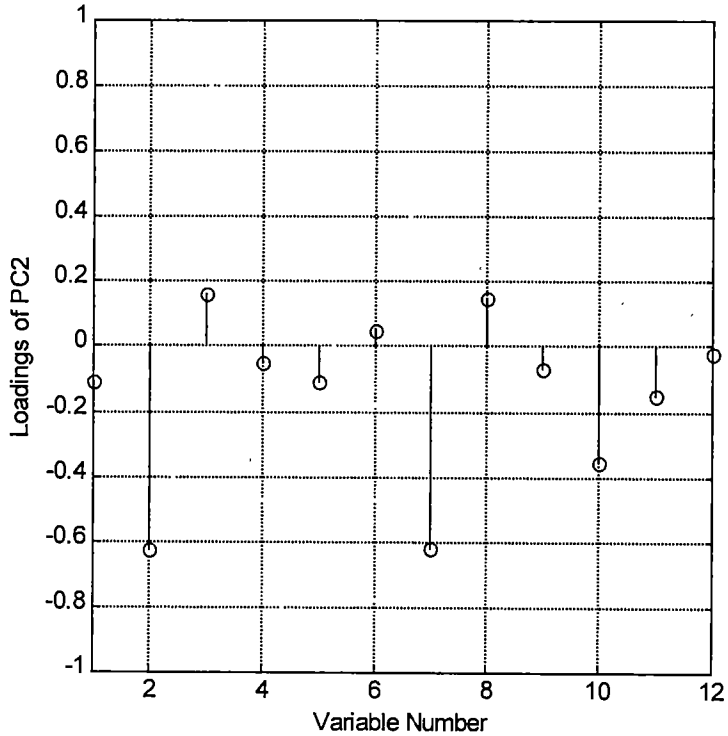

Figure 4-8. Loadings Plot for PC2

positively correlated. This trend can also be observed in the variance-retention plot shown later. PC2 may be readily interpreted as measuring the autotrophic biomass concentrations in the effluent stream from the anoxic reactor (x2) and the clarifier (x7). Any factors that might impact the growth of autotrophic biomass will affect the scores onto the PC2 loadings. For instance, in a later figure on page 158, the abnormal case deviates in the scores on PC2. This is an alarm for the operating personnel. Whenever this kind of behavior is observed, attention should be paid to the root causes that might lead to factors that have impact on the autotrophic biomass kinetics. As will be shown, in this specific case depicted by the figure on page 158, the abnormality is caused by the introduction of a minus change in $\mu_{m,\,A}$, the maximum specific growth rate of autotrophic biomass. This change will directly impact the growth rate of the autotrophic biomass, thus its steady state value in the process streams. By means of interpreting the PCA plots, the operating personnel can more effectively gain a handle in isolating a probable root cause for the abnormal process operations.

From the loadings plot, one notes that x2 and x7 are highly positively correlated. This correlation can be easily observed in all the closed-loop time response simulation plots as shown previously in Figures 4-1 and 4-2 and later, in the figures on pages 135 and 141. In each case, x2 and x7 correlated response trajectories. They increase/decrease concordantly. Their changes are comparable in magnitudes.

Simulation has been carried out for the open-loop system with a change in the sludge age to demonstrate this pattern. Figures 4-9 and 4-10 are the open-loop response to the -10% and +10% changes occurring in the sludge age at t=10 days. Figure 4-9 shows that -10% change of sludge age causes about -12% variation in both x2 and x7. Figure 4-10 shows that +10% change in sludge age causes about +12% variation in both x2 and x7. Monitored variables x2 and x7 in the two figures have similar time response trajectories. This supports the correlation pattern observed in the loadings plot for PC2.

4.4.1.3 Principal Component 3

Figures 4-11 is the loadings plot for PC3, which contributes 10% to the overall variation. According to the plot, the third PC is loaded mainly with x5 ($S_{NO\ (Anoxic\ Reactor\ Effluent)}$), and a bit with x1 ($X_{B,\ H\ (Anoxic\ Reactor\ Effluent)}$) and x12 (Sludge Age). PC3 can be interpreted as a measurement of x5, the effluent concentration of $[NO_3^-]$ from the anoxic reactor, which is independent of the loadings in PC1 and PC2 (the loadings vectors are mutually orthogonal).

Deviation from the acceptable region along the PC3 direction indicates possible root causes related to a deviation in x5, the anoxic effluent concentration of $[NO_3^-]$. The figure on page 152 will be such an example. In this figure, abnormal observations deviate from the 'normal operation' region along the directions of PC1 and PC3. The abnormality occurring along PC3 is caused by introducing a bigger than normal values in $\mu_{m,\ H}$ and $K_{s,\ [COD]}$. These bigger than normal bio-parameter

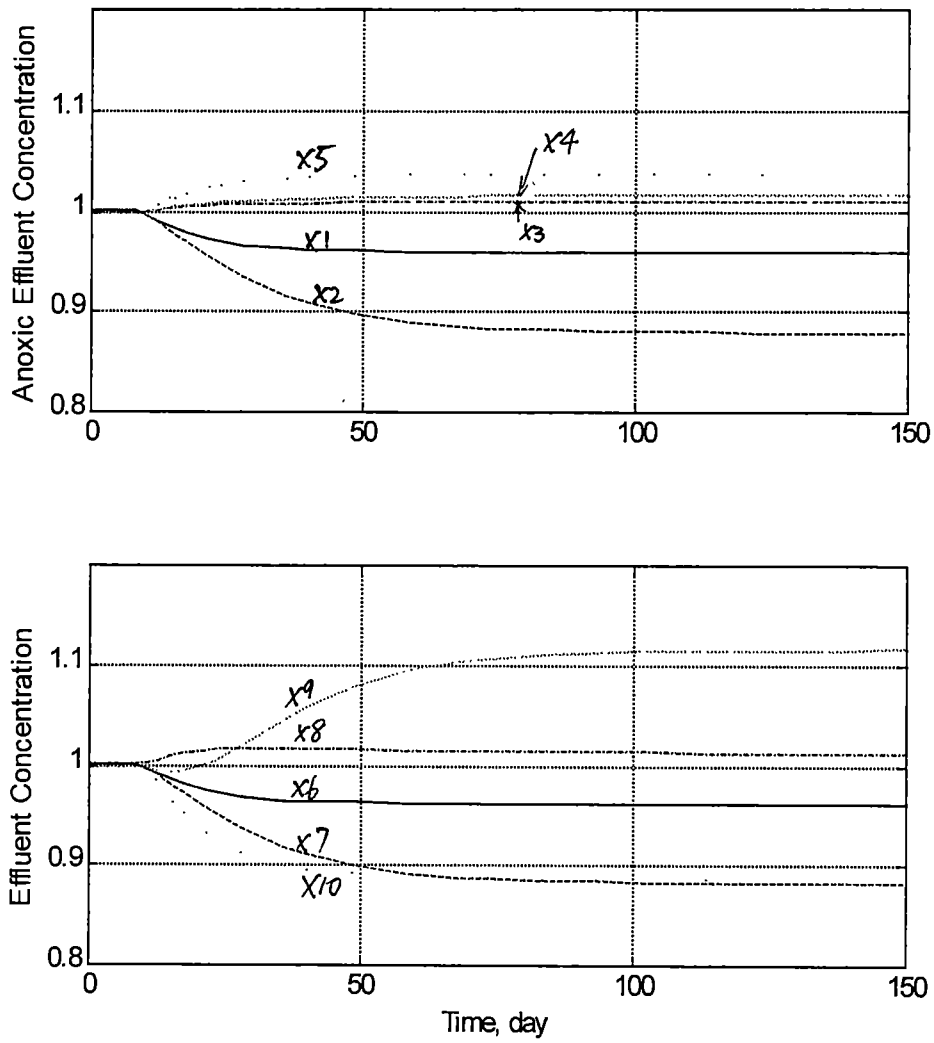

Figure 4-9. Open-Loop Response with –10% Change in the Sludge Age (x12) a) b) Process Variables: [Biomass], $_H$ (x1, x6) -; [Biomass], $_A$ (x2, x7) --; [BOD] (x3, x8), -.; [NH_4^+] (x4, x9), ...; [NO_3^-] (x5, x10), . .

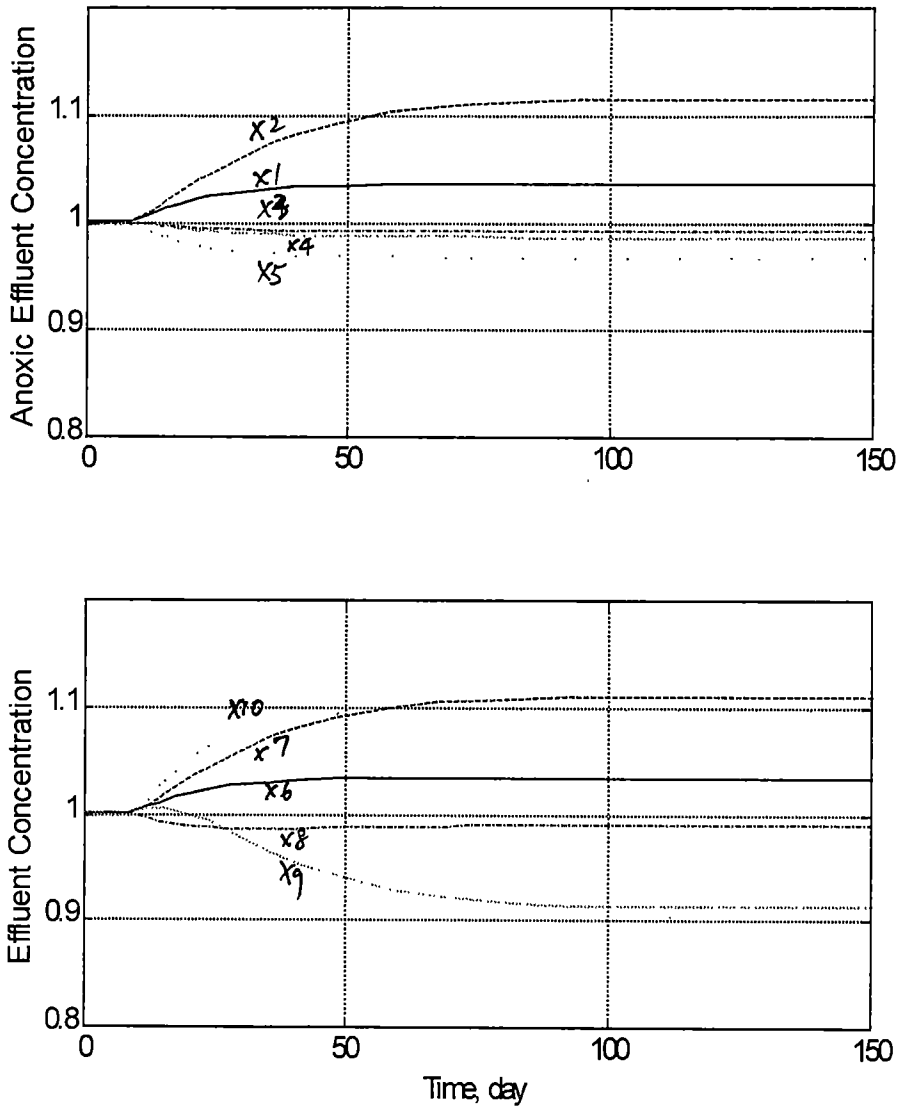

Figure 4-10. Open-Loop Response with +10% Change in the Sludge Age (x12) a) b) Process Variables: [Biomass], $_H$ (x1, x6), -; [Biomass], $_A$ (x2, x7), --; [BOD] (x3, x8), -.; [NH_4^+] (x4, x9), ...; [NO_3^-] (x5, x10), . .

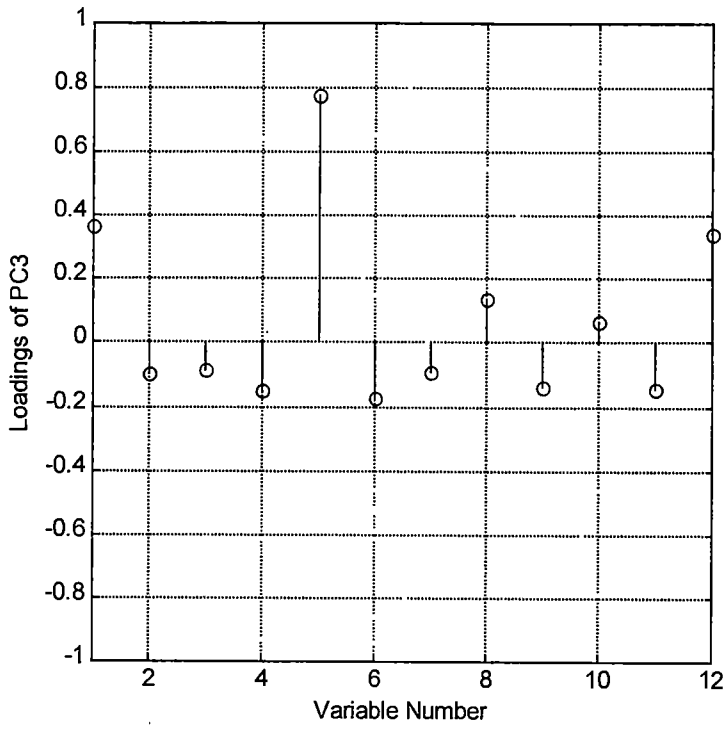

Figure 4-11. Loadings Plot for PC3

changes in the hetorotrophic biomass growth and COD degradation will affect the heterotrophic biomass growth in the anoxic reactor correspondingly. The bio-growth is associated with the denitrification in the same reactor occurring simultaneously. Biomass uses nitrate as energy and nitrogen supplement for growth. Therefore, the anoxic effluent nitrate concentration is closely related to the rate of bio-growth. Factors that might impact the biological growth that depends on nitrate will then influence the anoxic effluent nitrate concentration, x5.

Figure 4-12 is the closed-loop time response of the system with –50% change in $\mu_{m,\,H}$ and +60% change in $K_{s,\,[COD]}$. It corresponds to the sample with the maximum deviation in the figure on page 152. According to this figure, it deviates along both PC1 and PC3 direction. In the time response figure, x5 increases to 2.5 times of its original value, which causes the observation to migrate out of the acceptable region along the PC3 direction. Apparently, there are other process variables deviating greatly from their nominal values, such as, x3, x4, x8, x10 and x11. These variables are exactly the ones loaded in PC1. Appreciable amount of variations in these variables will lead to a large shift in PC1. That is why the observation in the figure on page 152 has bigger than normal deviation along PC1 as well. Observation and analysis of Figure 4-12 curves again support the interpretation of PC1's make-up.

Variables that load heavily onto PC4, PC5 and PC6 (x6, x9 and x12) as will be seen below, are the very ones that are not represented well by the first three PC's, which together capture 68% of the overall variation exhibited by the base

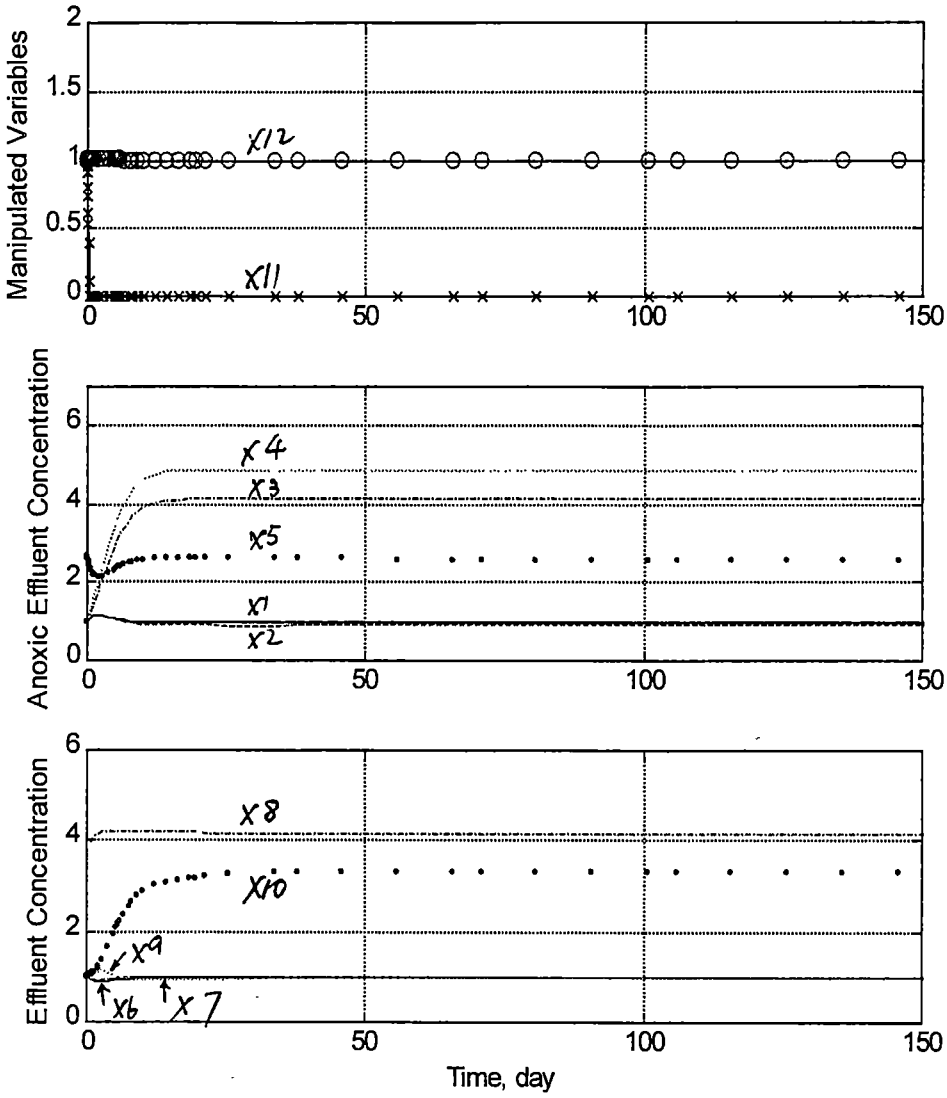

Figure 4-12. 2x2 IMC Closed-Loop Response with -50% $\mu_{m,\,H}$ and +60% $K_{s,\,[COD]}$ Changes

a)Manipulated Variables: Recirculation Ratio(x11), x; Sludge Age(x12), o;

b) c) Other Process Variables: [Biomass], $_H$ (x1, x6), -; [Biomass], $_A$ (x2, x7), --; [BOD] (x3, x8), -.; [NH_4^+] (x4, x9), ...; [NO_3^-] (x5, x10), . .

Controlled Variables: Effluent [BOD] (x8) and Effluent [NH_4^+] (x9)

case data. Therefore, the interpretation is that these variables are relatively resilient to changes introduced in the construction of the base case data, and their variation in the base case data may reflect more of the noise nature than real process variation. As a result, physically valid interpretation of these PC's are more elusive and probably less meaningful.

4.4.1.4 Principal Component 4 and 5

Figure 4-13 is the loadings plot for PC4, which contributes 7% to the overall system variation.

Figures 4-14 is the loadings plot for PC5. For this PC, x6 ($X_{B,\ H\ (System\ Effluent)}$) is the dominant variable. Besides x6, x12 (Sludge Age) also contributions a little to this PC. The correlation pattern between x6 and x12 is supported by their open-loop correlated time responses as shown in Figures 4-9 and 4-10 when the sludge age (x12) is changed. When there is a +10% change in the sludge age, heterotrophic biomass concentration from the clarier, x6, yields a +4% change; when there is a –10% change in the sludge age, x6 yields a –4% change. Considering PC4 and PC5 together, they can be readily represented as the measurement of x6 and x12. Other variables' contribution to these two PC's is negligible.

4.4.1.5 Principal Component 6

Figures 4-15 is the loadings plot for PC6. Apparently, x9 ($S_{NH\ (System\ Effluent)}$) is dominant in explaining PC6. Other variables have little contribution to PC6.

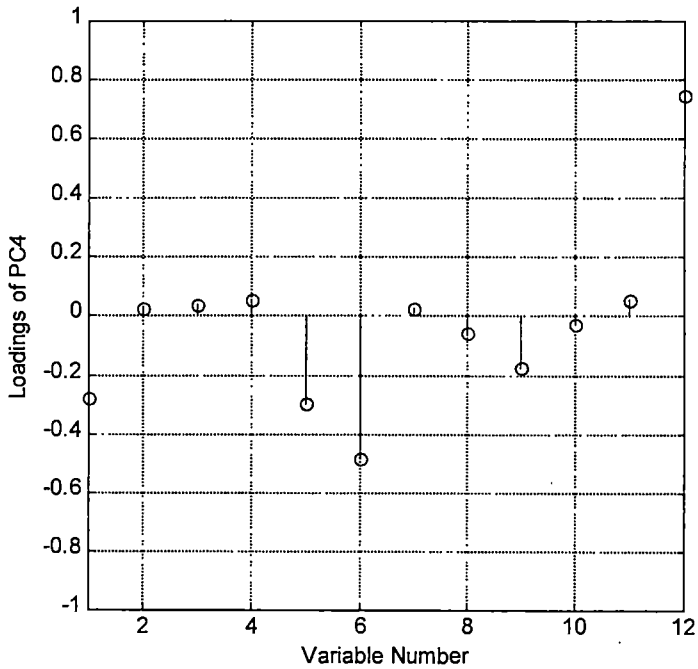

Figure 4-13. Loadings Plot of PC4

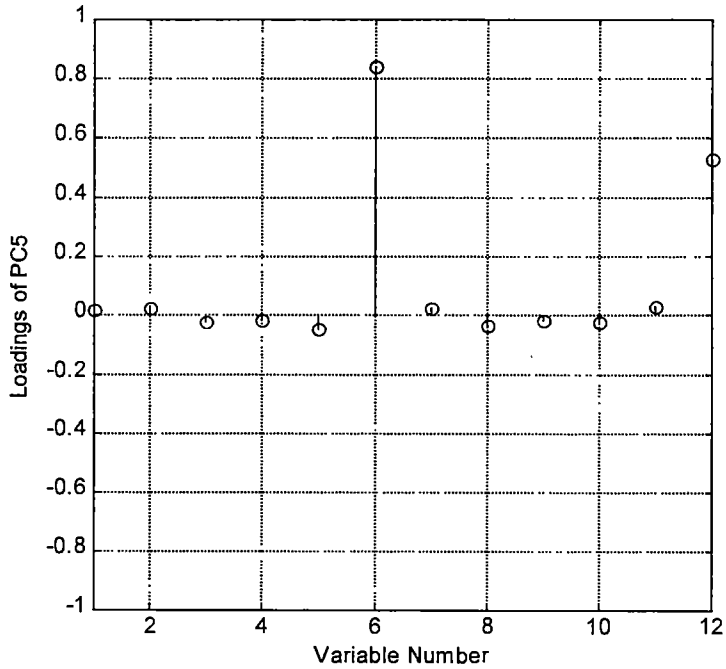

Figure 4-14. Loadings Plot for PC5

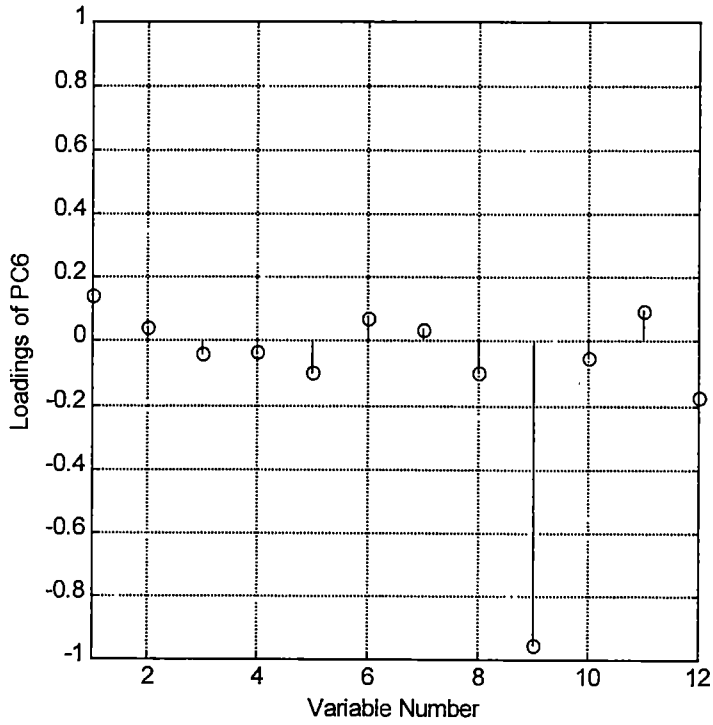

Figure 4-15. Loadings Plot for PC6

Therefore, PC6 information of observations can readily reflect the behavior of the $N\text{-}NH_4^+/NH_3$ in the system effluent.

4.4.2 Variance-Retention Plot

The variance-retention plot delivers similar information as the loadings plot, but with more emphasis on the quantitative information for variables that contribute to by each PC.

4.4.2.1 Principal Component 1

Figure 4-16 is the variance-retention plot for PC1. It is similar to the loadings plot in showing how much each variable contributes to the first PC. The most heavily loaded ones are again x3 ($S_{S\ (Anoxic\ Reactor\ Effluent)}$), x4 ($S_{NH\ (Anoxic\ Reactor\ Effluent)}$), x8 ($S_{S\ (System\ Effluent)}$) and x11 (Recirculation Ratio). PC1 explains more than 80% of the normalized overall variation of each of these four process variables. PC1 explains 60% variation of x10 ($S_{NO\ (System\ Effluent)}$). Variance-retention graph is more informative in that it is able to tell exactly how much each variable contributes to each PC. Loadings plot is more informative in that it provides correlation pattern information for the process variables. Therefore, a combination of these two plots provides a clear indication of the contributions of the process variables to the principal components' construction as well as of the correlation between the variables.

4.4.2.2 Principal Component 2

Figures 4-17 is the variance-retention plot for PC2. Consistent with the previous conclusion for loadings plot in Section 4.4.1.2, this PC is loaded mainly

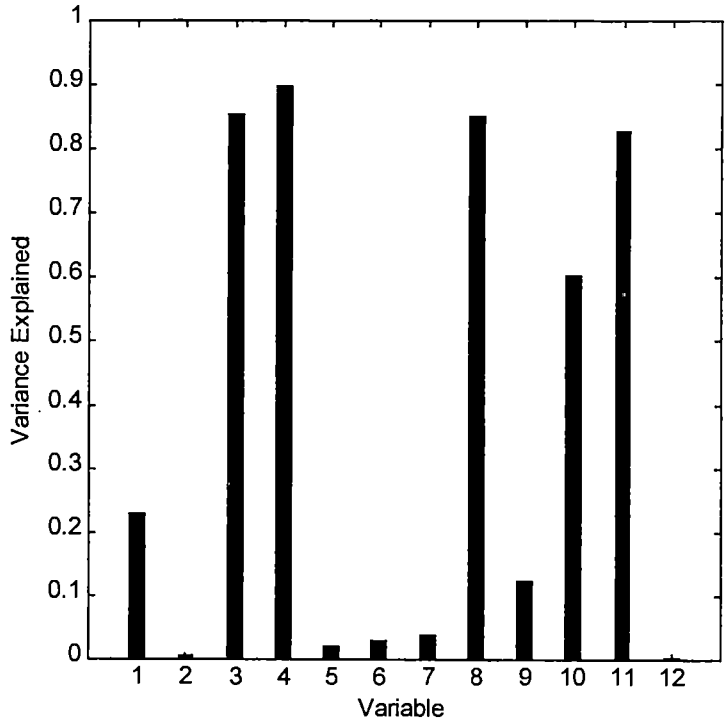

Figure 4-16. Variance-Retention Plot for PC1

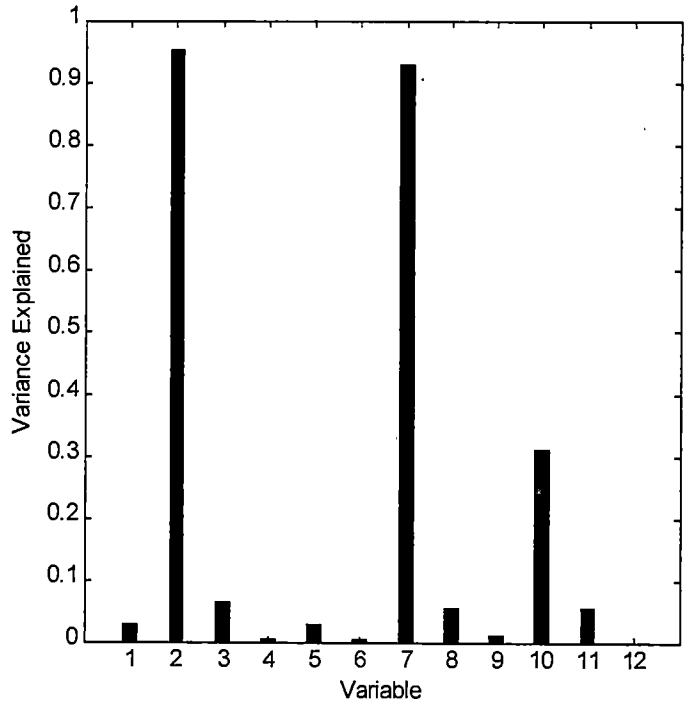

Figure 4-17. Variance-Retention Plot for PC2

with autotrophic biomass concentration in both effluent streams, x2 ($X_{B,\ A\ (Anoxic\ Reactor\ Effluent)}$), x7 ($X_{B,\ A\ (System\ Effluent)}$) and a bit with x10 ($S_{NO\ (System\ Effluent)}$). The contribution of x10 on PC2 is not comparable to that of x2 and x7. This trend is apparent in Figure 4-17. PC2 captures more than 90% of the overall variation of x2 and x7 while it can explain only 30% of x10. Therefore, x2 and x7 are dominant variables for PC2 construction. PC2 can be readily interpreted as measuring the autotrophic biomass concentrations in the effluent stream of the anoxic reactor (x2) and of the clarifier (x7).

4.4.2.3 Principal Component 3

Figure 4-18 is the variance-retention plot for PC3. According to it, x1, x5 and x12 have contribution to PC3 and x5 ($S_{NO\ (Anoxic\ Reactor\ Effluent)}$) contributes much more than x1 ($X_{B,\ H\ (Anoxic\ Reactor\ Effluent)}$) and x12 (Sludge Age). Therefore, PC3 is readily interpreted as a measurement of x5, the effluent concentration of [NO_3^-] from the anoxic reactor.

4.4.2.4 Principal Component 4

Figure 4-19 is the variance-retention plot for PC4. It is observed that the fourth PC is most heavily loaded by x12 (Sludge Age). x6 ($X_{B,\ H\ (System\ Effluent)}$), x1 and x5 also have some contributions on PC4. More than 50% of the variation for x12 is explained while other variables retain 10% to 25% of their overall variation by PC4. Compared with x12, the contribution of these variables onto the make-up of PC4 is not significant. Therefore, PC4 is readily interpreted by x12.

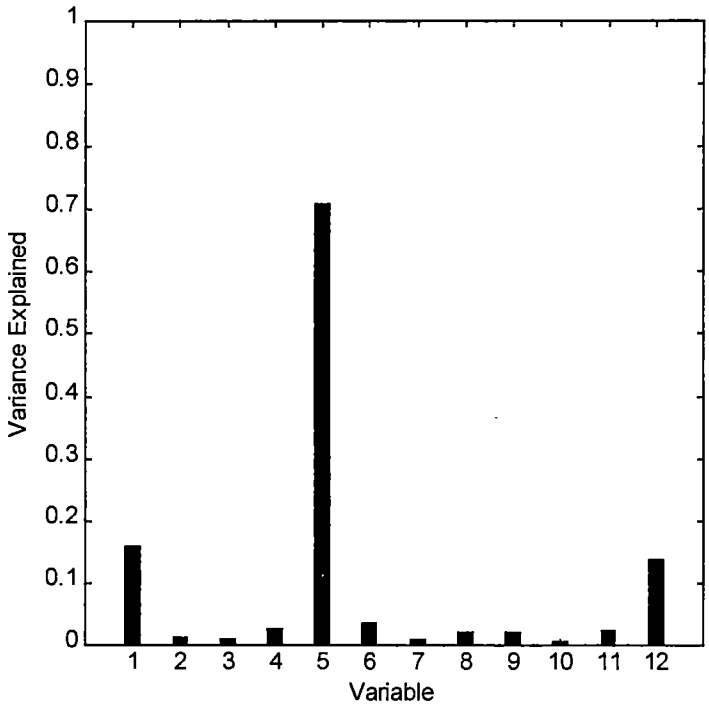

Figure 4-18. Variance-Retention Plot for PC3

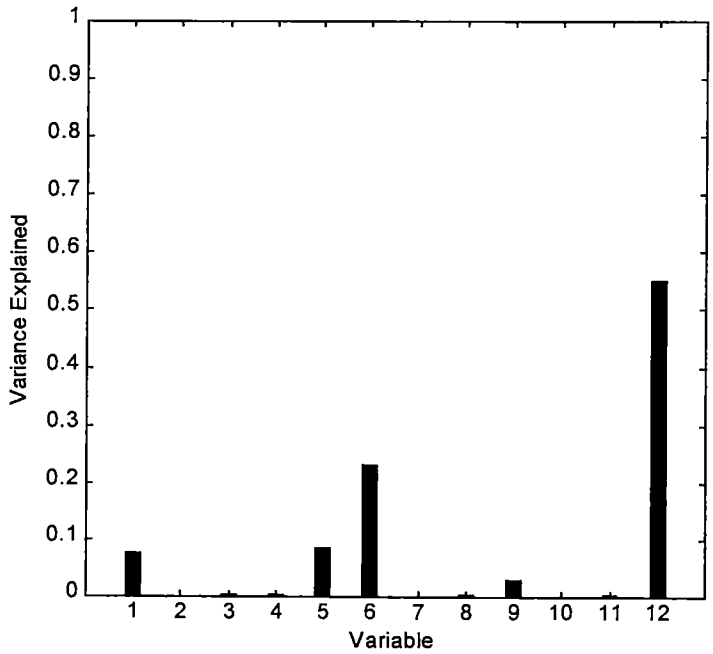

Figure 4-19. Variance-Retention Plot for PC4

4.4.2.5 Principal Component 5

Figure 4-20 is the variance-retention plot for PC5. For this PC, x6 ($X_{B,H\ (System\ Effluent)}$) and x12 (Sludge Age) have some contribution on it. But x12 has only less than half of the contribution as x6 does on PC5. Therefore, x6 is the dominant variable on PC5.

4.4.2.6 Principal Component 6

Figure 4-21 is the variance-retention plot for PC6. Apparently, the variable x9 ($S_{NH\ (System\ Effluent)}$) is the only dominant variable in PC6 construction.

4.4.3 Gabriel's Plot for PC1, PC2 and PC3

Three-dimensional Gabriel's plots for the first three PC's of the base PCA model are shown in Figures 4-22 and 4-23. Figure 4-23 is the same plot as Figure 4-22 but with a different view. Figure 4-22 shows that except for x6, x12, x9 and x1, vectors representing other variables have relatively long vector lengths. Since all the vectors plotted in the Gabriel's plot are normalized, the longer length implies the better interpretation of this variable by this specific plot. Figure 4-22 shows the relationship between x2 to x5, x7, x8, x10 and x11. Although Figure 4-22 is not sufficient in explaining x1, x6, x9 and x12, more information is available for these process variables in the later figures plotted for other PC's.

In Figure 4-22, it appears that x4 and x10 are highly collinear to each other, and the same for x2 and x7. x8 and x11 comprise a highly negatively correlated group in this figure. Besides the correlation information between variables, Gabriel's plot also tells relationships between the variables and the principal

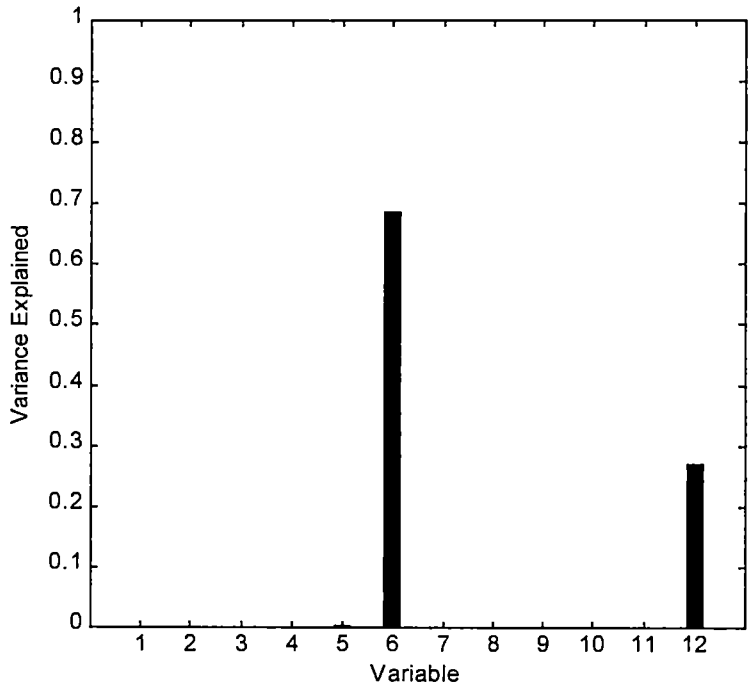

Figure 4-20. Variance-Retention Plot for PC5

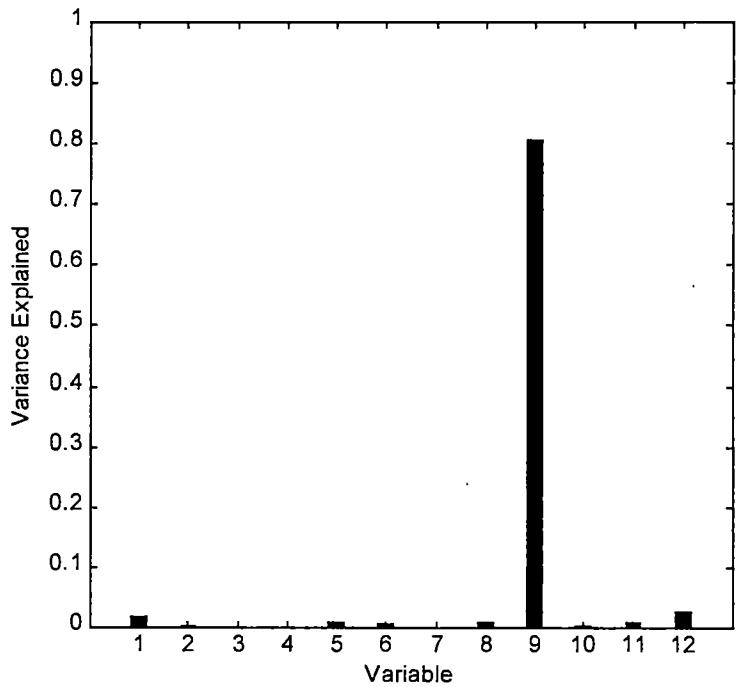

Figure 4-21. Variance-Retention Plot for PC6

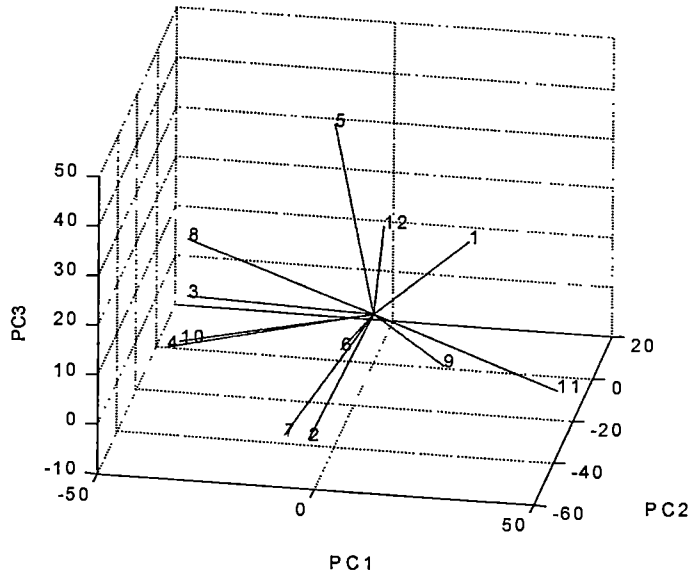

Figure 4-22. Gabriel' s Plot for PC1, 2 and 3

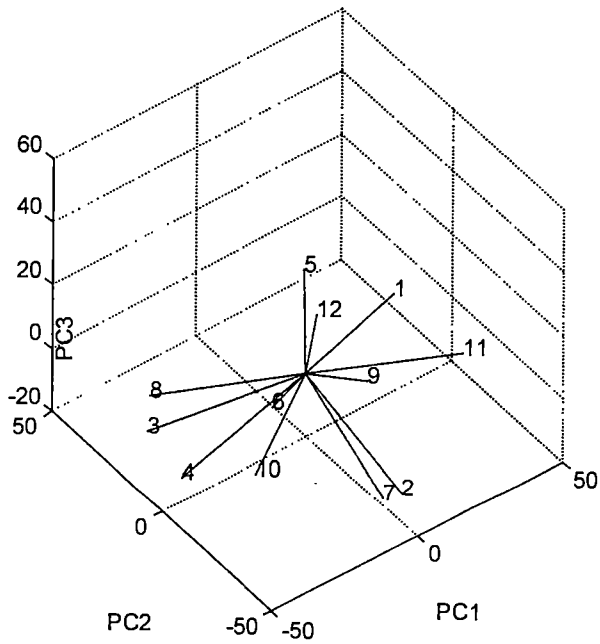

Figure 4-23. Gabriel' s Plot for PC1, 2 and 3 (Different View from Figure 4-22)

components. The vectors for the complex of the two negatively correlated variables, x8 and 11, are closely aligned with the axis of the first principal component. Variables x3, x4 and x10 are also more aligned with PC1 axis. Therefore, the first principal component is defined primarily by the five process variables of x3, x4, x8, x10 and x11. This conclusion is consistent with those obtained from the loadings plot and the variance-retention plot for PC1.

Figures 4-24 to 4-26 are the two-dimensional Gabriel's plots for PC1 and 2, PC1 and 3 and PC2 and 3, respectively. After observing all five figures, most conclusions obtained by analyzing Figure 4-22 remain applicable.

Information supported by all of the five Gabriel's plots are: 1) x2 and x7 are very highly correlated. They contribute strongly to PC2. 2) x5 is closely aligned with PC3. PC3 is then primarily defined by x5. x5 has little contribution to PC1 and PC2. 3) x2, x7 are very much orthogonal to x5. This implies that their variations are physically independent. 4) x8 and x11 are closely aligned on principal component 1. They are negatively correlated to each other. 5) x3 and x4, to some extent, also contribute to PC1.

The physical interpretation for conclusion 3) above can be: that x2 and x7 are autotrophic biomass concentration from the anoxic reactor and the clarifier, respectively. The growth of autotrophic biomass occurs in the aerobic reactor only when oxygen is provided as the electron acceptor. Therefore, only the factors relating to aerobic reactions will have impact on x2 and x7. x5 is the anoxic

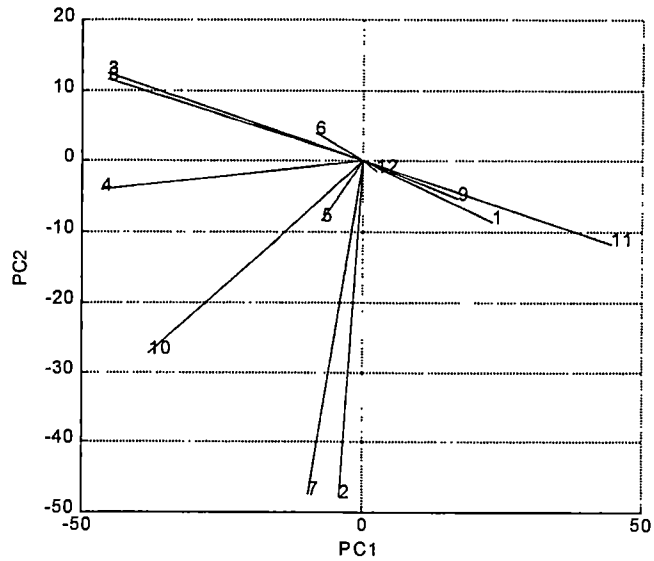

Figure 4-24. Gabriel' s Plot for PC1 and 2

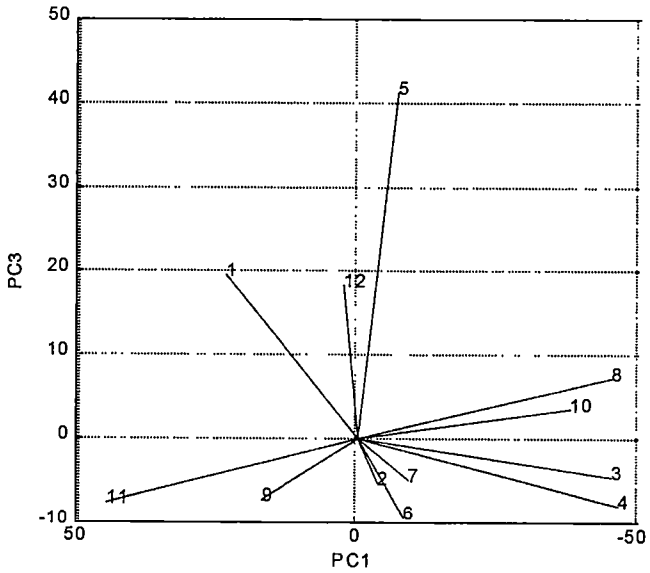

Figure 4-25. Gabriel' s Plot for PC1 and 3

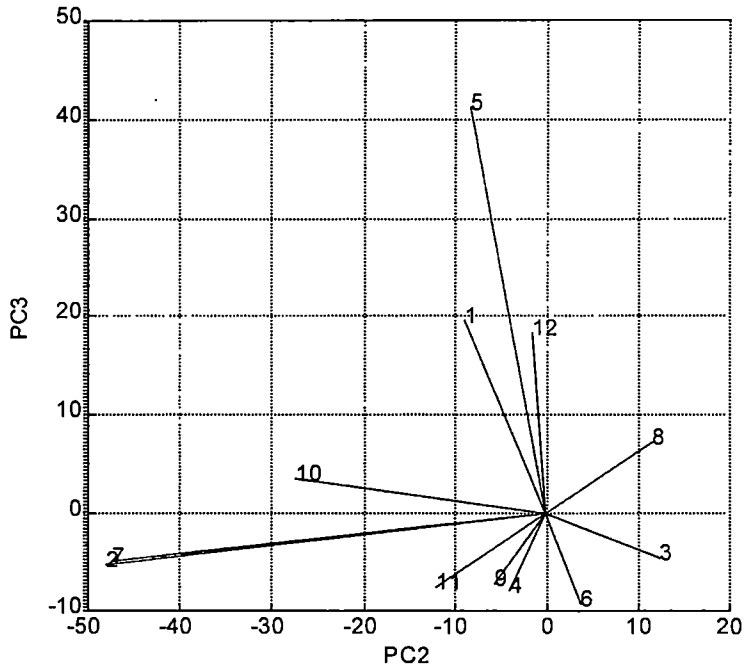

Figure 4-26. Gabriel' s Plot for PC2 and 3

effluent of nitrate concentration. This amount of nitrate will pass through the aerobic reactor unchanged. Therefore, x5 is independent of x2 and x7.

Most of the conclusion gained by analyzing Gabriel's plot supports the conclusion obtained in the previous sections. Therefore, the same physical phenomenon and interpretation can be obtained by several different types of the PCA plots. They deliver consistent and complementary information.

4.4.4 Scores Plot for Samples Projected onto PC's

Scores plot for samples projected onto PC's tells us information about how the 2401 samples score onto each of the PC' s, and patterns of similarity among the samples can be discerned from them.

4.4.4.1 Principal Component 1

Figure 4-27 is the scores plot for PC1, plotted against index numbers, of the 2401 noisy samples. This figure exhibits the pattern of contributions of the 2401 samples to the construction of the first score. This pattern is consistent with the original approach by which the reference database is generated – a factorial design of points for simulation. The seven major groups from left to right represent the seven levels of changes in the influent [NO_3^-]. The seven subgroups inside each of the seven major groups represent the seven levels of changes in the influent [NH_4^+]. Close-up plot of each subgroup gives similar patterns. The larger the absolute score value of each sample, the bigger is the associated projection of that sample onto PC1. As shown, for PC1, sample 301 is the one with the maximum scores, –9. This sample is simulated under the extremal operating condition of –21% change in the

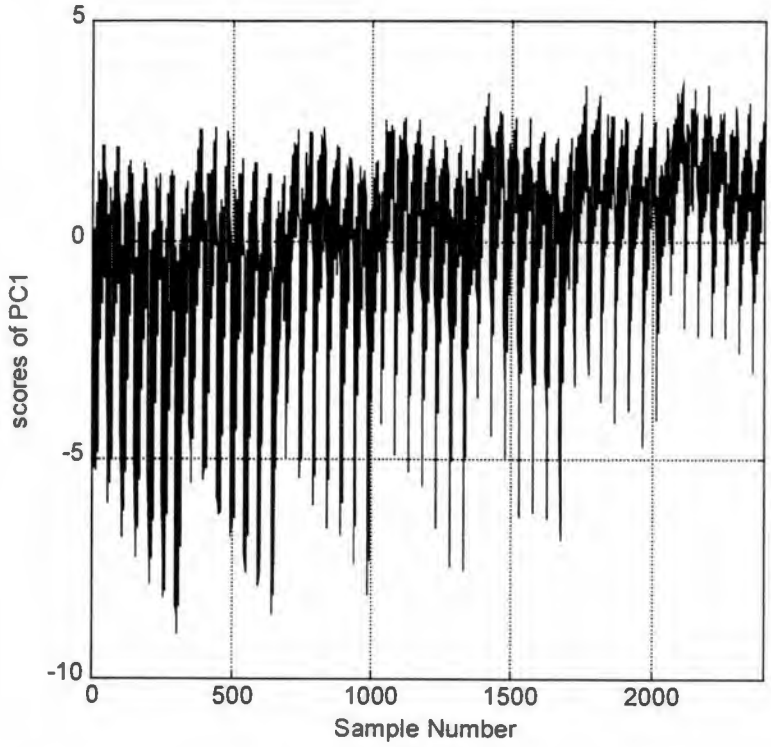

Figure 4-27. Scores Plot of PC1 for Samples

influent $[NO_3^-]$, +15% $[NH_4^+]$, -21% $\mu_{m,\ H}$ and +21% $K_{s,\ [COD]}$. This is the reason why sample 301 was chosen in Figure 4-7 to show the closed-loop collinear relationship exhibited by PC1. The observation of the general trend for Figure 4-27 leads to the conclusion that: with all the other operating conditions fixed, the combination of decreasing influent $[NO_3^-]$, increasing influent $[NH_4^+]$, decreasing $\mu_{m,\ H}$ and increasing $K_{s,\ [COD]}$ lead to an increase in the corresponding sample scores on PC1. This trend is well exhibited by sample 301 which has the biggest scores onto PC1, because this sample is simulated with the lowest influent $[NO_3^-]$, $\mu_{m,\ H}$ and highest influent $[NH_4^+]$ and $K_{s,\ [COD]}$ among all the samples in base case.

4.4.4.2 Principal Component 2

Figure 4-28 shows the scores of the samples on the second principal component. In contrast to the scores for PC1, there is no sample with extremely large scores on PC2. Scores are distributed evenly between -3 to +4. It is clear that there are again seven major groups of samples corresponding to the seven levels of changes in the influent $[NO_3^-]$. Samples within each group are differentiated by the influent $[NH_4^+]$. The repeating pattern of the seven groups indicates that difference of the influent $[NO_3^-]$ change does not cause big difference in the sample scores on the PC2. Inside each group, the scores change gradually from positive scores to negative scores as the influent $[NH_4^+]$ changes from –15% to +15% of its nominal value. The bigger the deviations from the nominal cases, the bigger the sample scores are on PC2.

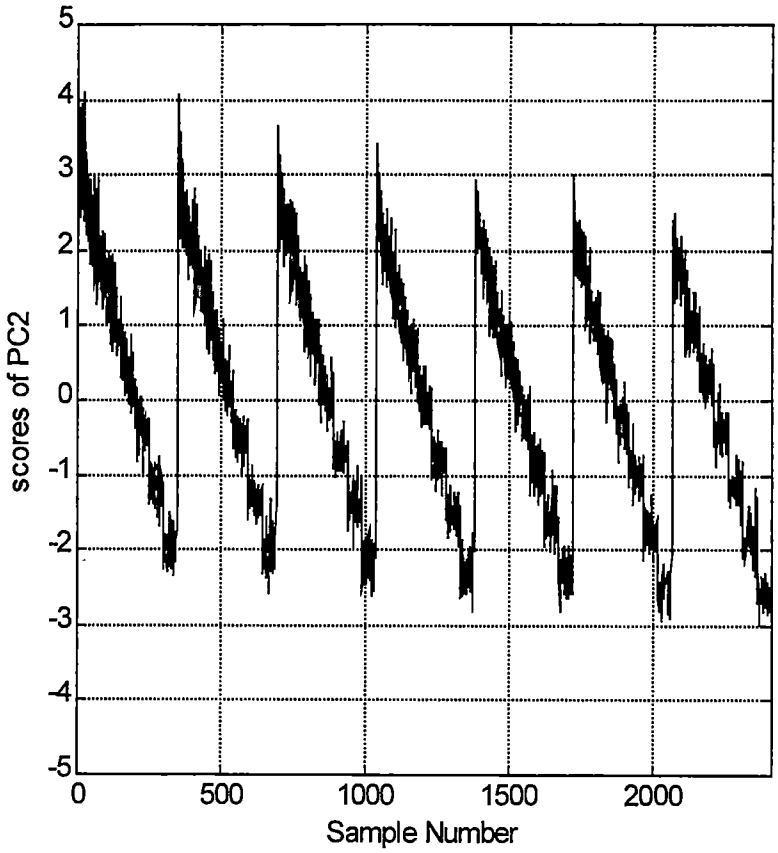

Figure 4-28. Scores Plot for PC2

4.4.4.3 Principal Component 3

Figure 4-29 is the scores plot for PC3. The pattern is less clear for this case than that for PC1 and PC2 cases. The scores of samples are distributed around zero. Similar to scores plot of PC2, there is no sample having much larger scores than others.

4.4.4.4 Other Principal Components

Scores plot for PC4 to PC6 exhibit less trend than PC3. They will not be discussed further here.

4.5 Establishing 'Nominal Operation' Domain

A PCA model is calculated from the historical data that represents the nominal operation region. Under 'normal' operation, the process measurements are shown to cluster in a well-defined region in the (t1-t2) and (t1-t2-t3) space with small values of Squared-Prediction-Error (SPE). This clustering region is defined as the 'nominal operation' region. Future process observations are then referenced against this 'nominal' model. The two most popular graphical presentations of the reference model are the monitoring charts of two/three dimensional plots of the scores, and the SPE plots. These two types of MSPC charts are used in this study to monitor the process.

A PCA model has been developed by keeping the first 6 principal components. Pretreated base case data is projected onto the subspace spanned by these 6 PC's. The error of fitting by the PCA model is defined as the length of the difference vector between each sample in the original pretreated data and its

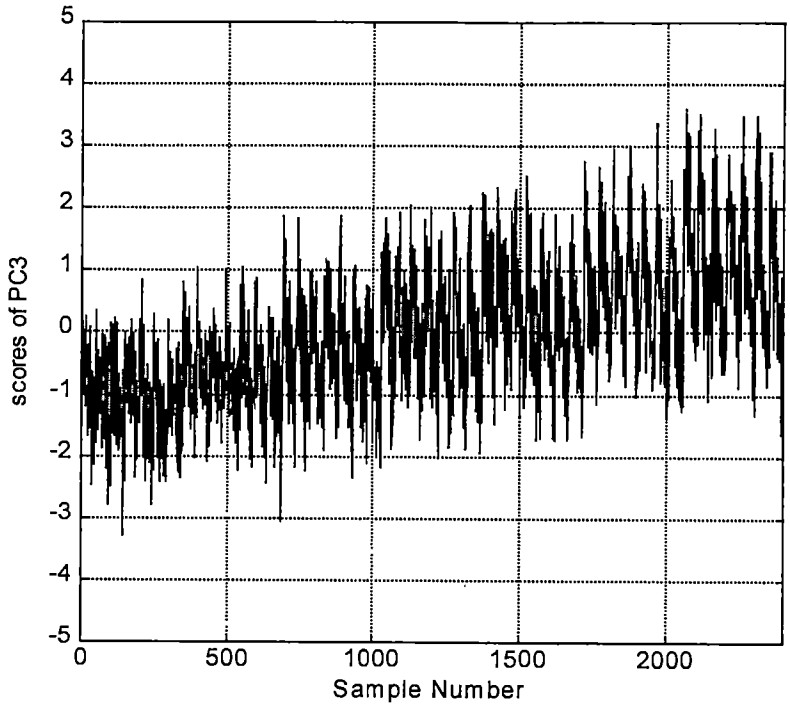

Figure 4-29. Scores Plot for PC3

corresponding projection in the 6-dimensional subspace. SPE for each sample is calculated by equation (8) in Section 3.5.2.

Figure 4-30 is the scores plot of the 2401 samples onto PC1 and PC2. Figure 4-31 is the three-dimensional scores plot with scores on PC3 as well. A highly clustering region around the origin exists in both figures. This clustering region defines the 'nominal operation' domain for the monitoring scores chart.

Figures 4-32 and 4-33 are SPE plots. Figure 4-32 is the SPE versus PC1 and PC2 chart. Figure 4-33 is a chart of SPE versus indexed sample numbers. Both SPE charts show that most of the samples cluster in the low residual area. This area has higher sample density. The biggest SPE occurs at sample number 1915. Its SPE is 10.92. The operating conditions of this sample is +14% [NO_3^-], +5% [NH_4^+] and –21% $\mu_{m,\ H}$ and +7% $K_{s,\ [COD]}$. Different from expectation, the sample with maximum error did not result from the combination of the extremal operating conditions. It may be a result of the nonlinearity of the system.

4.6 Simulating 'Abnormal Operations'

To evaluate the capability of such a series of multivariate statistical process control charts to detect abnormal operating deviations, several cases of faults have been simulated. Abnormalities can enter the system in two different ways. The first type of abnormalities is simulated by introducing a larger than normal change in one or more of the operating variables, such as the influent flow rate or concentrations. In this case, the essential relationship among the process

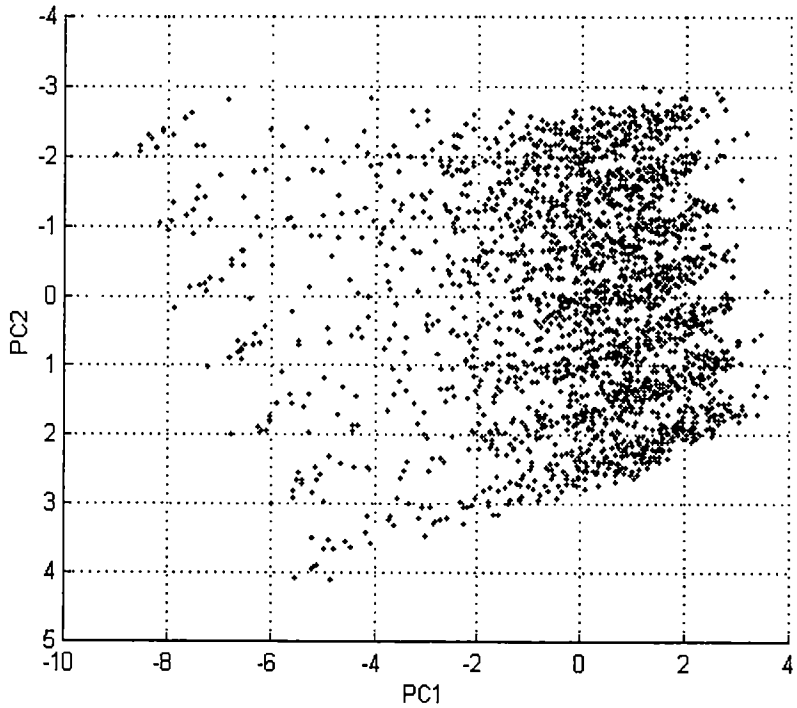

Figure 4-30. Scores Plot for Principal Components 1 and 2

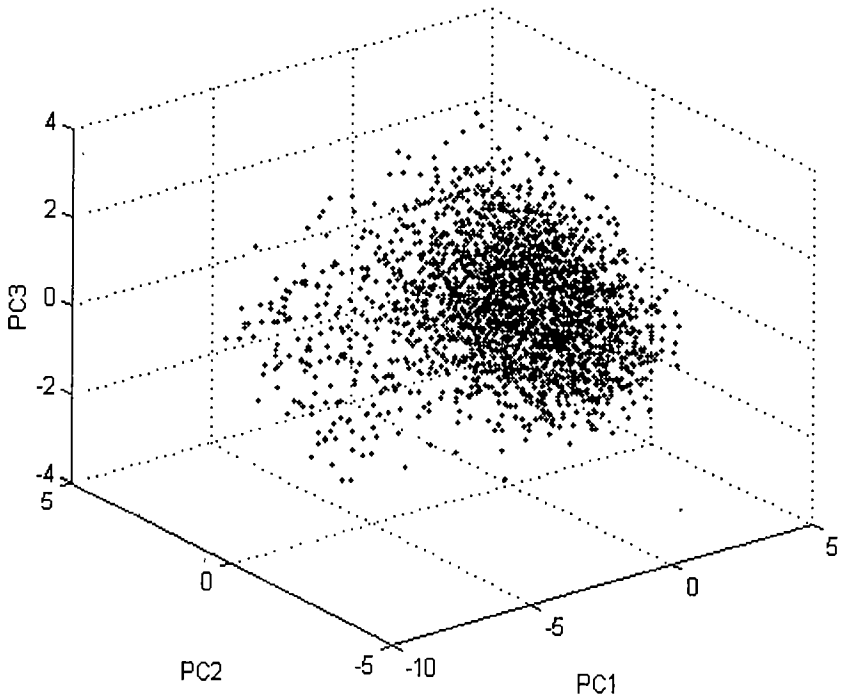

Figure 4-31. Scores Plot for Principal Components 1, 2 and 3

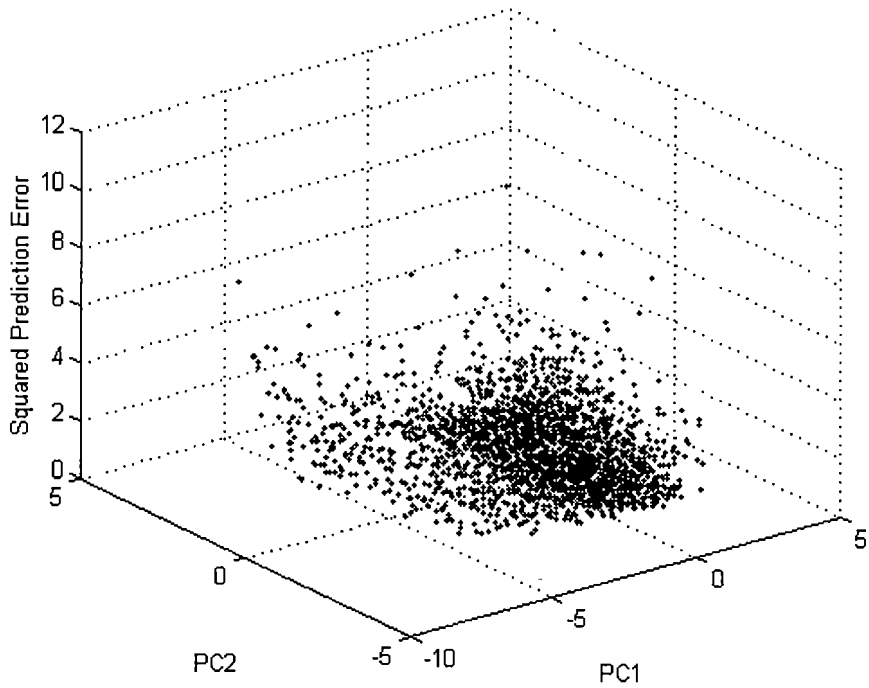

Figure 4-32. SPE Plot for PC1- 2

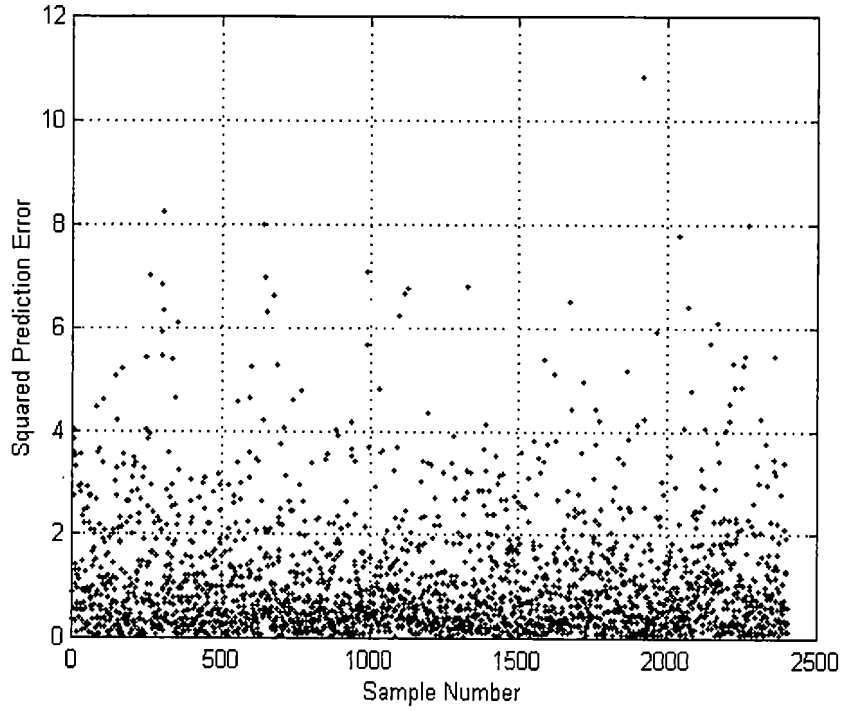

Figure 4-33. SPE Plot (SPE versus Sample Number)

variables has not been altered, only the forcing function terms are different. Therefore, this type of abnormality will possibly result in a shift of the t1-t2-t3 scores to outside the normal operating region but should not result in a shift of the SPE to outside of the acceptable region, indicating the PCA model still fit the new data relatively well.

The second type of abnormality is simulated by introducing plant/model mismatch. In this case, the relationship among the process variables is being changed, because one or more of the process dynamic equations' parameters are being changed. Therefore, after fitting with the base case PCA model, this type of abnormality would most probably increase the associated SPE, possibly together with a drift out of the normal t1-t2-t3 scores region.

In this study, four cases of abnormalities, belonging to the above two categories, are simulated. The first two are non-plant/model mismatch abnormalities. The last two are abnormalities related to model variation.

The first group is simulated by introducing a new disturbance to the system that was not encountered in the reference database generation. The new disturbance is a +20% change in the influent flow rate.

The second group is simulated by introducing bigger than 'normal' disturbance to the system. An increase in the influent [NO_3^-] to 30% - 40% of its nominal value and the influent flow rate to 10% - 20% of its nominal value was introduced. The amount of changes for these two inputs in the base case are from –21% to +21% and zero, respectively. All the other operating conditions remain at

some values within the set regarded as normal. Factorial design is used to generate a small data matrix of the abnormal operations based on varying the two factors: the influent [NO_3^-] and the influent flow rate. The data matrix size for this group is 36x12, 36 observations in 12 variables.

The third group is generated by introducing larger than 'normal' biological parameters with –50% to –40% change in the $\mu_{m,\ H}$ and +50% to +60% in the $K_{s,\ [COD]}$. The amount of changes for these two parameters in the base case is from –21% to +21%. The other two operating conditions taken into account in the base case model, the influent [NO_3^-] and the influent [NH_4^+], are fixed at their nominal values in this case. The data size obtained is 100x12.

The fourth group is simulated with a new biological event: changes in the maximum growth rate of autotrophic biomass, $\mu_{m,\ A}$. This bio-parameter is the only operating condition changed in this group of simulations. The other four operating conditions varied in the base case generation remain at their nominal values. The parameter $\mu_{m,\ A}$ varies from –30% to –20% of its nominal value. The data size for this group of abnormality is 51x12.

4.7 Validating PCA Model Using 'Normal'/'Abnormal' Cases and Identifying Causes for 'Abnormal' Cases

Now the PCA model has been developed and different sets of data corresponding to 'abnormal operations' have been generated. It is time to test how good the base case model is in serving as a reference to flag 'out of normal' operations. The new observations, mean-centered and scaled with that used for the

base case model, are projected onto the reference PCA model to assess its fitness. Thus, abnormality is expected to be detected by plotting various monitoring charts and possible root causes to be identified. Before testing the PCA model with 'abnormal cases', one case from the reference database development is displayed below to show the performance of 'normal' case on the PCA monitoring charts.

Once an abnormality is detected, it is useful to find an assignable cause so that the operating personnel will be advised as to which combination of variables to look into to drive the system back to the normal situation. MSPC is much more powerful than USPC and other process control methods in providing diagnostic information in this regard. By observing the t-scores plot and the SPE plot, one can distinguish between a bigger-than-normal disturbance and a plant/model mismatch. Besides that, contribution plot discussed in Section 3.9 makes it possible to trace back the responsible measurement variables for the deviation occurring in the t-scores and SPE plot. For a well-developed monitoring and diagnostic system, contribution plot can be made on-line, along with the monitoring charts. Once fault is detected by either the t-scores or the SPE plot, contribution plot will indicate the group of variables that might cause this abnormality and to help the operating personnel to hypothesize for an assignable cause. Therefore, for some of the following abnormal case studies, diagnostic plots (contribution plots) are shown in association with the monitoring charts.

4.7.1 Normal Case: +15% Changes in the Influent [NO_3^-] and [NH_4^+]

Figures 4-34 to 4-37 correspond to the MSPC charts for a +15% change in the influent [NO_3^-] and [NH_4^+] initiated at time t=10 days. This set of operating condition is one of the cases included in generating the reference database. The maximum positive changes for the influent [NO_3^-] and [NH_4^+] are +21% and +15%, respectively. It is expected that the steady state scores and SPE of this sample should fall inside the 'normal operation' region defined by the reference case.

Figures 4-34, 4-35 are the scores plot for PC1, 2, 3 and SPE plot for PC1, 2, respectively, but also showing the transient response scores as well. Some of the transient score observations fall outside of the 'normal operation' domain when disturbance introduced in the base case enters the system. At t=0, the system is at the original steady state. In both charts, the projection of the data corresponding to t=0 appears around the origin. At t=10 days, disturbance is introduced into the process which leads to eventual deviation from its original value. However, the deviation starting at t=10 days is not big enough for the system data to drift out of the acceptable region in both monitoring charts. At t=20 days, the projections of new operating points result in out-of-the-normal-clustering in both figures. In the scores plot, the projection at t=20 days deviates from the acceptable region somewhat while in the SPE plot, the SPE rises to a value much larger than the upper limit. After 20 days, the deviation decreases gradually and finally converges toward a new steady state within the 'normal operation' region. Because the

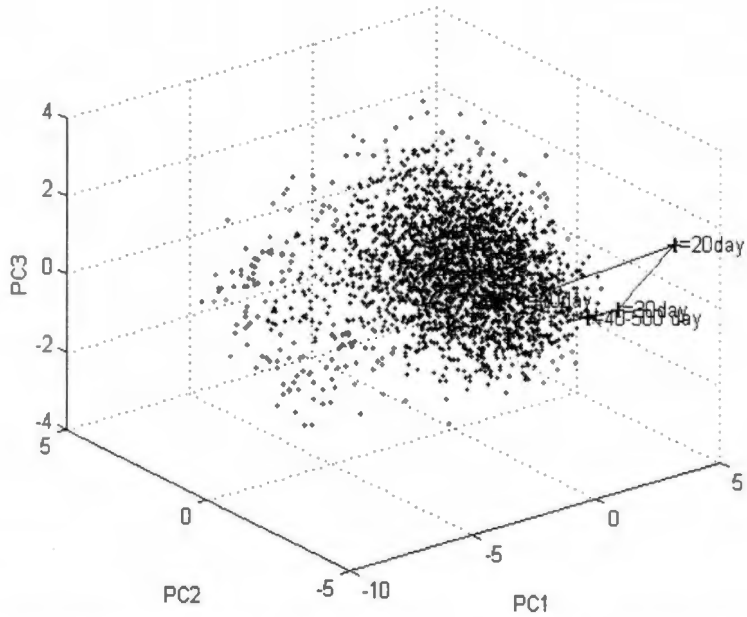

Figure 4-34. Scores Plot for Principal Component 1, 2 and 3. (. =Reference Data; + = Data from the Transient Response with +15% Influent [NH_4^+] and +15% [NO_3^-] Changes)

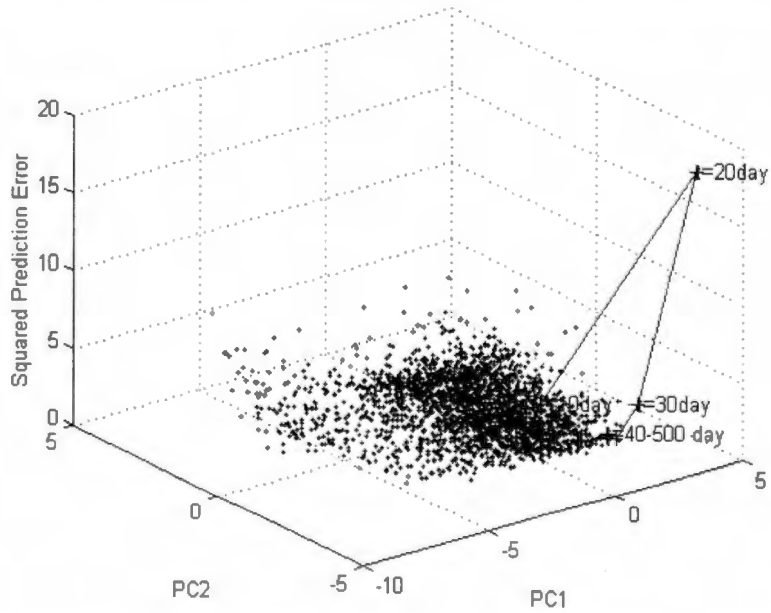

Figure 4-35. SPE Plot for Principal Component 1 and 2 (. =Reference Data; + = Data from the Transient Response with +15% Influent [NH_4^+] and +15% [NO_3^-] Changes)

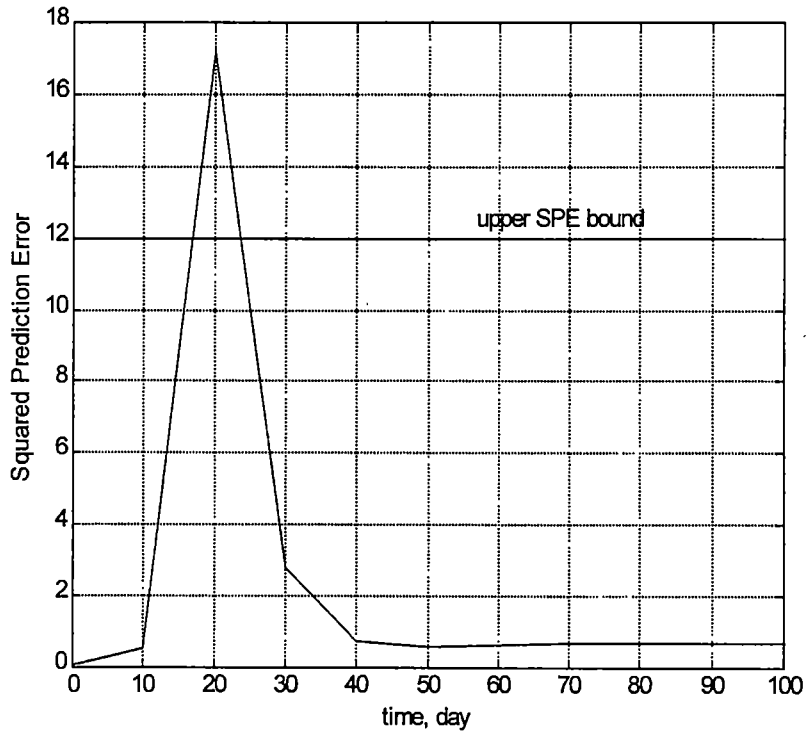

Figure 4-36. SPE Plot over Time. (Transient Response with +15% Influent [NH_4^+] and +15% [NO_3^-] Changes. Upper SPE Bound is Obtained from the SPE of Reference Case.)

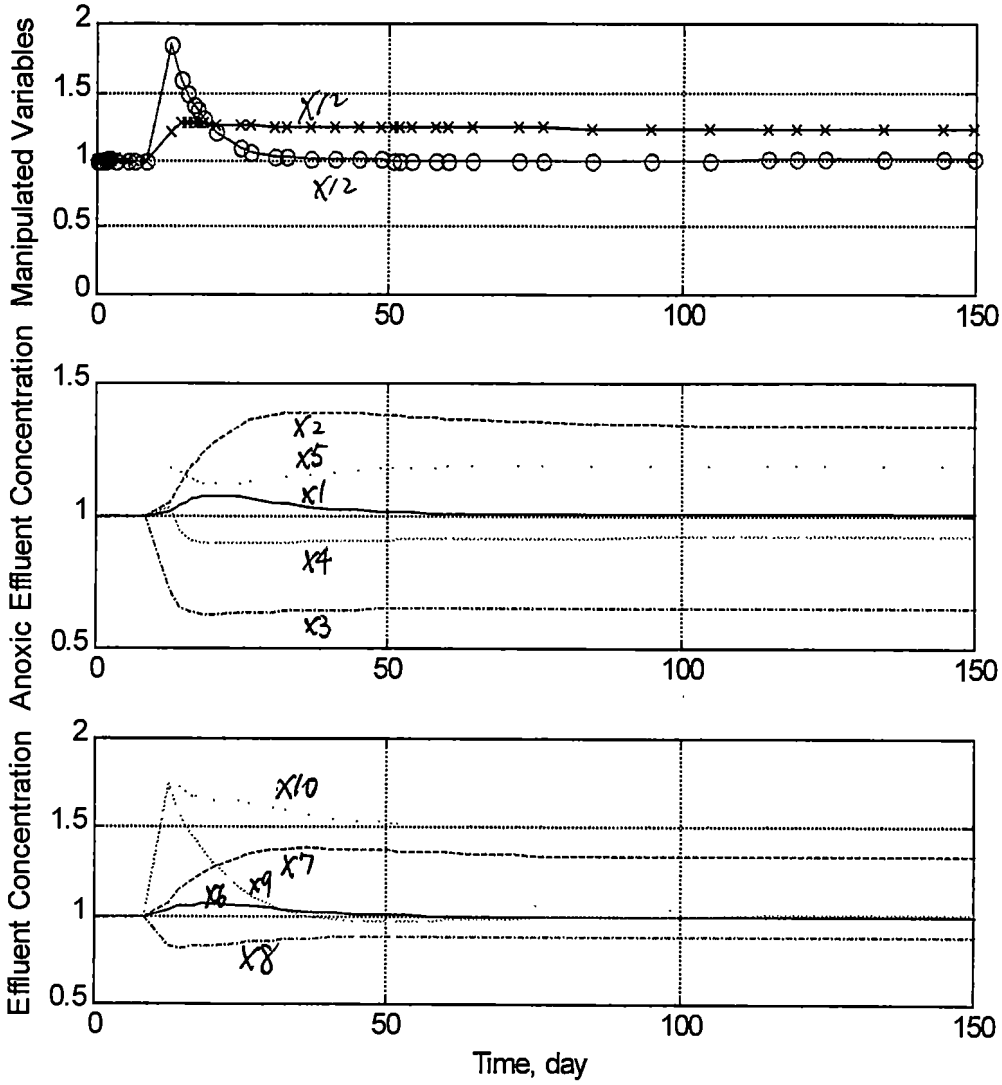

Figure 4-37. 2x2 IMC Closed-Loop Response with +15% Influent $[NH_4^+]$ and +15% $[NO_3^-]$ Changes
a) Manipulated Variables: Recirculation Ratio (x11), x; Sludge Age (x12), o;
b) c) Other Process Variables: [Biomass], $_H$ (x1, x), -; [Biomass], $_A$ (x2, x7), --; [BOD] (x3, x8), -.; $[NH_4^+]$ (x4, x9), ...; $[NO_3^-]$ (x5, x10), . .
Controlled Variables: Effluent [BOD] (x8) and Effluent $[NH_4^+]$ (x9)

case development, the final steady state value of this case is expected to be inside the 'normal operation' region, and is shown to be the case as seen in Figures 4-34 and 4-35.

Figure 4-36 is the SPE versus time plot. Its behavior is similar to that displayed in the previous figures. The SPE starts to increase from t=10 days, when the disturbance is introduced and reaches a maximum at t=20 days, followed by a decrease toward its new steady-state after 40 days.

In monitoring the system response, one may worry about the transient observations that start to migrate out of the acceptable region, for instance, starting at t=20 days in Figures 4-34 to 4-36. Previous investigation of the process suggests a time constant τ around 40 days. Therefore, adjustment of the process operation condition should not be undertaken more frequently for intervals shorter than that of the time constant. Persistent deviations that last longer than time constant would need attention from the operating personnel.

Figure 4-37 is the time response curve for each of the twelve process variables. The transient response lasts from t=10 to 20 days, approaching steady state thereafter by 50 days.

In this case, all observations after meeting new steady states are well within the 'normal operation' region, for both the scores and the SPE. Transient behavior is often out of the acceptable 'normal operation' region. This transient response should not be regarded as the system being in a state of 'out of control'. Rather one should assess the state of control when the system is more or less in a steady state

mode and should wait out for a period of time beyond that of the system's time constant before forming a conclusion.

4.7.2 Abnormal Case 1: +20% Changes in the Influent Flow Rate

Figures 4-38 to 4-42 are MSPC plots corresponding to the case with a +20% change in the influent flow rate introduced at time t=10 days. This operating condition is not included in the reference database generation. The flow rate term appears in the forcing function of the set of 'kinetic equations' used by the simulator development. Therefore, a change in the influent flow rate does not constitute a change in the basic model structure. It is expected that the scores of the new points may fall outside the 'normal' scores region but not the SPE. Instead of one group of data being simulated, it is only one observation simulated in this case. The migration of this new sample on the scores plot and SPE plot over time is shown in the following figures.

Figures 4-38 and 4-39 are the scores plots for PC1, 2, 3 and PC2, 3, respectively. The transient response curve starts around the origin and migrates out of the acceptable region, reaching a maximum at 20 days. After that time, the scores come back toward the normal clustering, and settle at a new steady state somewhat outside the 'normal operation' region. Figure 4-39 is a close up of Figure 4-38 showing the scores on PC2 and 3.

Figures 4-40 and 4-41 are the corresponding SPE plots. Figure 4-40 is the SPE for PC1 and PC2. Figure 4-41 is the SPE monitored over time. Both figures

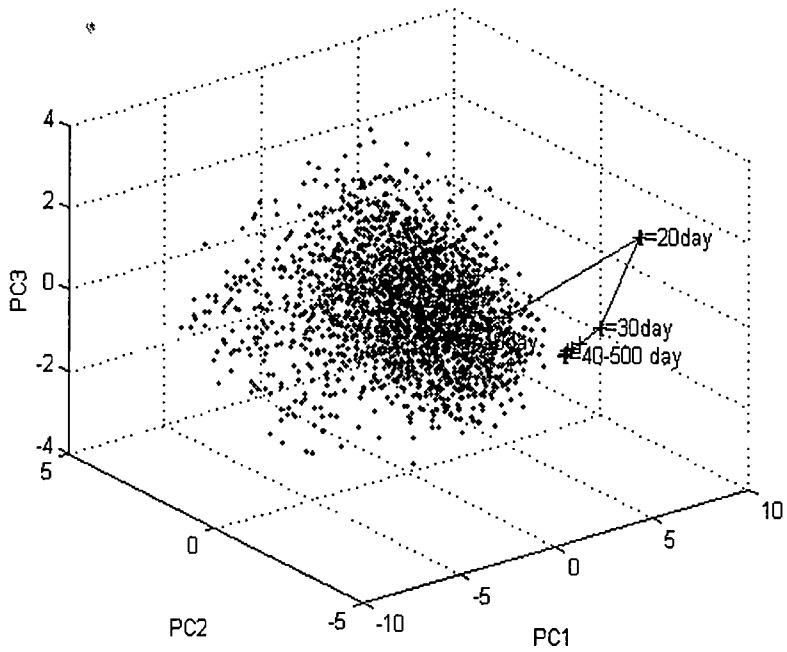

Figure 4-38. Scores Plot for Principal Component 1, 2 and 3. (. =Reference Data; + = Data from the Transient Response with +20% Influent Flow Rate Changes)

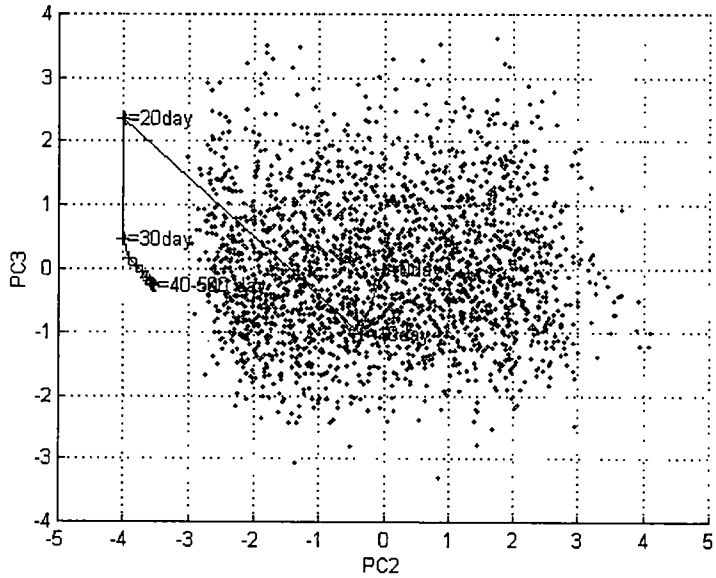

Figure 4-39. Scores Plot for Principal Component 2 and 3 (. =Reference Data; + = Data from the Transient Response with +20% Influent Flow Rate Changes)

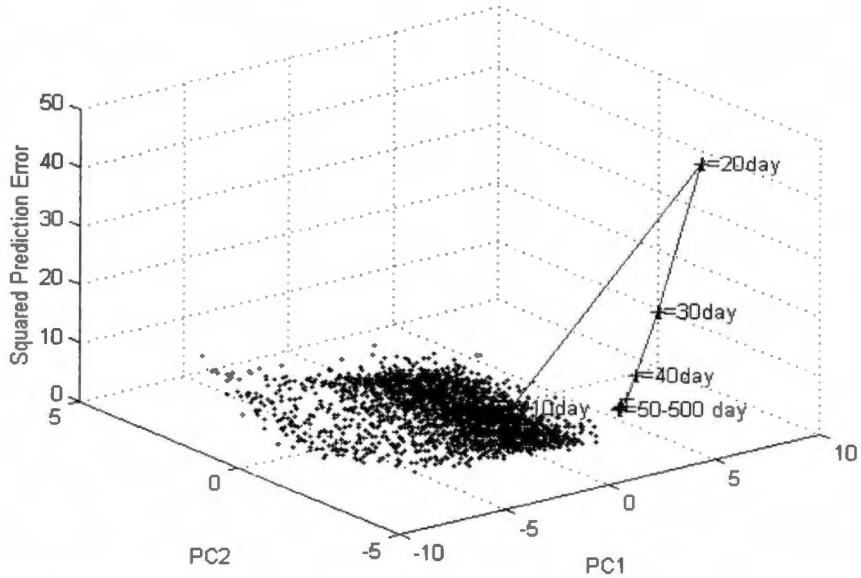

Figure 4-40. SPE Plot for Principal Component 1 and 2 (. =Reference Data; + = Data from the Transient Response with +20% Influent Flow Rate Changes)

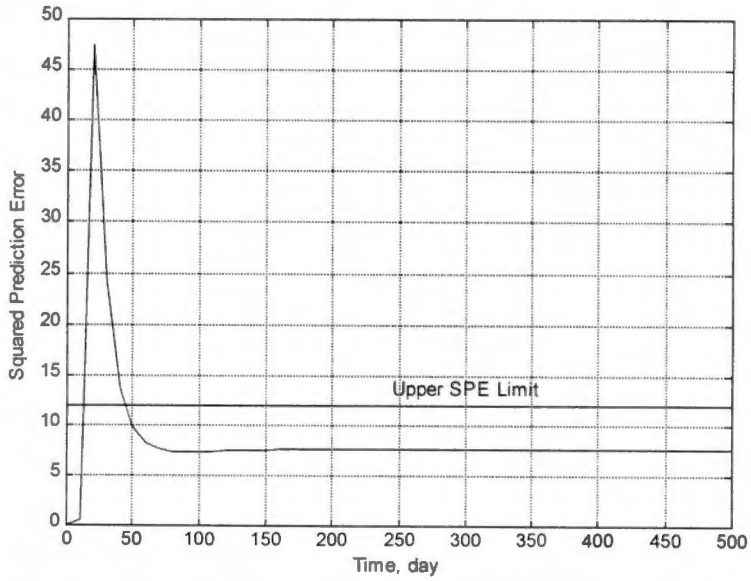

Figure 4-41. SPE Plot over Time. (Transient Response with +20% Influent Flow Rate Changes. Upper SPE Limit is Obtained from the SPE of Reference Case)

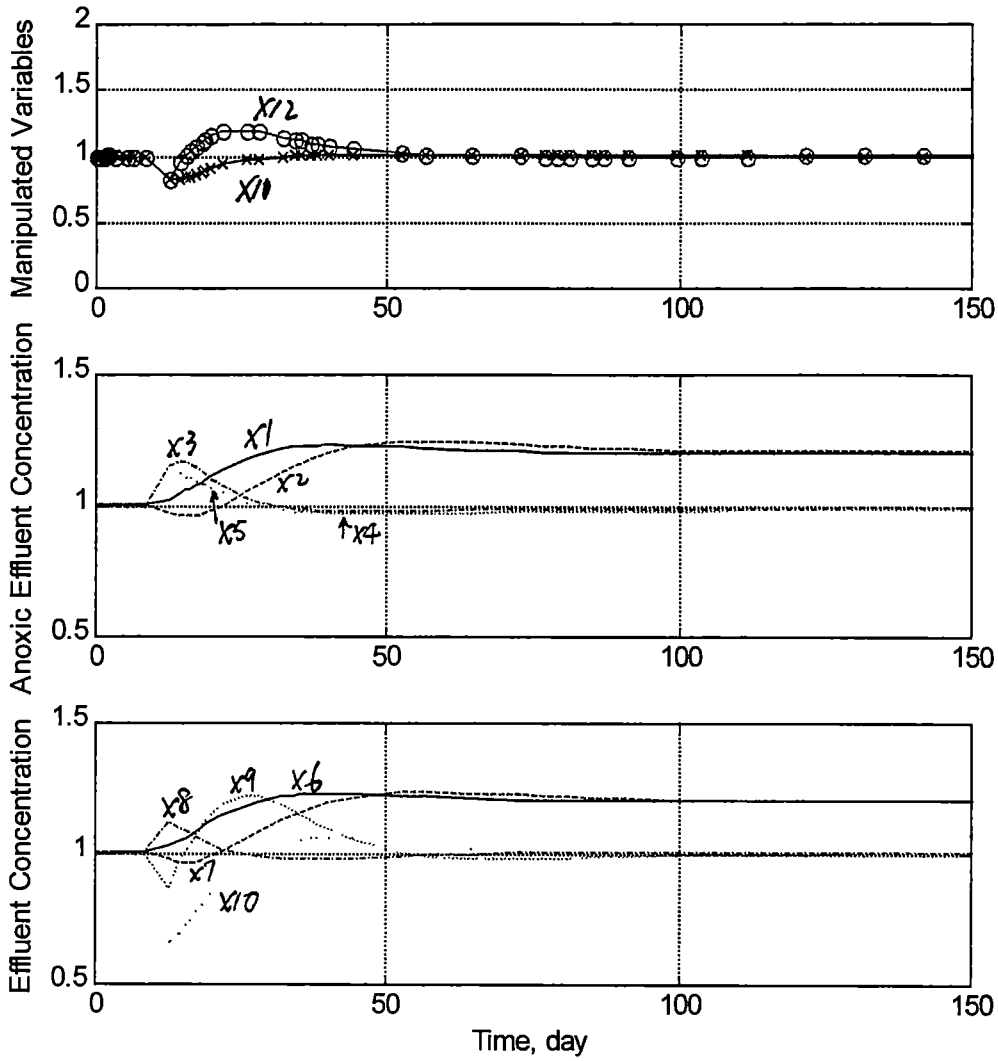

Figure 4-42. 2x2 IMC Close-Loop Response with +20% Influent Flow Rate Changes
a) Manipulated Variables: Recirculation Ratio (x11), x; Sludge Age (x12), o;
b) c) Other Process Variables: [Biomass], $_H$ (x1, x6), -; [Biomass], $_A$ (x2, x7), --; [BOD] (x3, x8), -.; [NH_4^+] (x4, x9), ...; [NO_3^-] (x5, x10), . .
Controlled Variables: Effluent [BOD] (x8) and Effluent [NH_4^+] (x9)

show that after a temporary out-of-'normal operation' occurring from around t=10 to t=45 days, the process settles down at a new steady state with a final SPE smaller than the upper SPE limit. The temporary 'out of bound' takes place within the time constant. These upsets should not be deemed as 'abnormal' and therefore the operating personnel should not yet to take corrective action. These plots imply that the new event does not reflect a change in the model itself. Otherwise, the new steady state SPE will be larger than that of the upper control limit. The influent flow rate shows up as a forcing term in the differential equations describing the process dynamics. Therefore it does not alter the intrinsic model of the process itself, but rather would result in the process operating at a higher (or lower) steady state regime compared to that of the base case.

Figure 4-42 is the IMC closed-loop time response for this case - +20% change in the influent flow rate introduced at t=10 days. The disturbance entering the system causes some of the process variables to reach new steady state. It takes 30-50 days for process variables to settle down to new stable values.

4.7.3 Abnormal Case 2: +30% to +40% Changes in the Influent [NO_3^-] and +10% to +20% Changes in the Influent Flow Rate

4.7.3.1 Modeling Abnormal Case 2

Figures 4-43 to 4-46 are the monitoring charts for this group of 'abnormal' operations, with fixed influent [NH_4^+], $\mu_{m,\ H}$ and $K_{s,\ [COD]}$, but bigger than normal influent [NO_3^-] and a new disturbance – that of flow rate change. Figures 4-47 and 4-48 are the charts for the transient response of one sample of the observations

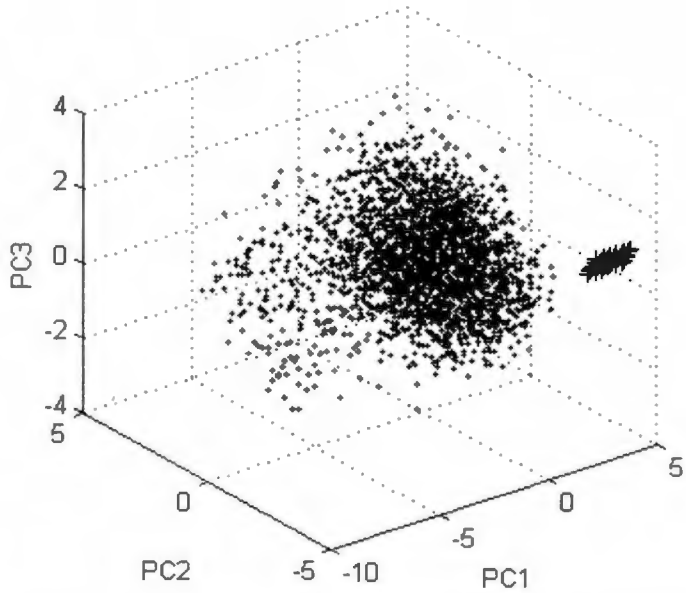

Figure 4-43. Monitoring Chart. Score Plot for Principal Component 1, 2 and 3 (. =Reference Data; + = Data of +15% Influent [NH_4^+], +21% $\mu_{m,\ H}$, -21% $K_{s,\ COD}$, +30%-+40% [NO_3^-] and +10%-+20% Flow Rate Changes)

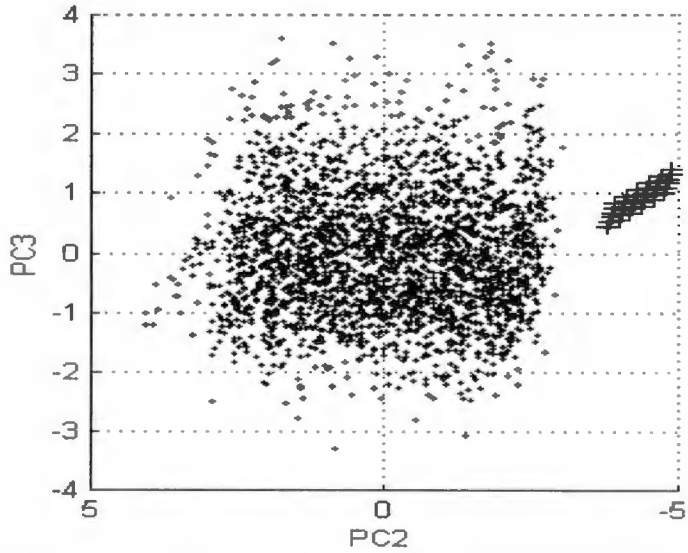

Figure 4-44. Monitoring Chart. Score Plot for Principal Component 2 and 3 (. =Reference Data; + = Data of +15% Influent [NH_4^+], +21% $\mu_{m,\ H}$, -21% $K_{s,\ COD}$, +30%-+40% [NO_3^-] and +10%-+20% Flow Rate Changes)

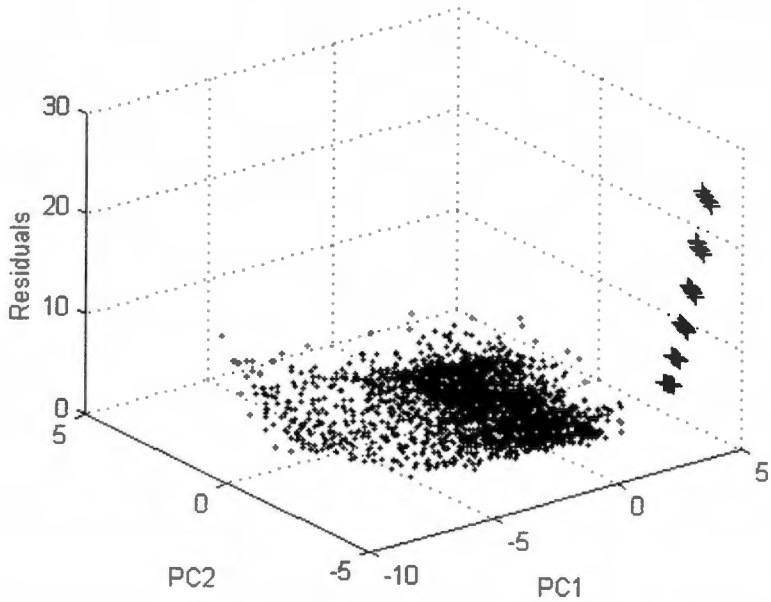

Figure 4-45. Monitoring Chart. SPE Plot for Principal Component 1 and 2 (. =Reference Data; + = Data of +15% Influent [NH_4^+], +21% $\mu_{m,\,H}$, -21% $K_{s,\,COD}$, +30%-+40% [NO_3^-] and +10%-+20% Flow Rate Changes)

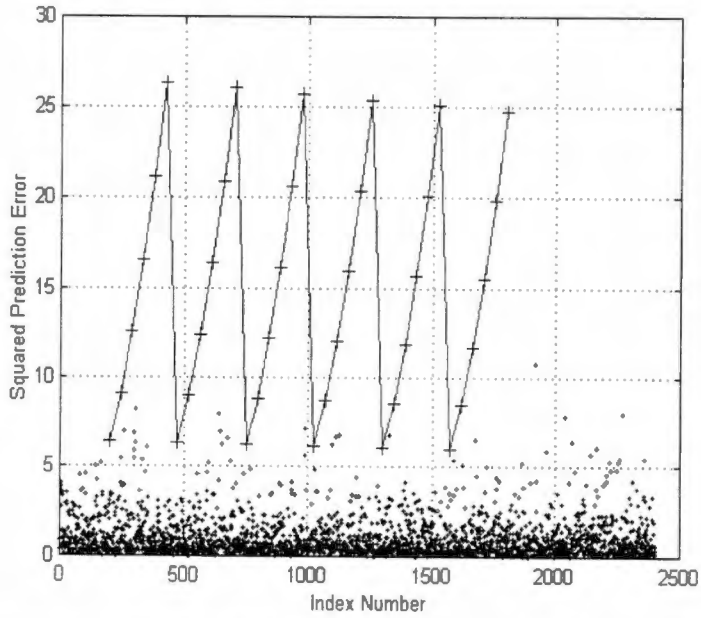

Figure 4-46. Monitoring Chart. SPE Plot (. =Reference Data; + = Data of +15% Influent [NH_4^+], +21% $\mu_{m,\,H}$, -21% $K_{s,\,COD}$, +30%-+40% [NO_3^-] and +10%-+20% Flow Rate Changes)

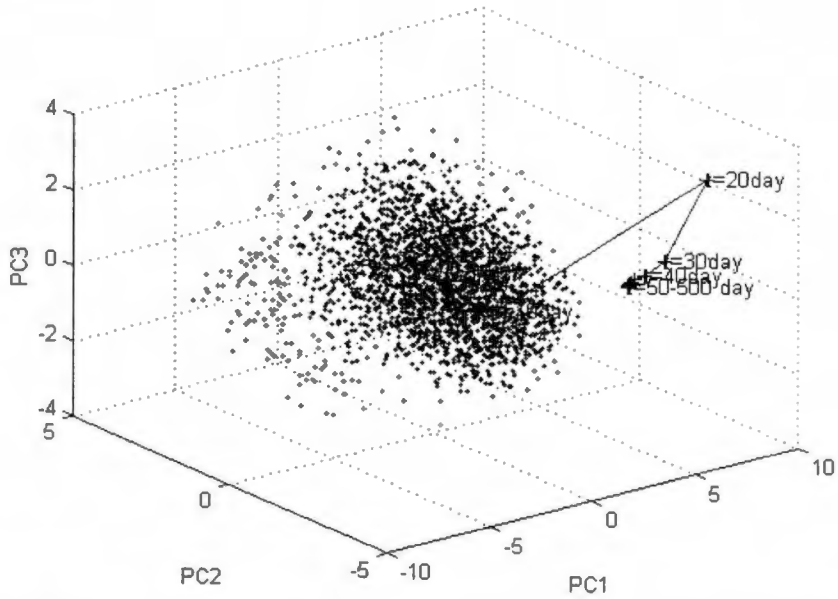

Figure 4-47. Monitoring Chart. Score Plot for Principal Component 1,2, 3 (.=Reference Data; + = Data of Transient Response of +15% Influent [NH_4^+], +21% $\mu_{m,\ H}$, -21% $K_{s,\ COD}$, +40% [NO_3^-] and +10% Flow Rate Changes)

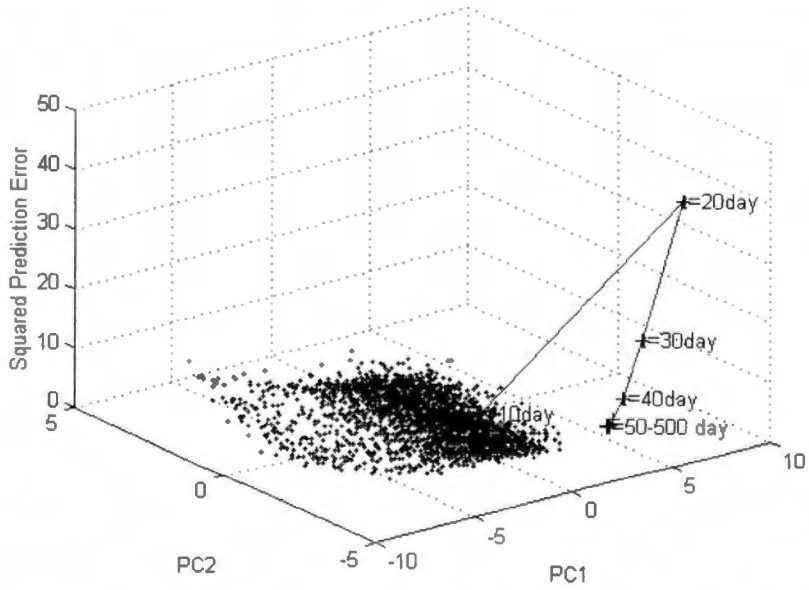

Figure 4-48. Monitoring Chart. SPE Plot for Principal Component 1 and 2 (. =Reference Data; + = Data of the Transient Response of +15% Influent [NH_4^+], +21% $\mu_{m,\ H}$, -21% $K_{s,\ COD}$, +40% [NO_3^-] and +10% Flow Rate Changes)

from this group. Its operating condition is: +10% change in the influent flow rate, +40% change in the influent [NO_3^-], +15% change in influent [NH_4^+], +21% change in the $\mu_{m,\,H}$ and –21% change in the $K_{s,\,[COD]}$.

In Figures 4-43 and 4-44, steady state values of the new observations obtained at several new levels of the influent [NO_3^-] and feed rate conditions are observed to be out of the 'normal operation' region, which is an early warning that some kind of abnormal deviation has occurred. According to the previous section, out-of-bound in the scores plot suggests a root cause of bigger than normal variation in the operating condition. Whether this abnormality is associated with a model shift or not is determined by the SPE plot. Figures 4-45 and 4-46 are the corresponding SPE plots for this case. It seems that most of the observations lie beyond the upper SPE limit, which suggests a model shift as well. A clearer view is shown in Figure 4-46, in which sample index is in the x-axis. It is apparent that a range of SPE variation exists, peaking at about 26 SPE units. Tracing the SPE variation back, it is found that each of the six groups, from left to right, is in the order of increasing influent [NO_3^-]; each of the six observations within a group, from left to right, is in the order of increasing influent flow rate. It shows that increasing the influent [NO_3^-] does not affect SPE much; but increasing influent flow rate raises SPE drastically. In Figure 4-46, the six smallest SPE observations are those with +10% change in the influent flow rate and different levels of the influent [NO_3^-]. The highest six observations are those with +20% change in the influent flow rate and different levels of [NO_3^-]. The twelve observations with

smallest SPE in this figure are below the upper SPE limit. Compared with the abnormal case 1 with +20% flow rate change alone, it is very possible that the phenomenon of out of control limit in this case is caused by the nonlinearity of the system. The +20% change in the flow rate alone does not alter the plant model, as supported by the SPE plot in Figures 4-40 and 4-41. In the small neighborhood of the nominal values, which are used to build the process model, the process model describes the process well. Beyond this small neighborhood, plant/model mismatch always exists. In Figures 4-45 and 4-46, the out-of-'normal operation' phenomenon can be explained as the model shift caused by the variation of the operating conditions beyond the linear region of the process model. This SPE deviation may also be caused by the conjunction of two large perturbations to the operating condition. In other words, although bigger than normal [NO_3^-] alone or feed rate change alone will not cause SPE deviation, if they are combined, the overall effect could exceed the upper SPE limit and display an abnormality pattern in the SPE monitoring chart.

Monitoring charts 4-43 to 4-46 provide the information that there are larger than 'normal' changes in the operating conditions because new observations move out of the acceptable region of the scores plot. This is apparently caused by the +30% to +40% change in the influent [NO_3^-] and +10% to +20% in the influent flow rate. In the reference case, the influent [NO_3^-] is changed at most to +21% and flow rate has zero change. It also appears that plant/model mismatch occurs when

the above amount of variations are introduced to the process. It may be either due to the nonlinearity or due to the conjunction of multi-operating condition changes.

Figures 4-47 and 4-48 show the transient scores response for one sample from this case. Since the influent flow rate chosen in this transient study is +10% change of its nominal value, it moves back to the 'normal operation' at its new steady-state in SPE plot 4-48. Scores plot still shows the trend of moving out of the normal region and staying out at steady state.

4.7.3.2 Identifying Cause for One Sample from Abnormal Case 2: +40% Change in the Influent [NO_3-] and +20% Change in the Influent Flow Rate

Figures 4-49 and 4-50 are the contribution plots for one sample from the abnormality case 2, when the influent flow rate has +20% change from its nominal value and the influent [NO_3^-] has +40% change. The t-scores plots, Figures 4-43 and 4-44, show that the deviation in the scores plot occurs along the second principal component direction. Therefore, contribution plot for PC2 is carried out as shown in Figure 4-49. It shows that deviation in the second PC consists mostly of x2 ($X_{B,\ A\ (Anoxic\ Reactor\ Effluent)}$) and x7 ($X_{B,\ A\ (System\ Effluent)}$). Each variable of the two accounts for more than 30% of overall contribution of all twelve variables. Consequently, deviation along PC2 can be assigned to the deviations in the autotrophic biomass concentration from both the anoxic reactor and the clarifier. This conclusion is consistent with the interpretation of loadings plot for PC2 shown

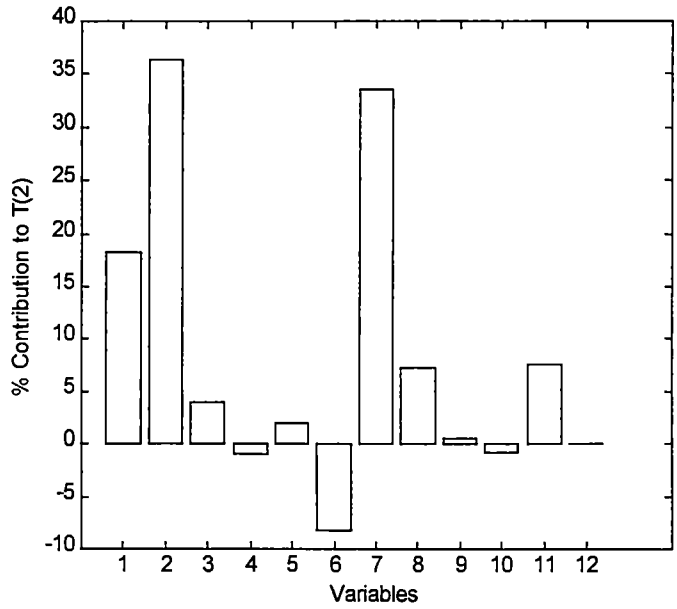

Figure 4-49. Contribution Plot to t-score2 for Abnormality Case 2: +20% Change in the Influent Flow Rate and +40% Change in the influent [NO_3^-]

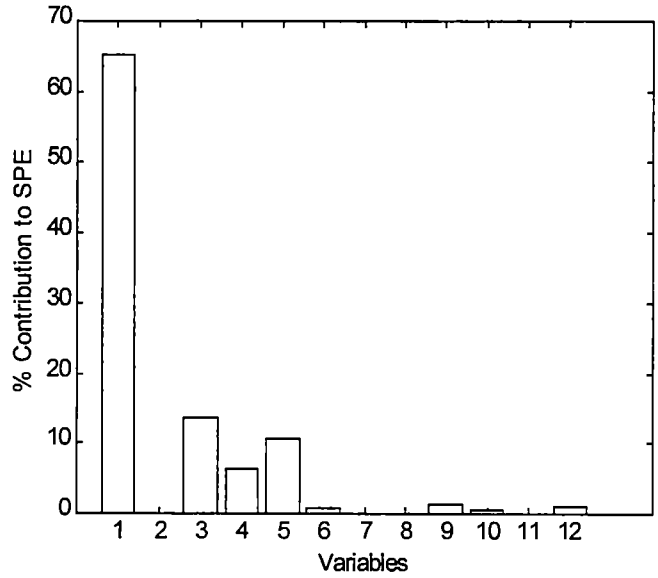

Figure 4-50. Contribution Plot to SPE for Abnormality Case 2: +20% Change in the Influent Flow Rate and +40% Change in the influent [NO_3^-]

earlier in Section 4.4.1.2. PC2 is highly contributed by x2 and x7. Therefore, abnormality in PC2 direction implies an abnormality in either x2 or x7 or both. Also based on Section 4.4.1.2, x2 and x7 are always highly correlated to each other. Hence, deviation in PC2 can be reasonably assigned to x2 and x7.

The contribution plot in Figure 4-49 can suggest to the operating personnel that some factors causing x2 and x7 to deviate from their nominal values are undergoing some bigger than normal variation. Since autotrophic biomass growth is occurring in the aerobic reactor together with the nitrification, its concentration is closely related to the $[NO_3^-]$ in the system. Therefore, this set of contribution plot suggests a bigger than normal deviation in the influent $[NO_3^-]$. Operating personnel is then able to accordingly take corrective actions to this process input in an attempt to drive the system back to 'normal'. Besides this, other inputs possibly responsible for the abnormality are the influent flow rate and $[NH_4^+]$. MSPC can not guarantee to assign the root-cause for any abnormal operation. Instead, it can sometimes provide a handle from where to trace back for those root-causes.

Figure 4-50 shows that the deviation in the corresponding SPE chart is primarily caused by x1 ($X_{B,\ H\ (Anoxic\ Reactor\ Effluent)}$), hetorotrophs concentration from the anoxic reactor. Its contribution to the overall error is bigger than 65%. According to Section 2.2.4, theories of denitrification, larger amount in the influent flow rate as well as $[NO_3^-]$ causes more nitrogen to be removed in the anoxic reactor. More heterotrophic biomass will need to be produced in this reactor to counterbalance against the increased nitrogenous load. Consequently, x1, which

represents the heterotrophic biomass effluent concentration from the anoxic reactor, will depart from its nominal value. That is the major reason causing model misfit error in this case. By means of this, when the SPE monitoring chart indicates unacceptable deviation, contribution plot for the SPE should be developed to indicate responsible process variables. The operating personnel will observe the deviation of x1 from this contribution plot. A deviation on the SPE chart is classified as 'a model shift'. Therefore, the root cause can be hypothesized accordingly to either bio-parameter related to heterotroph growth, for instance, $\mu_{m,H}$, or nonlinearity of the current operation. In our case, it is the nonlinearity or the conjunction of two abnormal operating conditions that cause the abnormality.

4.7.4 Abnormal Case 3: -50% to –40% Changes in the $\mu_{m,H}$ and +50% to +60% Changes in the $K_{s,[COD]}$

4.7.4.1 Modeling Abnormal Case 3

Figures 4-51 to 4-56 show the analysis results for abnormal case 3. In this case, bigger than normal changes are made in the bio-parameters of the process, which will change the process model. It is expected that at least a larger than normal SPE will result.

Figures 4-51 and 4-52 show that the scores of the new observations also move beyond the 'normal' region in PC1, 2 and 3. This trend implies larger than normal changes in the process variables have taken place. In the base case, the biggest negative change in $\mu_{m,H}$ is –21% from its nominal value and the biggest positive change in $K_{s,[COD]}$ is +21%. However, in this case, both biological

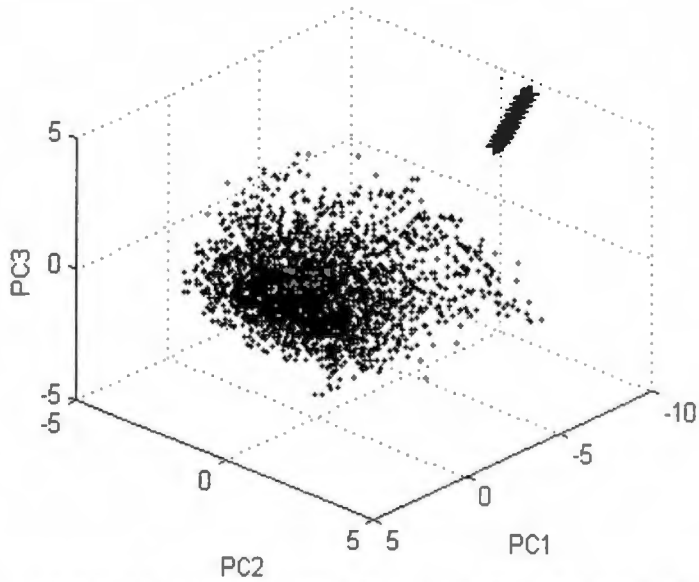

Figure 4-51. Monitoring Chart. Scores Plot for Principal Component 1, 2 and 3 (. =Reference Data; + = Data of -50% to –40% $\mu_{m,\ H}$, +50% to +60% $K_{s,\ COD}$, Changes)

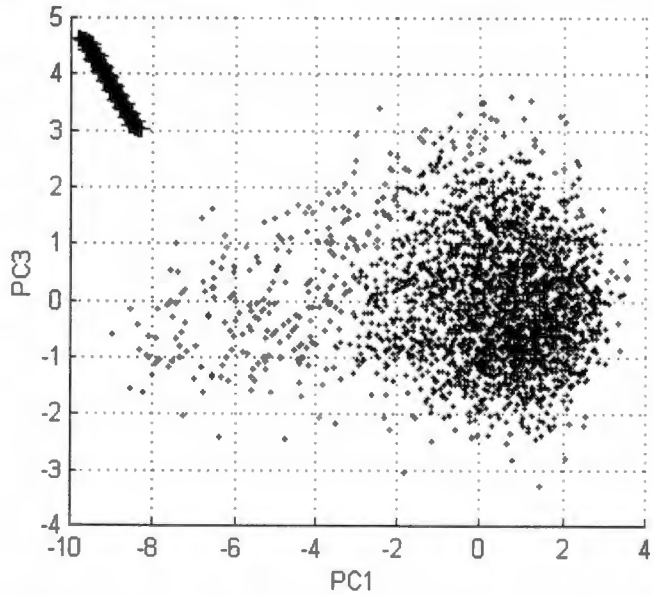

Figure 4-52. Monitoring Chart. Scores Plot for Principal Component 1 and 3 (. =Reference Data; + = Data of -50% to –40% $\mu_{m,\ H}$, +50% to +60% $K_{s,\ COD}$, Changes)

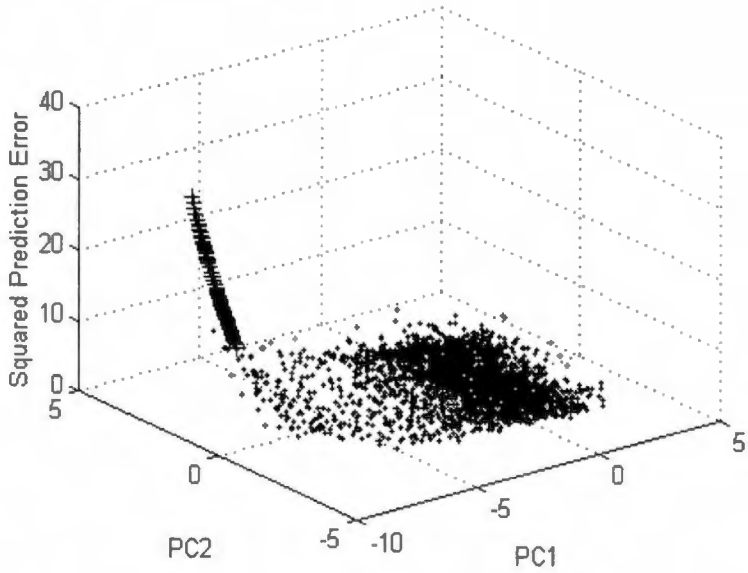

Figure 4-53. Monitoring Chart. SPE Plot for Principal Component 1 and 2 (. =Reference Data; + = Data of -50% to –40% $\mu_{m,\ H}$, +50% to +60% $K_{s,\ COD}$, Changes)

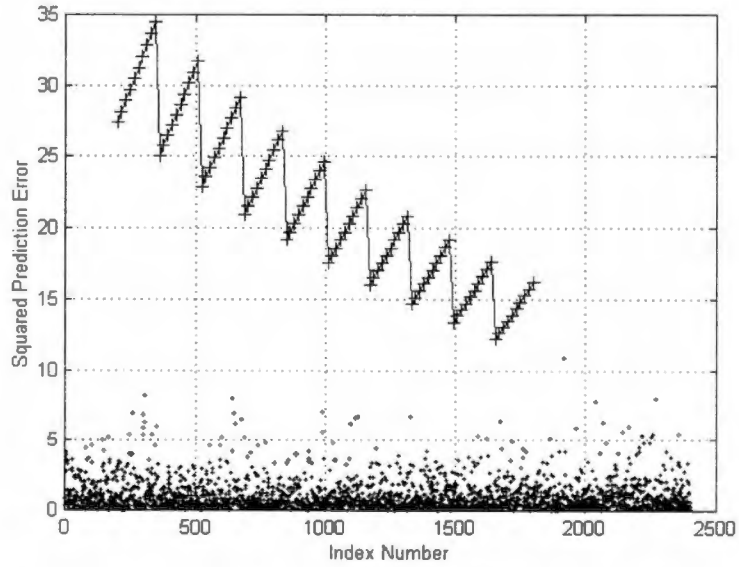

Figure 4-54. Monitoring Chart. SPE Plot (. =Reference Data; + = Data of -50% to -40% $\mu_{m,\ H}$, +50% to +60% $K_{s,\ COD}$ Changes)

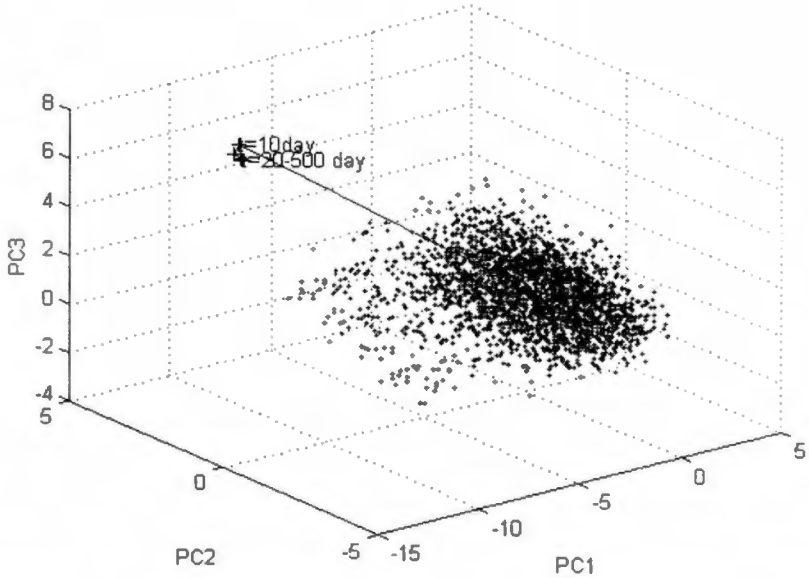

Figure 4-55. Monitoring Chart. Scores Plot for Principal Component 1, 2 and 3 (. =Reference Data; + = Data of Transient Response of -50% $\mu_{m,\,H}$, +60% $K_{s,\,COD}$, Changes)

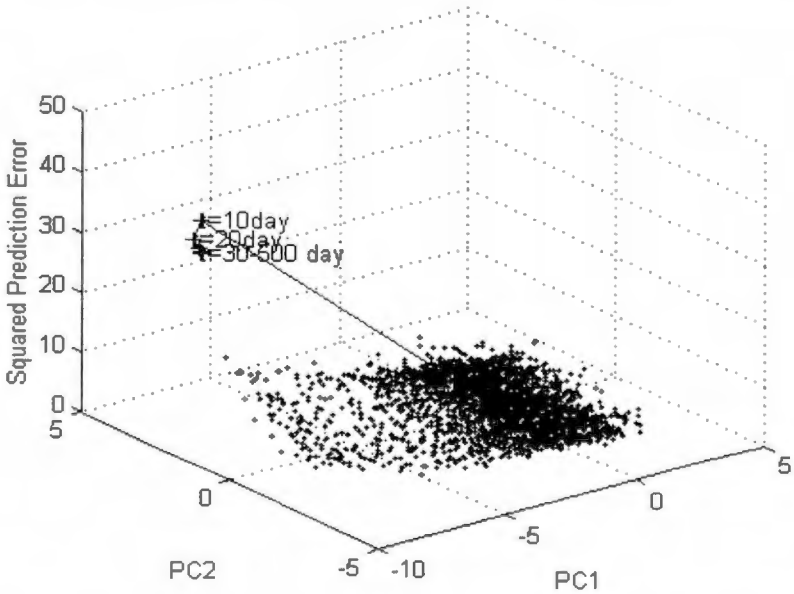

Figure 4-56. Monitoring Chart. SPE Plot for Principal Component 1 and 2 (. =Reference Data; + = Data of Transient Response of -50% $\mu_{m,\,H}$, +60% $K_{s,\,COD}$, Changes)

constants are changed to a level much larger than their maximum changes in the base case, forcing the growth of the heterotrophs to slow down thereby slowing the breakdown of the carbonaceous components as well as the nitrification process. This explains the migration of points to that of out-of-bound occurring in the t-scores plot.

The more drastic impact of changing bio-parameters on the process behavior is shown in the SPE plot of Figures 4-53 and 4-54. The SPE increases to as big as 35 units corresponding to a change of a –50% change in the $\mu_{m,\ H}$ and a +60% change in the $K_{s,\ [COD]}$. The upper SPE limit obtained from the reference case is less than 11. From Figure 4-54, the SPE values are seen to be above the upper limit for the entire range of parameter variation. This clearly indicates that a model shift has occurred. This is caused by the biological parameter variation in the $\mu_{m,\ H}$ and $K_{s,\ [COD]}$ which occur in the terms involving the biomass as well as the organic and nitrate concentrations in the overall mass balance differential equations. In the figure, it is evident that there are ten groups with ten observations in each group. According to the simulation process, from left to right, the groups correspond to increasing values of the $\mu_{m,\ H}$; within each group, from left to right, each sample corresponds to increasing values of the $K_{s,\ [COD]}$ parameter. The behavior of the points illustrates that increasing $K_{s,\ [COD]}$, the half saturation constant for heterotrophs thus slowing down μ, leads to larger errors in the system description; whereas increasing $\mu_{m,\ H}$, the maximum specific growth rate of heterotrophs toward that of nominal, leads to smaller model errors. In this case, $\mu_{m,\ H}$ is varied from

–50% to –40% of its nominal value. Increasing $\mu_{m,\ H}$ towards its nominal value will certainly reduce the modeling error. In contrast, increasing $K_{s,\ COD}$ from +50% to +60% away from its nominal value, is expected to increase plant-model mismatch. It is indeed reflected in the increasing SPE. The consistency between the monitoring charts and the physical interpretation is one of the attractions of the PCA methodology.

Figures 4-55 to 4-56 are the scores and SPE for the transient response for the parameter combination that leads to the worst process deviation in this case of abnormality. At t=0, each response starts from inside the 'normal operation' domain around the origin. It then migrates out of the acceptable bound starting at t=10 days and stays outside at steady state, in both the t-scores and the SPE charts.

4.7.4.2 Identifying Causes of One Sample from Abnormal Case 3: -50% Change in the $\mu_{m,\ H}$ and +60% Change in the $K_{s,\ [COD]}$

In this case, instead of +21% and -21% maximum changes in the $\mu_{m,\ H}$ and $K_{s,\ [COD]}$, -50% change in the $\mu_{m,\ H}$ and +60% change in the $K_{s,\ [COD]}$ are introduced, respectively. Contribution plots are carried out for the sample with -50% change in the $\mu_{m,\ H}$ and +60% change in the $K_{s,\ [COD]}$. Figures 4-57 to 4-59 are the contribution plots for this case.

According to figure 4-51 and 4-52, since new observations do not deviate along the PC2 direction, contribution plot for PC2 is omitted. Figure 4-57 is the contribution plot for PC1 and Figure 4-58 is that for PC3. Figure 4-57 shows that the deviation along PC1 direction is mainly caused by the behavior of x8 ($S_{S\ (System}$

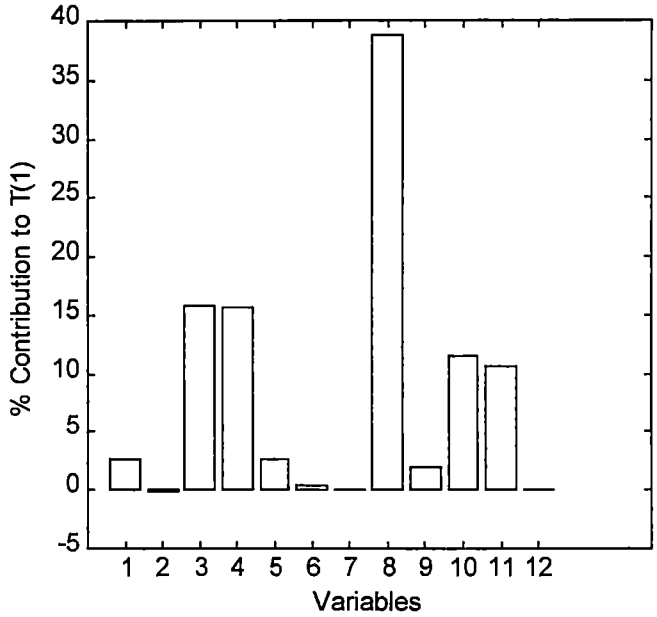

Figure 4-57. Contribution Plot to PC1 for Abnormality Case 3 -50% Change in the $\mu_{m,H}$ and +60% Change in the $K_{s,[COD]}$

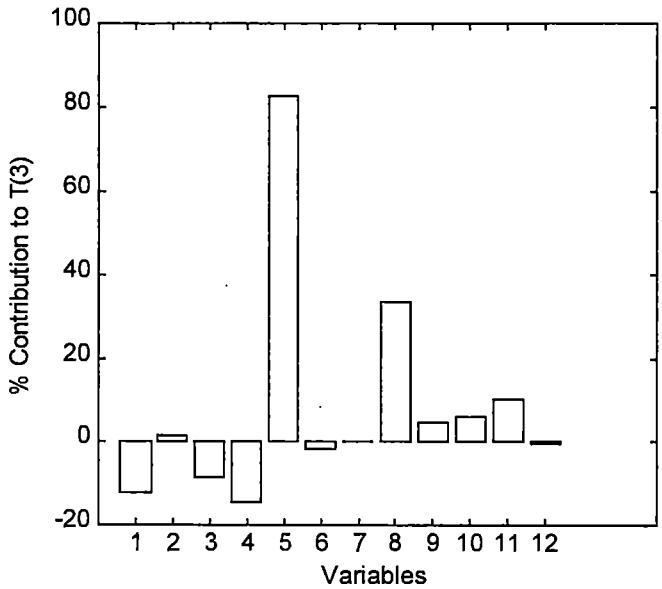

Figure 4-58. Contribution Plot to PC3 for Abnormality Case 3 -50% Change in the $\mu_{m,H}$ and +60% Change in the $K_{s,[COD]}$

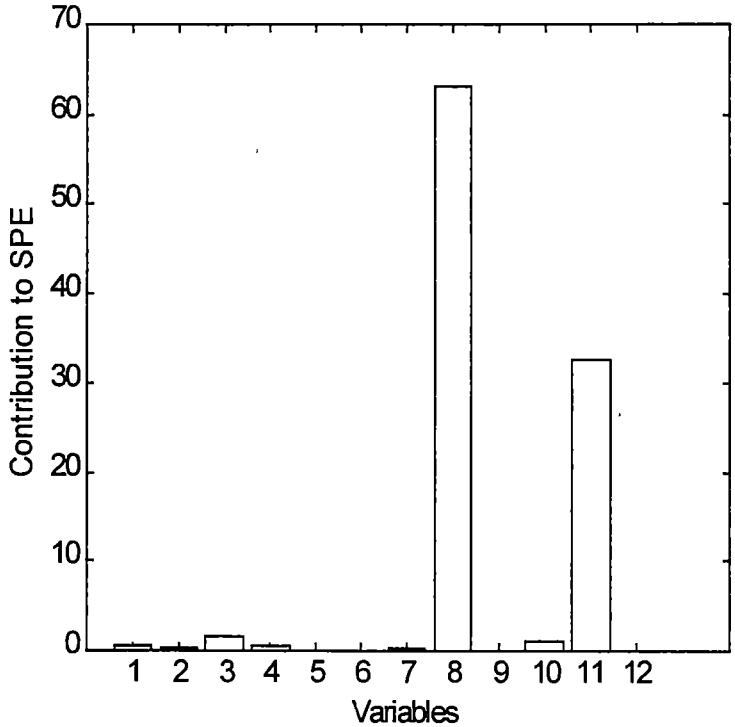

Figure 4-59. Contribution Plot to SPE for Abnormality Case 3 -50% Change in the $\mu_{m,H}$ and +60% Change in the $K_{s,[COD]}$

$_{Effluent)}$), effluent [BOD]. It is also somewhat associated with the deviation in x3 ($S_{S\ (Anoxic\ Reactor\ Effluent)}$), x4 ($S_{NH\ (Anoxic\ Reactor\ Effluent)}$), x10 ($S_{NO\ (System\ Effluent)}$) and x11 (Recirculation Ratio). These variables are exactly those contributing the most to the construction of PC1, as discussed earlier in Section 4.4.1.1. They are the responsible variables for the PC1 deviation. Figure 4-58 shows that deviation in PC3 is mainly caused by x5 ($S_{NO\ (Anoxic\ Reactor\ Effluent)}$). This is also consistent with the conclusion in Section 4.4.1.3.

The error in this case is obviously caused by the bigger amount of changes in the bio-parameters of the system. Figure 4-59 shows that x8 is primarily responsible for the residual of this case. It contributes more than 65% of the overall error of the process. x11 (Recirculation Ratio) is more or less responsible, too. The abnormal case studied here is simulated with a much smaller $\mu_{m,\ H}$ and much larger $K_{s,\ [COD]}$ compared with the reference model. Both reducing $\mu_{m,\ H}$ and increasing $K_{s,\ COD}$ will lead to slower biomass growth, therefore slower carbonaceous compound degradation. This will definitely have strong impact on the effluent [BOD], x8. In the biological wastewater plant under study, effluent [BOD] is paired with recirculation ratio in the feedback control loop. Deviation in the effluent [BOD] will automatically influence the recirculation ratio, x11, in an attempt to bring the effluent [BOD] back to its setpoint value. Therefore, the error between that predicted by the model and that from the abnormal observation is assignable to x8 and x11.

4.7.5 Abnormal Case 4: New Biological Event - -30% to –20% Changes in $\mu_{m,A}$

4.7.5.1 Modeling Abnormal Case 4

In this case, there is a completely new biological event not included in the base case model development. The maximum specific growth rate of autotrophic biomass, $\mu_{m,A}$, is varied from –30% to –20% change from its original value. This change in the bio-parameter constitutes a model shift. The following figures are the associated monitoring charts for this case.

Figures 4-60 and 4-61 are monitoring charts for PC1, 2, 3 and PC1, 2, respectively. This set of variation in $\mu_{m,A}$ results in out-of-bound changes in not only the PCA scores, but also the corresponding SPE. This implies that not only the base case model is a poor fit, but also that the corresponding scores are larger than normal.

Figures 4-62 and 4-63 show the impact on SPE of introducing this biological new event into the process. Clearly, SPE goes to a magnitude as high as 60 units. It is more than five times of the upper SPE limit. It is also about two folds as much as the SPE value obtained from the previous two cases of abnormalities. This large SPE is caused by a new type of biological constant change not considered in the reference case. In Figure 4-63, the decreasing trend in SPE is associated with a decreasing deviation of $\mu_{m,A}$ from that of nominal.

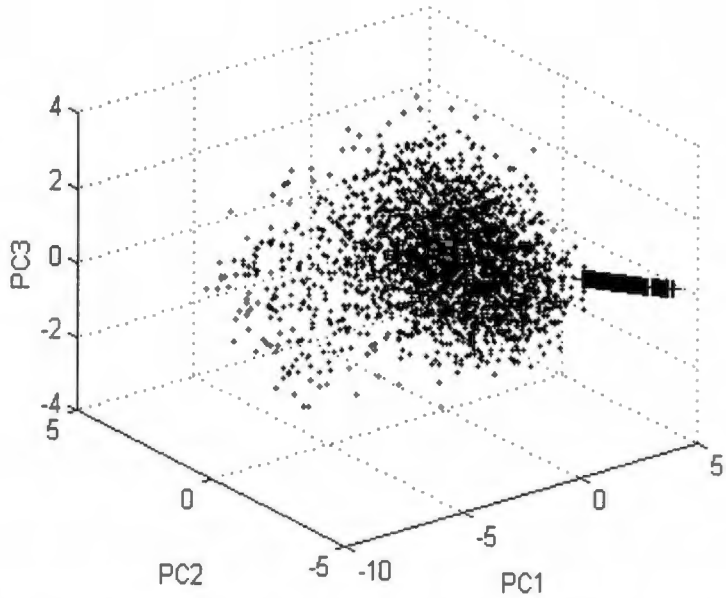

Figure 4-60. Monitoring Chart. Scores Plot for Principal Component 1, 2 and 3 (. =Reference Data; + = Data of -30% to –20% $\mu_{m,A}$ Changes)

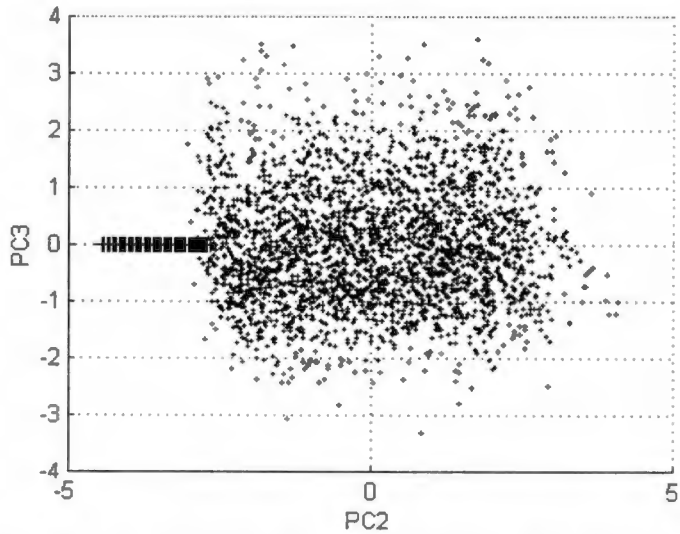

Figure 4-61. Monitoring Chart. Scores Plot for Principal Component 2 and 3 (. =Reference Data; + = Data of -30% to –20% $\mu_{m,A}$ Changes)

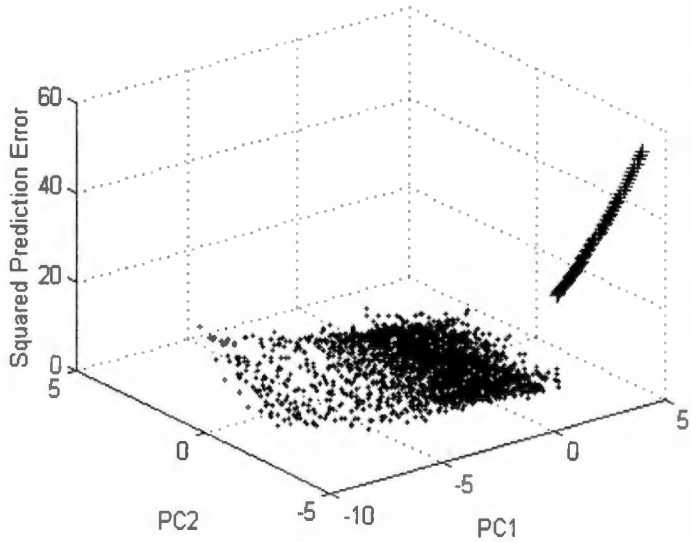

Figure 4-62. Monitoring Chart. SPE Plot for Principal Component 1 and 2 (. =Reference Data; + = Data of -30% to –20% $\mu_{m,A}$ Changes)

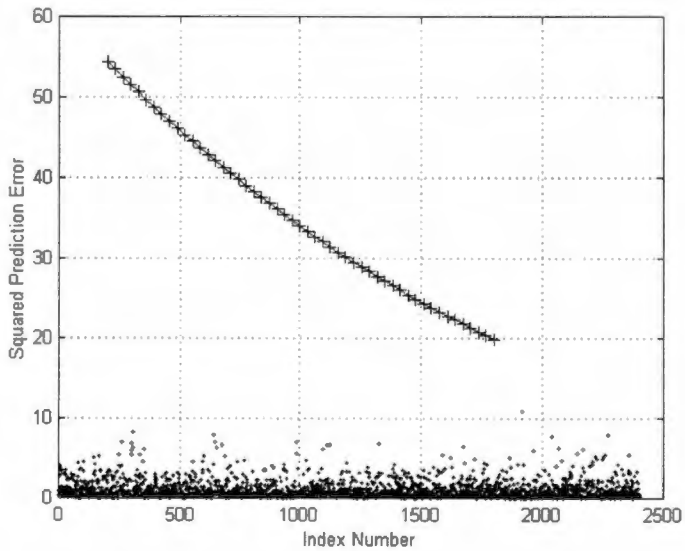

Figure 4-63. Monitoring Chart. SPE Plot (. =Reference Data; + =Data of -30% to –20% $\mu_{m,A}$ Changes)

Figures 4-64 and 4-65 show the scores and SPE for the transient responses for the case with the biggest variation in this group, when $\mu_{m,A}$ has a -30% change. Both plots show that the final steady state values stay well outside the original normal clustering region. This is a clear indication that the process is out of control. Causes need to be identified and eliminated if possible. Contribution plots can again be brought into suggest process variables responsible for the deviation.

4.7.5.2 Identifying Causes of One Sample from Abnormal Case 4: -30% Change in the $\mu_{m,A}$

Abnormality Case 4 is generated under a totally new biological event, changes in $\mu_{m,A}$. A -30% change in the $\mu_{m,A}$ is used to create contribution plots for this case. Figures 4-66 and 4-67 are the contribution plots.

Figures 4-60 and 4-61 show that the deviation in the t-scores plot is along the PC2 direction. The contribution plot for PC2 shows that this deviation is consisted of x2, the autotrophic biomass concentration from the anoxic reactor, x7, the autotrophic biomass concentration from the clarifier and x9, the effluent [NH_4^+], again due to the fact that PC2 is loaded by x2 and x7 mostly.

Figure 4-67 shows that error of this case is mainly caused by x1, the hetorotrophic biomass concentration from the anoxic reactor. Since $\mu_{m,A}$ decreases, the growth rate of autotrophic biomass in the aerobic reactor decreases accordingly. Therefore, the rate of nitrification occurring in the aerobic reactor slows down, too. Then less NO_3^- is produced in the aerobic reactor and fed into the anoxic reactor. Consequently, the hetorotrophic biomass growth rate in the anoxic reactor will be

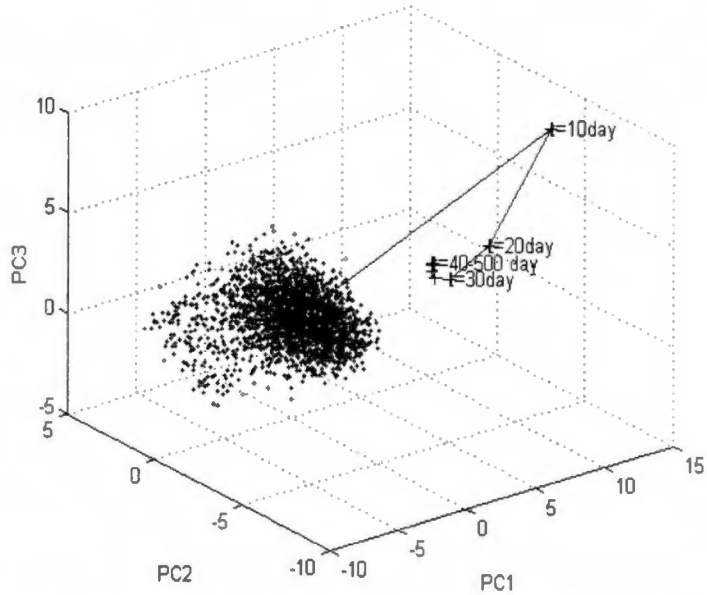

Figure 4-64. Monitoring Chart. Scores Plot for Principal Component 1, 2 and 3 (. =Reference Data; + = Data of Transient Response of -30% $\mu_{m,A}$ Changes)

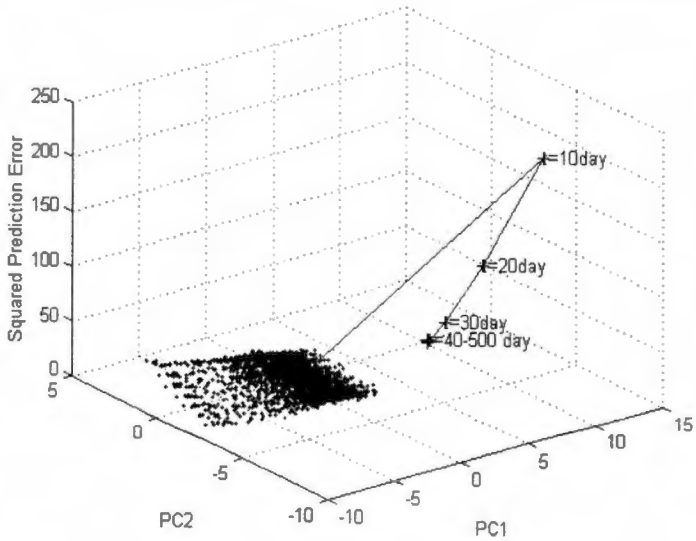

Figure 4-65. Monitoring Chart. SPE Plot for Principal Component 1 and 2 (. =Reference Data; + = Data of Transient Response of -30% $\mu_{m,A}$ Changes)

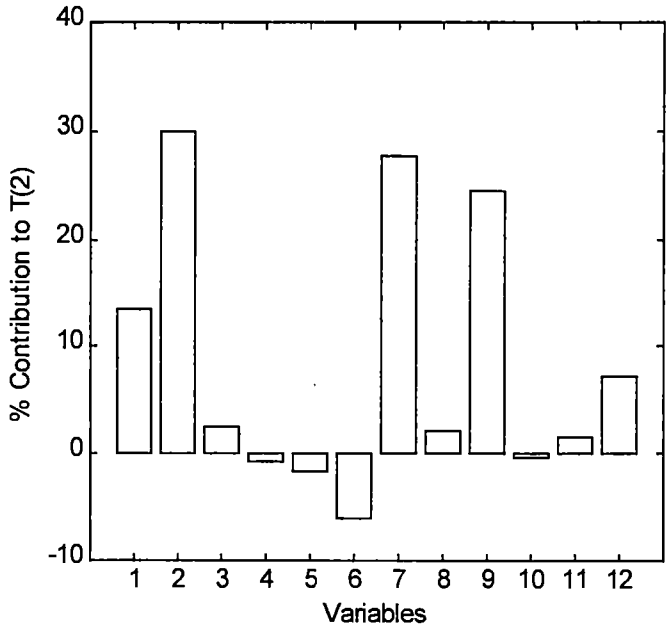

Figure 4-66. Contribution Plot to PC2 for Abnormality Case 4 -30% Change in the $\mu_{m,A}$

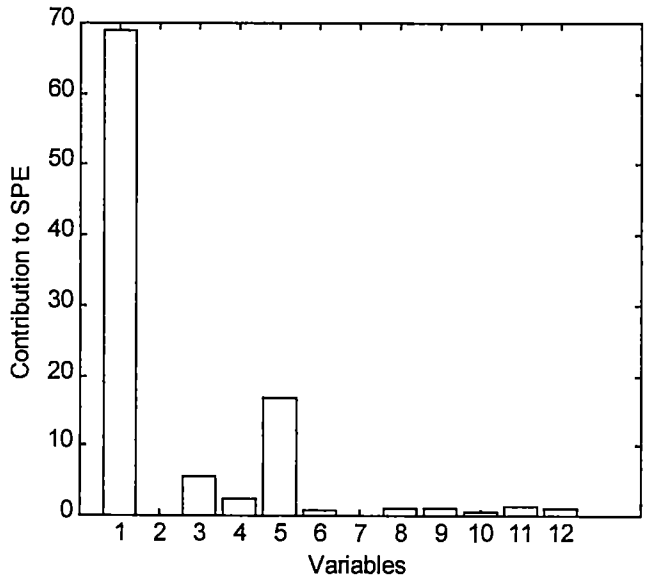

Figure 4-67. Contribution Plot to SPE for Abnormality Case 4 -30% Change in the $\mu_{m,A}$

affected, too. Therefore, x1, the hetorotrophic biomass concentration from the anoxic reactor, will deviate from normal value as well.

4.7.6 Conclusion

In each of the above four case studies of abnormalities, various multivariate statistical charts effectively detect abnormal deviations and deliver warnings to the operating personnel. By observing the out-of-bound behavior depicted in each plot, one can obtain some insight to the nature of the deviation. Larger-than-normal shift in the process variables is usually reflected in a shift of the scores; whereas a model shift is reflected by increased SPE. In addition, by observing the SPE plot, one can assess how much the process deviates from its nominal condition. The larger the SPE, the higher the disturbance or modeling error. These PCA charts correspond well to the physical interpretation of the observed events. In addition, the usage of contribution plots provides the potential to possibly identify the root causes for the observed abnormal deviations.

Chapter 5

Conclusions and Recommendations

5.1 Conclusions

In this study, the development of a monitoring and diagnostic framework using Multivariate Statistical Process Control (MSPC) methodology is presented for a multi-stage industrial prototype biological wastewater treatment plant. Results show that MSPC is capable of effectively detecting abnormality occurring during plant operation, and sometimes is capable of identifying possible root-cause for the abnormality. It is concluded that MSPC is a feasible tool for future application to wastewater treatment plant operations to improve plant effluent quality and to reduce process down times.

During the development of the MSPC monitoring and diagnostic framework, close attention must be paid to the following three aspects. First, data that are to be included in the base case profile should be from more or less steady state values, because they are indicative of the true state of the process operation. Transient data is not to be considered in the reference case. Second, the degree of variation reflected by the historical data should be chosen with care, in that they should be regarded as 'normal', arising from variations that are deemed normal. If the variation chosen is too broad, some malfunction or fault may later be regarded as 'normal', because it is within the boundary of the base case pattern. Conversely, if the acceptable variation chosen is too narrow, some otherwise acceptable operations will be judged as 'abnormal'. In addition, one should also be assured

that the underlying feedback controllers are chosen appropriately and are properly tuned to reach the control objective. Third, future data being monitored should be pretreated with the same mean and scaling factor as used in the base case profile. Otherwise, the two sets of data are not being compared with equal base line and bounds.

Based on this study, future application of such a MSPC framework to wastewater bio-treatment plant is expected to provide the operating personnel with a visual detection of the occurrence as well as the possible cause of a process abnormality. MSPC has the potential of detecting the onset of abnormal behavior of the process and providing the operating personnel an opportunity to take timely corrective step in the hope of driving the system back to that of normal.

5.2 Recommendations

Before this MSPC monitoring and diagnostic framework can be brought on-line in industry, implementation issues need to be addressed and analyzed. For instance, how often should the measurements should be taken; how long should the operator wait after observing from the MSPC charts, the onset of abnormal deviation before they take actions in hopes of driving the system back to the normal region; how often should the base case profile be updated to reflect recent changes in operation practice; some variable behavior changes periodically with the season or other operating conditions; therefore using multi-databases as the reference database may be warranted. Another important consideration is the availability of measurements for analysis. The question of how often, how feasible and how costly

for the additional measurement values required for MSPC are all very relevant and practical issues that need to be addressed and well thought about.

In summary, a properly designed MSPC is expected to yield timely information to the operating personnel, in regard to the 'state' of the process, thus avoiding possible irreversible decay of the process, which implies, always, additional time and resources that would be required to restore the process to that of 'normal'.

REFERENCES

REFERENCES

1. Bakshi, B. R., "Multiscale PCA with Application to Multivariate Statistical Process Monitoring", *AIChE journal*, vol. 44, no. 7, (1998), 1596-1609.

2. Chen, G. and McAvoy, T. J., "Predictive On-Line Monitoring of Continuous Processes", *Journal of Process Control*, vol. 8, nos. 5-6, (1998), 409-420.

3. Chen, G., McAvoy, T. J. and Piovoso, M. J., "A Multivariate Statistical Controller for On-Line Quality Improvement", *Journal of Process Control*, vol. 8, no. 2, (1998), 139-149.

4. Dayal, B., MacGregor, J. F., Taylor, P. A., Kildaw, R. and Marcikic S., "Application of Artificial Neural Networks and Partial Least Squares Regression for Modeling Kappa Number in a Continuous Kamyr Digester", *Control Systems '92,* (1992), 191-196.

5. Diaconis, P. and Efron, B., "Computer-intensive Methods in Statistics", *Scientific American*, (1983), 96-108.

6. Evangelisti, F. and Zunin, P., "Stability to Oxidation of Virgin Olive oils as Related to Olive Conditions: Study of Polar Compounds by Chemometric Methods", *Journal of the American Oil Chemists Society*, vol. 74, no. 8, (1997), 1017-1023.

7. Gan, F. F., "Joint Monitoring of Process Mean and Variance", *Nonlinear Analysis, Theory, Methods & Applications*, vol. 30, no. 7, (1997), 4017-4024.

8. Grosdidier, Pierre, Morari, Manfred, and Holt, Bradley R., "Closed-Loop Properties from Steady-State Gain Information", *Industrial Engineering Chemical Fundamentals*, vol. 24, no. 2, (1985), 221-235.

9. Grove, J. M., *Analysis of Controllability of a Wastewater Treatment Plant*, M.S. Thesis, University of Tennessee, (1995).

10. Henze, M., Grady, C.P.L., Jr, Gujer, W., Marais, G.v.R., Matsuo, T., "Activated Sludge Model No. 1", *IAWPRC Scientific and Technical Reports*, no. 1, IAWQ, London (1986).

11. Hoskuldsson, A., "A Combined Theory for PCA and PLS", *Journal of Chemometrics*, vol. 9, (1995), 91-123.

12. Jackson, J. E., *A User's Guide to Principal Components*, John Wiley & Sons, Inc., New York, (1991), Chapter 1.

13. Jackson, J. E., "Principal Components and Factor Analysis: Part I - Principal Components", *Journal of Quality Technology*, vol. 12, no. 4, (1980), 201-213.

14. Jones, R. M., MacGregor, J. F., Murphy, K. L. and Hall, E. R., "Towards a Useful Dynamic Model of the Anaerobic Wastewater Treatment Process: a Practical Illustration of Process Identification", *Water Science and Technology*, vol. 25, no. 7, (1992), 61-71.

15. Kambhatla, N. and Leen, T. K., "Dimension Reduction by Local Principal Component Analysis", *Neural Computation*, vol. 9, no. 7, (1997), 1493-1516.

16. Kaspar, M. H. and Ray, W. H., "Chemometric Methods for Process Monitoring and High-performance Controller Design", *AIChE Journal*, vol. 38, no. 10, (1992), 1593-1608.

17. Kassidas, A., Taylor, P.A. and MacGregor, J. F., "Off-line Diagnosis of Deterministic Faults in Continuous Dynamic Multivariable Processes Using Speech Recognition Methods", *Journal of Process Control*, vol. 8, nos. 5-6, (1998), 381-393.

18. Kourti, T. and MacGregor, J. F., "Process Analysis, Monitoring and Diagnosis, Using Multivariate Projection Methods", *Chemometrics and Intelligent Laboratory Systems*, vol. 28, (1995), 3-21.

19. Kramer, M. A., "Nonlinear Principal Component Analysis Using Autoassociative Neural Networks", *AIChE Journal*, vol. 37, no. 2, (1991), 233-243.

20. Kresta, J. V., MacGregor, J. F. and Marlin, T. E., "Multivariate Statistical Monitoring of Process Operating Performance", *the Canadian Journal of Chemical Engineering*, vol. 69, (1991), 35-47.

21. Ma, X. H., Sinha, N. K. and MacGregor, J. F., "Linearizing Transformation for the Study of Nonlinear Systems", *1987 IEEE*, (1987), 159-162.

22. MacGregor, J. F., Marlin, T. E., Kresta, J. and Skagerberg, B., "Multivariate Statistical Methods in Process Analysis and Control", *Chemical Process Control--CPC IV, Proceedings of International Conference 4th*, (1991), 79-99.

23. Majcen, N., Rius, F. X. and Zupan, J., "Linear and Non-linear Multivariate Analysis in the Quality Control of Industrial Titanium Dioxide White Pigment", *analytica chimica acta*, vol. 348, nos. 1-3, (1997), 87-100.

24. Martin, E. B., Morris, A. J. and Zhang, J., "Process Performance Monitoring Using Multivariate Statistical Process Control", *IEE Process Control Theory and Application*, vol. 143, no. 2, (1996), 132-144.

25. Martin, E. B. and Morris, A. J., "An Overview of Multivariate Statistical Process Control in Continuous and Batch Process Performance Monitoring", *Transactions. Institute of Measurement & Control*, vol. 18, no. 1, (1996), 51-59.

26. Metcalf & Eddy, Inc. *Wastewater Engineering Treatment, Disposal, and Reuse*, 3rd ed., McGraw-Hill Book Co., New York (1991).

27. Morari, M. and Zafiriou, E., *Robust Process Control*, Prentice-Hall, Inc., (1989).

28. Morsing, T. and Ekman C., "Comments on Construction of Confidence Intervals in Connection with Partial Least Squares", *Journal of Chemometrics*, vol. 12, (1998), 295-299.

29. Mujunen, S. P., Minkkinen, P., "Modeling of Activated Sludge Plants Treatment Efficiency with PLSR: a Process Analytical Case Study", *Chemometrics and Intelligent Laboratory Systems*, vol. 41, (1998), 83-94.

30. Negiz, A. and Cinar A., "Statistical Monitoring of Multivariable Dynamic Processes with State-space Models", *AIChE Journal*, vol. 43, no. 8, (1997), 2002-2020.

31. Neogi, D. and Schlags, C. E., "Multivariate Statistical Analysis of an Emulsion Batch Process", *Industrial Engineering in Chemical Research*, vol. 37, (1998), 3971-3979.

32. Nomikos, P., *Statistical Process Control of Batch Processes*, Ph.D. Dissertation, McMaster University, Canada, (1995).

33. Nomikos, P., and MacGregor, J. F., "Monitoring Batch Processes Using Multiway Principal Component Analysis", *AIChE Journal*, vol. 40, no. 8, (1994), 1361-1375.

34. Nomikos, P. and MacGregor, J. F., "Multivariate SPC Charts for Monitoring Batch Processes", *Technometrics*, vol. 37, no. 1, (1995), 41-59.

35. Ogunnaike, B. A. and Ray, W. H., *Process Dynamics, Modeling, and Control*, Oxford University Press, Inc., New York, (1994).

36. Orhon, D. and Artan, N., *Modeling of Activated Sludge Systems*, Technomic Publishing Company, Inc., Pennsylvania, (1994).

37. Pearson, K., "On Lines and Planes of Closest Fit to Systems of Points in Space", *Philosophy Magazine*, vol. 2, (1901), 559-572.

38. Piovoso, M. J. and Kosanovich, K. A., "The Use of Multivariate Statistics in Process Control", CRC Press, Inc., New York, (1996).

39. Pringle, T. C. and MacGregor, J. F., "Product Quality Control in Reduced Dimensional Spaces", *Industrial Engineering in Chemical Research*, vol.37, (1998), 3992-4002.

40. Qin, S. J. and Dunia, R., "Determining the Number of Principal Components for Best Reconstruction", P*reprint of AIChE Meeting, Nov., 1998,* (1998).

41. Rosen, C. and Olsson, G., "Disturbance Detection in Wastewater Treatment Plants", *Water Science and Technology*, vol. 37, no. 12, (1998), 197-205.

42. Schlags, C. E. and Anani, A. S., "Waste Treatment Process Analysis Using Multivariate Statistical Methods", *Preprint of AIChE Meeting, Nov., 1998*, (1998).

43. Schmidt, B. T., *Analysis of Closed-loop Control Strategies for a Wastewater Treatment Plant*, M.S. Thesis, University of Tennessee, (1996).

44. Shewhart, W. A., *Economic Control of Quality of Manufactured Product*, Van Nostrand Reinhold, New York, (1931).

45. Skagerber, B., MacGregor, J. F. and Kiparissides, C., "Multivariate Data Analysis Applied to Low-density Polyethylene Reactors", *Chemometrics and Intelligent Laboratory Systems*, vol. 14, (1992), 341-356.

46. Sparks, R., Adolphson, A. and Phatak, A., "Multivariate Process Monitoring Using the Dynamic Biplot", *International Statistical Review*, vol. 65, no. 3, (1997), 325-349.

47. Strang, G., *Linear Algebra and Its Applications*, 3rd ed., Harcourt Brace Jovanovich College Publishers, Orlando, FL, (1988).

48. Teppola, P., Mujunen, S. P. and Minkkinen P., "A Combined Approach of Partial Least Squares and Fuzzy C-means Clustering for the Monitoring of an Activated-Sludge Waste-Water", *Chemometrics and Intelligent Laboratory Systems*, vol. 41, (1998), 95-103.

49. Teppola, P., Mujunen, S. P. and Minkkinen P., "Partial Least Squares Modeling of an Activated Sludge Plant: A Case Study", *Chemometrics and Intelligent Laboratory Systems*, vol.38, (1997), 197-208.

50. Tesch, S. and Otto, M., "Application of Principal-Component Analysis to the Interpretation of Brown Coal Properties", *Fuel*, vol. 74, no. 7, (1995), 978-982.

51. Westerhuis, J. A., Kourti, T. and MacGregor, J. F., "Analysis of Multiblock and Hierarchical PCA and PLS Models", *Journal of Chemometrics*, vol. 12, (1998), 301-321.

52. Wikstrom, C., Albano, C., "Multivariate Process and Quality Monitoring Applied to an Electrolysis Process", *Chemometrics and Intelligent Laboratory Systems*, vol. 42, (1998), 221-231.

53. Wise, B. M. and Gallagher, N. B., "The Process Chemometrics Approach to Process Monitoring and Fault Detection", *Journal of Process Control*, vol. 6, no. 6, (1996), 329-348.

54. Wise, B. M., Ricker, N. L., Veltkamp, D. F. and Kowalski, B. R., "A Theoretical Basis for the Use of Principal Component Models for Monitoring Multivariate Processes", *Process Control and Quality*, vol. 1, (1990), 41-51.

55. Wold, S., "Chemometrics: What Do We Mean with It, and What Do We Want from It?", *Chemometrics and Intelligent Laboratory Systems*, vol. 30, no. 1, (1995), 109-115.

56. Wold, S., Esbensen, K. and Geladi, P., "Principal Component Analysis", *Chemometrics and Intelligent Laboratory Systems*, vol. 2, (1987), 37-52.

57. Wold, S., Geladi, P, Esbensen, K. and Ohman, J., "Multi-Way Principal Components and PLS Analysis", *Journal of Chemometrics*, vol. 1, (1987), 41-56.

58. Wold, S. and Sjostrom, M., "Chemometrics, Present and Future Success", *Chemometrics and Intelligent Laboratory Systems*, vol. 44, nos. 1, 2, (1998), 3-14.

59. Zhang, J. Martin, E. B. and Morris, A. J., "Process Monitoring Using Non-linear Statistical Techniques", *Chemical Engineering Journal*, vol. 67, (1997), 181-189.

VITA

Bei Fu was born in Beijing, CHINA on July 12, 1973. She graduated from Beijing Shiyan High School in 1992. She passed the highly-competitive National College Entrance Examination with outstanding scores and since September, 1992 became a student of Tsinghua University, the top engineering school in CHINA. In July, 1997 she received the Bachelor of Science degree in Chemical Engineering and Technology. While at Tsinghua University, she participated in many research projects in her department and did two summer internships in industry. In addition, she joined the Beijing University Students' Symphony Orchestra and played cello there for three years.

Being a self-motivator, she took all the necessary English tests for foreigners to study in U.S. and entered the Master' s program in Chemical Engineering at the University of Tennessee, Knoxville in January, 1998, officially receiving the Master's degree in December, 1999.

Upon graduation, she accepted a job with Umetrics, Inc. of New Jersey, as an engineer intending to work with the application of MSPC methodology to industrial processes.